

From side streams to building blocks: gas phase conversion of biomass-derived feedstocks to valuable monomers

Dissertation
zur Erlangung des akademischen Grades
Doctor rerum naturalium (Dr. rer. nat.)
der Mathematisch-Naturwissenschaftlichen Fakultät
der Universität Rostock

vorgelegt von
Fatima El Ouahabi, M. Sc.
Geboren am 18.09.1992 in Larache (Morocco)

Rostock, 22.08.2019



Dieses Werk ist lizenziert unter einer
Creative Commons Namensnennung - Nicht kommerziell - Keine Bearbeitungen 4.0
International Lizenz.

Die vorliegende Dissertation wurde im Zeitraum von Mai 2016 bis August 2019 gefertigt am Leibniz-Institut für Katalyse e.V. an der Universität Rostock im Bereich von Prof. Dr. Johannes G. de Vries.

Gutachter 1: Prof. Dr. Johannes G. de Vries
Leibniz-Institut für Katalyse e.V. an der Universität Rostock
Albert-Einstein-Straße 29a
18059 Rostock, Germany

Gutachter 2: Prof. Dr. G.J.M. (Gert-Jan) Gruter
University of Amsterdam
Postbus 94157
1090 GD Amsterdam

Datum der Einreichung: 26.08.2019

Datum der Verteidigung: 10.12.2019

Acknowledgments

The execution of this doctoral thesis has been a very nice journey. I must admit it changed me for ever. I have learned a big deal. It was a journey that conducted me through a pathway of meeting great people, and I am grateful to all of them.

My special thanks to Prof. Johannes G. de Vries, for giving me the opportunity to be part of the project where not only I developed such excellent skills, but it also allowed me to grow from the human perspective. It has been a wonderful program and I am again grateful.

This thesis would not have been possible without the help of the group leaders Dr. Sandra Hinze and Dr. Sergey Tin. All your suggestions and inputs were of a great help.

Acknowledgments also come to all the LIKAT colleagues who supported me from the very beginning, Richard van Heck, Dr. Pim Puylaert, Dr. Bartosz Wozniak, Dr. Tian Xia, Dr. Ronald Farrar-Tobar, Bernhard Stadler, Brian Spiegelberg, Dr. Arianna Savini, Andrea Dell'Acqua, Dr. Swechchha Pandey, Justus Diekamp, Roberto Sole, Dr. Sarah Kirchhecker, and Thibault Tannoux. Thank you for the warm welcoming as well as for the nice time we spent together. Dr. Pim Puylaert, you are a special gift I am taking with me from this adventure. I hope our friendship prevails for many and many years more.

I would like to thank all the people who contributed to this work from the industrial partnership with Avantium chemicals in Amsterdam. Dr. Jan-Kees van der Waal, I cannot tell you how glad I am for all the high-quality time spent where I adsorbed the excellent knowledge you transmitted me. Thank you so much!

Dr. Gerard van Klink, thanks for considering all the crazy ideas that I wanted to try and trusting me. Thanks to our project manager Dr. Erica Ording, especially for being always very supportive and understanding. Dr. Carlo Angelici, although we had some differences in personality, through a tough project, a very nice friendship has been established and I am extremely happy. I would like to thank you for the nice skills transferred such as synthesis of heterogeneous catalysts or others as organization skills...

Pierluigi Tosi, Anna Sangregorio, Layla Filiciotto and Anitha Muralidhara, thank you for being such nice colleagues, for the knowledge shared during the meetings and of course for the great time we shared as flat mates in Amsterdam and during our trips. It was a great experience!

Dr. Narayana Kalevaru, Dr. Sebastian Wohlrab, Dr. Mykola Polyakov and Annemarie Marckwordt it was a nice experience working with you over the past year! Thanks for allowing me to work in your labs and use your equipment. Dr. Hadis Amani, you cannot imagine how important you have been. Thanks a lot for keeping me sane!

To the analytical department of LIKAT, thank you so much for the amazing support!

I would also like to thank the HUGS board committee for the perfect job done during this past three years. All the business meetings and the training schools have been a great success! I thank the European Union for funding my research that was part of a Marie Skłodowska-Curie Innovative Training Network (Industrial Doctorates) from the European Union's Horizon 2020 Research and Innovation program under Grant Agreement n° 675325 of which Avantium was the coordinator.

Finally, my deepest gratitude and appreciation goes to my family and friends for all their support and patience. Also, to Mohammad Omar Aljamal, I am very happy to share all of this with you.

I can think of an infinite list of people I would like to thank, but you already know who you are and deserve as well a thank you from the deepest part of my heart!

Abstract

This thesis describes the chemical conversion of methyl levulinate (ML), a biorefinery side stream, to the valuable monomers methyl vinyl ketone (MVK) and methyl acrylate (MA). The first part of the research was aimed at the demethoxycarbonylation of ML in the liquid and in the gas phase. Several approaches using homogeneous and heterogeneous catalyzed processes were investigated for this conversion. During the course of this investigation, it was found that the liquid phase reaction was not successful. Due to the high stability of the methyl ester moiety of ML, the demethoxycarbonylation reaction requires high temperatures (up to 250 °C) at which the catalyst does not survive. In addition, the obtained MVK easily polymerizes in the liquid phase at these high temperatures. Thus, it was found necessary to use a gas phase process in order to achieve the desired product. Therefore, the demethoxycarbonylation of ML to MVK was studied by feeding the starting material on a fixed-bed, continuous flow set-up. Platinum 5 wt% on sulfided carbon was found to be the most active catalyst, affording up to 18% yield of MVK. In addition to low yields, the catalyst suffered from fast deactivation with time-on-stream. Through mechanistic studies of the reaction, it was discovered that the most likely intermediate for the formation of MVK is levulinic acid (LA) which rapidly undergoes ring-closure to alpha angelica lactone (α -AL). The decarbonylation of the latest forms MVK and CO. The latter can act as a catalyst poison. It was possible to obtain MVK from LA in over 54% yield using the same catalyst at 350°C. Unfortunately, the catalyst suffers from deactivation. The properties of this catalyst were characterized using TEM, XRD, XPS, BET and ICP.

In the second part of the project, conversion of ML to methyl-3-acetoxypyranoate (M3AP) through a Baeyer-Villiger (BV) oxidation was studied. The acid-catalyzed BV of methyl levulinate investigated in this thesis, led to the formation of various oxidized as well as degraded compounds. However, an enzymatic approach was reported by Mihovilovic and co-workers, achieving 80% yield of the desired M3AP. The thus-formed M3AP could be successfully converted to methyl acrylate (MA) *via* elimination of acetic acid in the gas phase. During our studies, it was observed that at 600 °C, MA was obtained in 97% yield together with quantitative amounts of acetic acid. Catalytic tests were carried out aiming to lower the reaction temperature. Although higher conversions of M3AP were obtained at 300°C, the process suffered from lower selectivity.

Zusammenfassung

Diese Dissertation beschreibt die chemische Umwandlung von Methyllävulinat (ML), einem Nebenprodukt der Bioraffinerie, in die wertvollen Monomere Methylvinylketon (MVK) und Methylacrylat (MA). In dem ersten Teil dieser Forschungsarbeit lag der Schwerpunkt auf der Demethoxycarbonylierung von ML in flüssiger sowie in gasförmiger Phase. Für diese Umsetzung wurden verschiedene Ansätze unter Verwendung von homogenen und heterogenen Katalysatoren getestet. Im Verlauf dieser Untersuchung wurde allerdings festgestellt, dass die Reaktion in der flüssigen Phase nicht erfolgreich war. Aufgrund der hohen Stabilität der Methylesterseinheit von ML erfordert die Demethoxycarbonylierungsreaktion hohe Temperaturen (bis zu 250 °C), bei denen der Katalysator nicht beständig ist. Außerdem polymerisiert das gebildete MVK in der flüssigen Phase bei diesen hohen Temperaturen leicht. Daher erschien es notwendig, die Reaktion in der Gasphase durchzuführen. Die Demethoxycarbonylierung von ML zu MVK wurde daher in einem Festbett-Durchflussreaktor untersucht. Es wurde gefunden, dass für diese Reaktion 5 Gew.% Platin auf sulfidiertem Kohlenstoff der aktivste Katalysator war, mit einer Ausbeute an MVK von bis zu 18%. Neben geringen Ausbeuten litt der Katalysator unter einer schnellen Deaktivierung im laufenden Betrieb. Durch mechanistische Untersuchungen wurde entdeckt, dass das wahrscheinlichste Zwischenprodukt für die Bildung von MVK Lävulinsäure (LA) ist, die schnell einen Ringschluss zu α -Angelicalacton (α -AL) eingeht. Die Decarbonylierung von α -AL bildet MVK und CO. Letzteres kann als Katalysatorgift wirken. Mit LA als Ausgangsstoff war es möglich, eine Ausbeute von über 54% MVK unter Verwendung des gleichen Katalysators bei 350 °C zu erhalten. Leider wird der Katalysator mit der Zeit deaktiviert. Die Eigenschaften dieses Katalysators wurden unter Verwendung von TEM, XRD, XPS, BET und ICP charakterisiert.

Im zweiten Teil des Projekts wurde die Umwandlung von ML in Methyl-3-acetoxypentanoat (M3AP) durch eine Baeyer-Villiger (BV) -Oxidation untersucht. Die säurekatalysierte BV von Methyllävulinat führte zu der Bildung von verschiedenen oxidierten Verbindungen sowie von Degradationsprodukten. Mihovilovic et al. berichteten jedoch über einen enzymatischen Ansatz, bei dem eine Ausbeute von 80% des erwünschten M3AP erzielt wurde. Das so gebildete M3AP konnte durch Abspaltung von Essigsäure in der Gasphase erfolgreich in Methylacrylat (MA) umgewandelt werden. Während unserer Untersuchungen stellten wir fest, dass bei 600 °C MA in 97%iger Ausbeute zusammen mit quantitativen Mengen Essigsäure erhalten wurde. Katalytische Tests wurden durchgeführt, um die Reaktionstemperatur zu senken. Obwohl bei 300 °C höhere Umwandlungen von M3AP erhalten wurden, litt das Verfahren unter einer geringeren Selektivität.

Abbreviations

ac	acetyl
ad	adamantyl
aq.	aqueous
cat.	catalyst
conc.	concentration
conv.	conversion
dba	dibenzylideneacetone
dcpp	1,3-Bis(dicyclohexylphosphino)propane
DMF	dimethylformamide
DMPU	N,N'-Dimethylpropyleneurea
DMSO	dimethylsulfoxide
dppf	1,1'-Bis(diphenylphosphino)ferrocene
DPPB	1,4-Bis(diphenylphosphino)butane
dtbpx	1,2-Bis(di- <i>tert</i> -butylphosphinomethyl)benzene
<i>et al.</i>	lat. <i>et alia</i> – eng. and others
eq.	equivalent
GC-MS	gas chromatography coupled with mass spectrometry
GHSV	gas hourly space velocity
HR-MS	high-resolution mass spectrometry
IPr·HCl	1,3-Bis(2,6-diisopropylphenyl)imidazolium Chloride
KOtBu	potassium <i>tert</i> -butoxide
M	mol/L
MB	mass balance
Me	methyl
MIBK	methyl isobutyl ketone
MOF	metal-organic framework
NHC	N-Heterocyclic Carbene
NMP	N-Methyl-2-pyrrolidone
NMR	nuclear magnetic resonance
PEF	polyester polyethylene-2,5-furanoate
PET	polyethylene terephthalate
Ph	phenyl
Ref.	reference
RT	room temperature
SPhos	2-Dicyclohexylphosphino-2',6'-dimethoxybiphenyl
wt	weight
[X]	conversion

List of Figures

Figure 1. Levulinic acid (LA).	8
Figure 2. Selected ligands and a NHC-Pd complex for the Pd-catalyzed demethoxycarbonylation of ML.	25
Figure 3. Deactivation curves of 5%Pt on sulfided carbon for MVK formation obtained from the high throughput screening.	42
Figure 4. TEM pictures: a) fresh 5 wt% Pt on sulfide carbon b) spent 5 wt% Pt on sulfided carbon.	44
Figure 5. Time-on-stream behavior of Pt/C catalyst and the effect of reactivation on the yields of MVK and MEK from LA.	49
Figure 6. Time-on-stream stability of Pt/C catalyst and the effect of temperature on the yields of MVK and MEK from LA at 350°C.	51
Figure 7. The overview of the project.	60
Figure 8. QCS equipment. a) Reactor block, b) heating box.	65
Figure 9. Reaction scheme of Flowrence set-up.	67
Figure 10. PFR flow set-up.	70
Figure 11. PFR set-up P&ID diagram.	71
Figure 12. X-ray diffraction (XRD) fresh and spent catalyst.	74
Figure 13. Pyrolysis set-up.	76

List of Schemes

Scheme 1. Synthesis of useful chemicals from biomass-derived lignocellulose.	2
Scheme 2. Selected examples of products derived from 5-HMF.	3
Scheme 3. FDCA synthesis routes from lignocellulosic biomass.	4
Scheme 4. 5-HMF reaction pathways towards FDCA.	6
Scheme 5. PEF synthesis route from fructose.	7
Scheme 6. Synthesis of LA from lignocellulose.	9
Scheme 7. Selected compounds that can be synthesized from levulinic acid.	10
Scheme 8. Catalytic preparation of nylon monomer precursors from Levulinic acid	11
Scheme 9. Possible ways for the conversion of biomass to alkyl levulinates.	11
Scheme 10. Synthesis of alkyl levulinates from levulinic acid.	12

Scheme 11. Decarboxylation/decarbonylation reactions followed by other transformations.	13
Scheme 12. Pd-catalyzed decarboxylative cross-coupling mechanism.	14
Scheme 13. Decarboxylation of (unsaturated) vegetable oils or fatty acids.	15
Scheme 14. Levulinic acid decarboxylation to MEK.	15
Scheme 15. Ru-catalyzed tandem isomerization-decarboxylation of oleic acid.	16
Scheme 16. Metal-catalyzed decarbonylation of acids.	16
Scheme 17. Mechanism of the Pd-catalyzed decarbonylation of acids via anhydride formation.	17
Scheme 18. Pd-catalyzed decarbonylative dehydration of fatty acids for the synthesis of linear alpha olefins	18
Scheme 19. General methoxycarbonylation reaction.	19
Scheme 20. Palladium-catalyzed decarbonylative trifluoromethylation using trifluoroacetic acid esters.	19
Scheme 21. Tolman's Pd-catalyzed decarbonylation of <i>p</i> -nitrophenyl esters to olefins.	20
Scheme 22. Tolman Ru-catalyzed dehydrative decarbonylation of fatty acid methyl esters.	20
Scheme 23. Demethoxycarbonylation of ML to MVK.	21
Scheme 24. Baeyer-Villiger oxidation of ML followed by elimination to MA.	22
Scheme 25. Baeyer-Villiger oxidation of LA.	23
Scheme 26. Proposed mechanism for the Pd-catalyzed demethoxycarbonylation of ML.	25
Scheme 27. Proposed reaction pathway for the Ru-catalyzed decarbonylation of ML.	27
Scheme 28. Synthesis of 2-pyridylmethyl levulinate from ML.	27
Scheme 29. Synthesis of levulinic <i>p</i> -nitrophenyl ester from LA.	28
Scheme 30. Decarbonylation of <i>p</i> -nitrophenyl hexanoate to pentene.	29
Scheme 31. Preparation of levulinic acid anhydride.	30
Scheme 32. Ni-catalyzed decarbonylation of levulinic anhydride.	30
Scheme 33. Procedure for the synthesis of Pd supported catalysts.	31
Scheme 34. FDCA synthesis from biomass derived HMF and MMF.	36
Scheme 35. General reaction for the conversion of ML to MVK.	37
Scheme 36. Proposed reaction pathways for the conversion of ML to MVK.	47
Scheme 37. MA and AcOH from bio-based ML.	55

List of Tables

Table 1. Selected examples of sources used for the LA production.	9
Table 2. Some selected examples of homogeneous and heterogeneous catalysts employed in methyl levulinate production	12
Table 3. Ligand screening in the Pd-catalyzed decarbonylation of ML.	26
Table 4. Reductive decarbonylation of 2-pyridylmethyl ester using different metal precursors.	27
Table 5. Pd-catalyzed decarbonylation of <i>p</i> -nitrophenyl ester.	29
Table 6. Heterogeneous Pd-catalyzed decarbonylation of ML using different solvents.	31
Table 7. Overview of the selected results from liquid phase conversion of ML to MVK in toluene using heterogeneous supported catalysts.	32
Table 8. MVK and MEK yields in the conversion of LA in H ₂ O using silver and copper oxides as catalysts.	34
Table 9. Overview of the results from gas phase high through put screening of various supported metal catalysts for demethoxycarbonylation of ML.	40
Table 10. Effect of H ₂ O admixture on the activity and selectivity of 5wt% Pt/sulfided Carbon catalyst tested in a single reactor system	43
Table 11. Control experiments for the gas phase conversion of ML.	48
Table 12. BV oxidation of ML using peroxides.	56
Table 13. Gas-phase elimination of acetic acid from methyl 3-acetoxypropanoate.	57
Table 14. Catalytic elimination of acetic acid from methyl 3-acetoxypropanoate.	58
Table 15. GC (TDC and FID) response factors 1.	68
Table 16. GC (TDC and FID) response factors 2.	69
Table 17. Brunauer–Emmet–Teller (BET) fresh and spent catalyst.	73
Table 18. X-ray photoelectron spectroscopy (XPS).	73
Table 19. Elemental compositions were determined by ICP-OES.	73
Table 20. X-ray diffraction (XRD).	74

Table of Contents

1. Introduction	1
1.1. Biomass as future feedstock for platform chemicals	1
1.2. Platform chemicals from biomass	2
1.2.1. The Avantium process to 2,5-furandicarboxylic acid	4
1.2.2. Synthesis and applications of levulinic acid esters	8
1.3. Deoxygenation of biomass-derived feedstocks to chemicals via decarbonylation and decarboxylation	13
1.3.1. Decarboxylation and decarbonylation of carboxylic acids	14
1.3.2. Decarbonylation and dealkoxycarbonylation of esters	18
1.4. Goal of the research described in this thesis	21
1.4.1. Methyl vinyl ketone	21
1.4.2. Methyl acrylate	22
2. Chapter 1: Liquid phase conversion of methyl levulinate and levulinic acid to methyl vinyl ketone	24
2.1. Introduction	24
2.2. Objectives	24
2.3. Results and discussion	24
2.4. Conclusion	35
3. Chapter 2: Gas phase conversion of bio-based methyl levulinate to methyl vinyl ketone	36
3.1. Introduction	36
3.2. Objectives	39
3.3. Results and discussion	39
3.4. Conclusion	52
4. Chapter 3: Preparation of methyl acrylate from biomass-derived methyl levulinate	54
4.1. Introduction	54
4.2. Objectives	55
4.3. Results and discussion	55
4.4. Conclusion	59
5. Thesis summary	60
6. Experimental work and data analysis	62
6.1. Chapter 1	62

6.1.1.	General considerations	62
6.1.2.	Experimental procedures and analytical data	62
6.2.	Chapter 2.....	66
6.2.1.	Experimental procedures and analytical data	66
6.2.2.	Catalyst characterization	72
6.3.	Chapter 3.....	75
6.3.1.	Experimental procedures and analytical data	75
7.	Statement: Scientific Independence	80
8.	Curriculum Vitae	81
9.	References.....	85

1. Introduction

1.1. Biomass as future feedstock for platform chemicals

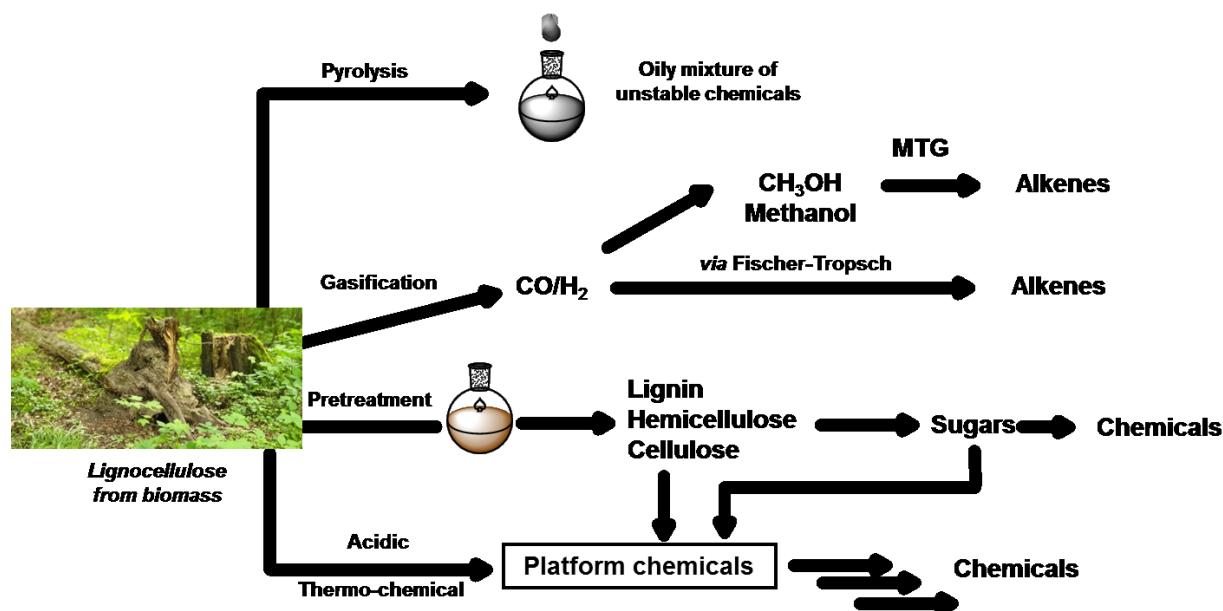
The imminent rapid exhaustion of fossil fuels forces mankind to look for new resources. We are currently strongly dependent on fossil fuels for our energy as well as for the chemicals and materials our daily lives depend on. Biomass, more specifically lignocellulosic biomass, is already becoming an important feedstock for sustainable chemicals and fuels which are essential for a growing bio-based economy.^[1]

Biomass is a well-known carbon source found in nature in the form of plants and wood. It may also be obtained in the form of agricultural residues. It mainly consists of lignocellulose, which itself contains cellulose, hemicellulose and lignin.^[2] The carbohydrates cellulose and hemicellulose are the largest constituents, comprising approximately 70–80wt% of the lignocellulose. For example, wood residues are found to be composed of 45-56% cellulose, 10-25% of hemicellulose and 18-30% of lignin. Lignocellulosic biomass is considered to be one of the major potential renewable feedstocks for chemicals and materials.^[3-4] The conversion of carbohydrates to platform chemicals and other value-added compounds is considered to be an important part of the bio-refinery concept.^[4] Other renewable resources present in lignocellulosic biomass are fats, other lipids, terpenes and proteins. These can be used for further application as for example in the polymer industry.^[5-6]

For the conversion of raw materials to chemicals, there are, however, major differences between the chemical composition of fossil and biomass resources. The high heteroatom content of biomass (mainly oxygen) presents an important barrier towards its use as fuel and chemical raw material.^[7-8] A process called deoxygenation (i.e. reducing the oxygen content), must often be carried out prior to the biomass application in the bio-refinery.^[9] Since this leads to a loss of molecular weight and requires additional chemical steps, the cost of bio-derived materials is often higher than that of their fossil counterpart.

Lignocellulosic biomass can be converted to useful chemicals through different processes (Scheme 1). The pyrolysis of lignocellulose is one of the simplest reaction where an oily mixture of unstable chemicals is formed.^[10] After this, a deoxygenation step is needed for the chemicals produced via pyrolysis to be used as fuels. The gasification reaction forms a mixture of CO and H₂ together with CO₂ and some carbon.^[11] This mixture can be converted into hydrocarbons in different ways. One possibility is to catalytically convert the syngas mixture to methanol which then through the methanol-to-gasoline (MTG) process can be further converted to a mixture of hydrocarbons. Another alternative is to form alkenes using CO/H₂ as the raw material

for the Fischer-Tropsch process. However, relative low selectivity is obtained in both processes. To allow for a hydrolytic depolymerization of polysaccharides to monomeric sugars such as xylose and glucose, pretreatment of lignocellulose is necessary. In this lignin-first process lignin is broken up leading to exposure of the polysaccharides. The sugars thus obtained can be used in fermentation processes to produce different types of chemicals. Although fermentation can produce natural metabolites such as succinic acid or citric acid in excellent yields and titers, this process also suffers from low selectivity towards desired bulk chemicals, such as caprolactam or adipic acid. Nevertheless, new routes have been developed to obtain bulk chemicals from platform chemicals in a more sustainable manner. Besides biocatalysis, homogeneously^[12] and heterogeneously^[13] catalyzed processes can be used for a highly selective conversion of platform chemicals to chemicals in multiple efficient steps.



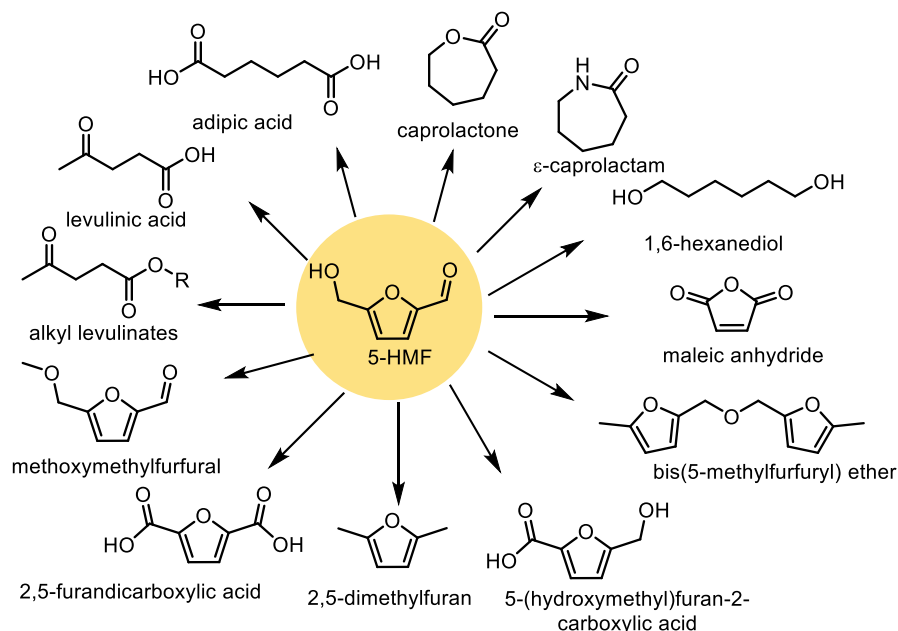
Scheme 1. Synthesis of useful chemicals from biomass-derived lignocellulose.^[14]

Addressing these challenges, researchers have identified several sugar-derived platform chemicals that serve as the feedstock for a diverse selection of commodity and fine chemicals. 5- (Hydroxymethyl)furfural (HMF) and levulinic acid (LA) are typical platform chemicals with great industrial potential.^{[15],[14]}

1.2. Platform chemicals from biomass

Due to the persistent attempts to use biomass as a potential replacement source of fossil fuels derived essential chemicals, it is easy to incorrectly use the term platform chemicals to rename the existing petrochemical building blocks. A platform chemical is

a molecule that is obtained in high selectivity from biomass through an efficient process, with a perspective of low-cost production on large scale, and that can be further converted into a range of several valuable products. An example of a well-known bio-based platform chemical is 5-hydroxymethylfurfural (5-HMF). It can be synthesized from fructose via an acid-catalyzed poly-dehydration.^[16] The Swiss company AVA-Biochem is producing HMF as a side product in their sugar carbonization process. In 2013, starting from sugar cane, their Biochem-1 plant in Muttenz was producing 20 tons of 5-HMF per year. At the end of 2014 the plant was expected to double the annual production of HMF.^[17] 5-HMF can be converted into a wide range of chemicals that can be further used in the production of valuable products, for example bio-based plastics.^[18] The functional, reactive groups present in the molecule are a hydroxyl and a formyl groups as well as the furan ring itself, allowing 5-HMF to be the basis of about 175 downstream chemical substances through reactions such as reduction, oxidation, esterification among others (some examples of 5-HMF derived industrially relevant chemicals are shown in Scheme 2).^[19-20]



Scheme 2. Selected examples of products derived from 5-HMF.

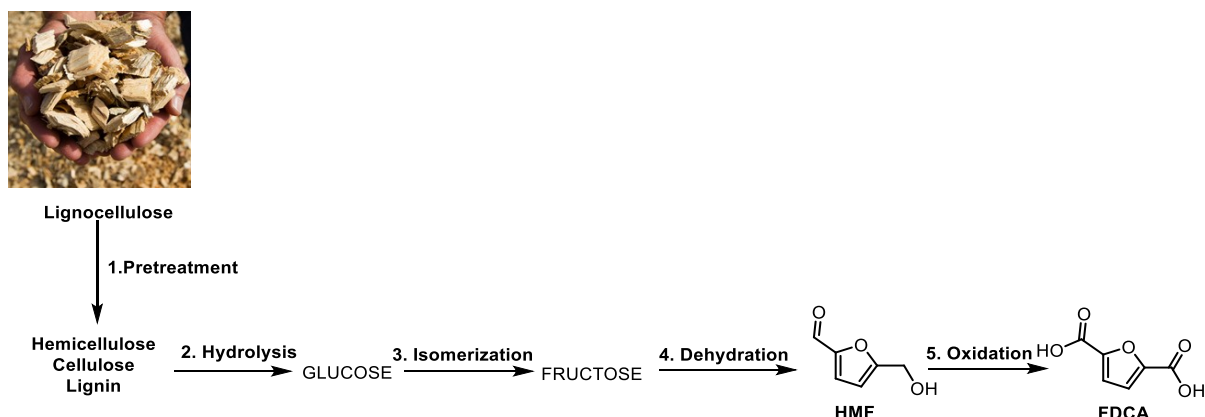
An important derivative which may be employed in the production of bio-based plastic bottles is 2,5-furandicarboxylic acid (FDCA).^[21] The production of this monomer is described later in this thesis.

Another valuable biomass-derived building block that has risen up as one of the top platform chemical is levulinic acid (LA).^[22] For a detailed description see section 1.2.1. Both LA and FDCA are present in the “Top 10 + 4” platform chemical list from the US Department of Energy (DOE) which contains the chemicals that can be obtained by the conversion of carbohydrates in good yields and which show potential to serve as the starting material for a range of functional chemicals.^[23]

1.2.1. The Avantium process to 2,5-furandicarboxylic acid

Among several important bio-derived building blocks, 2,5-furandicarboxylic acid (FDCA) has been a highly explored bio-derived monomer over the past decade. FDCA was rated by the DOE as one of the top 10 + 4 platform chemicals. FDCA is a molecule composed of two carboxylic acid groups attached to a furan ring in positions 2 and 5. In 1876 Rudikoh, Fittig and Heinzelman were the first to report FDCA as dehydromucic acid. It was produced from hydrobromic acid and mucic acid in 48% yield.^[24]

It was then found that FDCA can be produced via the acid-promoted dehydration of carbohydrates such as sugars coming from renewable sources. There are several routes established for the synthesis of FDCA.^[25] It is usually produced from sugars *via* 2,5-disubstituted furans. The oxidation of the latter in the presence of a catalyst delivers almost quantitative yields of FDCA. A stepwise pathway is shown in Scheme 3.^[26-27]^[25]



Scheme 3. FDCA synthesis routes from lignocellulosic biomass.

The production of FDCA from biomass starts first with the pretreatment of lignocellulose, thus improving the accessibility of cellulose and separating it from hemicellulose and lignin. Pretreatment of lignocellulosic biomass has great potential for the improvement of efficiency and lowering the cost of production.^[28] Various pretreatment options have been reported for the fractionation, solubilization, hydrolysis and separation of hemicellulose, cellulose and lignin from biomass,^[29] including: the much-used Kraft process (Na₂S and NaOH at high temperatures), steam explosion, ammonia fiber explosion (AFEX), use of SO₂, alkaline hydrolysis, organosolv processes, and enzymatic approaches.^[30] Some new technologies are also coming up for the production of chemicals and fuels from non-food materials (e.g. agricultural waste, forestry residues etc.) using second generation (2G) feedstocks. DAWN Technology (wood to sugar) developed by Avantium is one such good example.^[31]

Once cellulose is obtained, it is then converted into glucose through a hydrolysis process. This can either be done with a mixture of hydrolytic enzymes or through hydrolysis catalyzed by HCl (The Bergius process)^[32] as well as in the presence of solid

acids.^[33] In attempts to produce fuels and chemicals from glucose, it was found that the isomerized product fructose was the key intermediate being much more reactive and selective towards HMF.^[34] Currently, fructose is produced *via* isomerization of glucose in the presence of immobilized d-xylose ketoisomerase to further be commercialized as high fructose corn syrups (HFSs) employed as sweeteners or used as intermediate for the synthesis of other important chemicals, such as alkyl fructosides, and 5-ethoxymethylfurfural.^{[35],[36-40]}

The interconversion reaction of glucose to fructose was discovered as early as 1895 by Lobry de Bruyn and Alberda van Ekenstein.^[41] Since then, most interest has been focused on the biocatalytic approaches with enzymes and mineral acid/base catalysis. Generally, biocatalysts are utilized in their immobilized, heterogeneous form, as they can be recycled multiple times.^[42] However, because of the increased interest in the application of fructose in areas such as biomass valorization over the past decades, the exploration of chemocatalytic approaches with solid acid catalysts, chromium salts as well as tin containing heterogeneous catalysts has emerged in result.^[43]

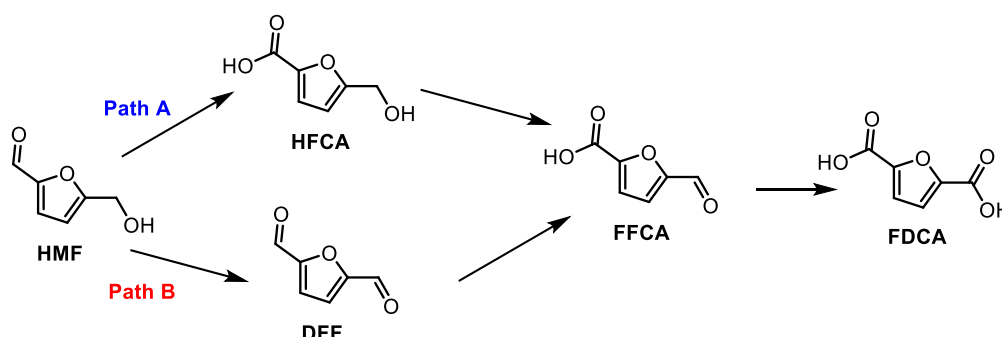
Although initially it was assumed that the enzymatic isomerization proceeds via an enediol mechanism, later work found that a hydride shift mechanism is also possible.^[43]

Lewis acid-catalyzed isomerization follows an intramolecular 1,2-hydride shift from the C2 to C1 position of the open-chain form of glucose by forming a six membered cyclic intermediate or a base-mediated enediol mechanism activated by abstracting a proton at the C2 position of glucose.^[44-46] Tessonnier *et al.* reported the selective isomerization of glucose to fructose via base catalysis, using amines, and found the same performance as the state-of-the-art Lewis acid catalysts with a yield of 32% and a selectivity of 63% for fructose after 20 min at 100°C.^[47-48] Furthermore, Delidovich and Palkovits developed an extraction assisted isomerization strategy involving consecutive chemocatalytic isomerization and fructose separation, which significantly improved the fructose yield, reaching 51% in water when a soluble phosphate buffer is used as catalyst.^[49]

HMF can be produced in higher yields starting from high purity fructose, such as crystalline fructose, HFS or inulin hydrolysate.^[34] Impurities in the raw material result in lower yields of HMF. Promising results with HMF yields and selectivities up to 90% were achieved using organic solvents or biphasic reaction systems.^[19, 50-52] However, to get good yields of HMF a continuous production is required. The dehydration was reported early to proceed in the presence of homogeneous acids in aqueous solutions under continuous extraction with MIBK as described early by the Cope^[53] and Kuster^[54] groups. Using similar systems, Shimanouchi *et al.*^[55] and Lueckgen *et al.*^[56] achieved 88% yield and 93% yield, respectively. The use of DMSO in the presence of ion-exchanged catalysts is reported to give high yields of HMF. In particular, up to 97% yield of HMF was obtained by the groups of Gaset *et al.*,^[57] Jeong *et al.*^[58] and Schön *et al.*^[59] using a continuous micro reactor for the catalytic dehydration of fructose in DMSO. All these authors claim HMF yields above 90%.

The main disadvantage shared by all the approaches mentioned above consists in the use of solvents with high boiling points such as DMSO resulting in difficult separation of the thermally unstable HMF.

FDCA can be obtained from HMF through an oxidation reaction. The catalytic oxidation of HMF to FDCA follows different routes depending on the catalysts used (Scheme 4).^[25] The highly reactive aldehyde group is oxidized first and HFCA is obtained (Scheme 4, pathway A). Then the primary alcohol is oxidized to the corresponding aldehyde delivering 5-formyl-2-furancarboxylic acid (FFCA). FFCA can also be obtained when the alcohol group of HMF is first converted to the aldehyde (DFF) and then oxidized to the carboxylic acid (Scheme 4, pathway B). Through both routes the FFCA precursor is formed which then is further oxidized to the dicarboxylic acid FDCA.^[25]

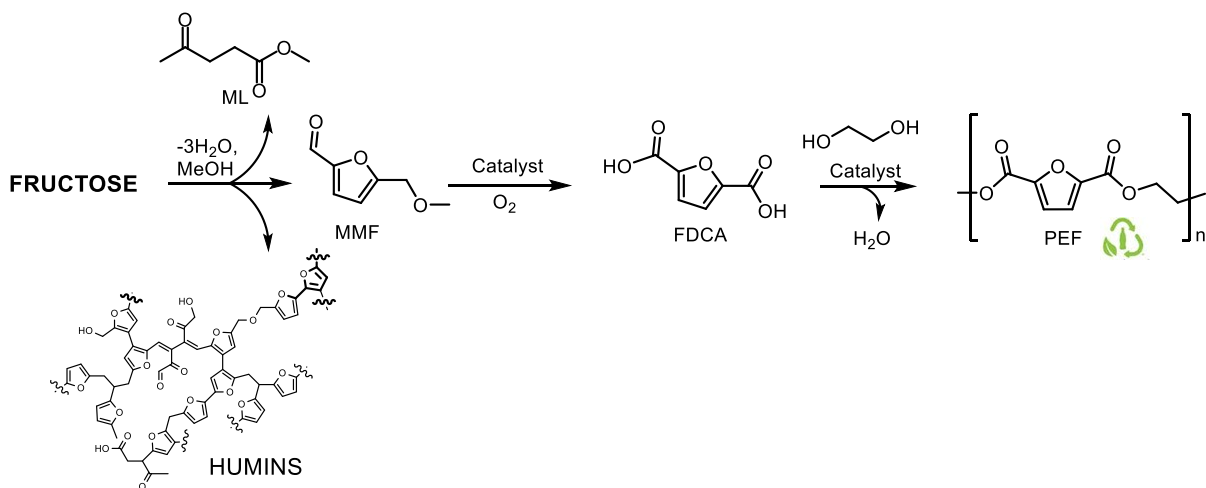


Scheme 4. 5-HMF reaction pathways towards FDCA.^[25]

In early studies, the oxidation of HMF to FDCA was performed either by using stoichiometric amounts of oxidants, such as oxygen with highly polluting catalysts (e.g., Pb) in basic conditions, or similar to the current production method of terephthalic acid, using oxygen with homogeneous metal salts as catalysts (e.g., Co/Mn/Br) in acidic solvents (i.e., acetic acid).^[26, 60] More recently, supported noble metal catalysts (mainly Pt, Au, Pd and Ru) supported on metal oxides or activated carbon were developed for HMF oxidation.^[25] Despite the high activity of the supported noble metals, these systems also require a homogeneous base, which leads to the production of salts as side-product and is therefore not desired at industrial scale. To overcome this problem, Gupta *et al.*^[61-63] developed a hydrotalcite-supported gold nanoparticle catalyst for aerobic oxidation of HMF. The yield of FDCA was close to 100% at 368 K for 7 h. However, leaching of the solid base, hydrotalcite into aqueous solution remained a problem. Wang *et al.*^[64] also demonstrated the base-free oxidation of HMF into FDCA to be possible when carbon nanotube supported Au-Pd alloy catalyst is used in water. This was attributed to the carbon nanotube-enhanced adsorption effect and the metal alloying effect. In 2013, Wang and co-workers reported the base-free aerobic oxidation of HMF to FDCA over Pt/C-O-Mg (Platinum on coated carbon with MgO). The yield of isolated FDCA reached 74.9% with very high purity (99.5%).^[65]

However, the preparation of FDCA from HMF still presents some drawbacks due to the low stability of the starting material. In the vast majority of the 5-HMF preparation procedures it is reported that starting from lignocellulose derivatives, 5-HMF was isolated as an oil of up to 98% purity. The HMF isolation as a pure solid was described by Konstantin *et al.* who obtained HMF in 99.9% purity. In addition, they performed a study on the stability of HMF. They observed a degradation of 5-HMF over 2 weeks into a polymeric black material composed of oligomers of HMF during the isolation process. This decomposition can be attributed to the highly reactive hydroxymethyl ($-\text{CH}_2\text{OH}$) and formyl ($-\text{CHO}$) groups present in HMF, which make the molecule sensitive to undesired side-reactions, such as condensation and polymerization. Therefore, chemical transformations in concentrated HMF solutions are always accompanied by the formation of a polymeric byproduct called humins.

An alternative would be to prepare FDCA starting from the ether analog of HMF, i.e. 5-methoxymethyl furfural (MMF), which is significantly more stable than the former compound. This method, developed by Avantium via their YXY Technology, allows preparing MMF in good yields by dehydration of fructose in methanol. This mixture is oxidized and further esterified to dimethyl FDCA. Avantium uses the latter ester for the preparation of the polyester polyethylene-2,5-furanoate (PEF) (Scheme 5), which could serve as a bio-based alternative for the well-known and widely used polyethylene terephthalate (PET).^[66-69] The PET bottle market alone amounts up to ca. 15 Mt per year, being approximately 5.9% of the total global plastics production and consuming ca. 0.2% of the global energy supply.^[70] Commercialization of PEF applications is carried out by Avantium in collaboration with third parties that are interested to bring applications to the market.^[71]



Scheme 5. PEF synthesis route from fructose.^[72]

Although the synthesis of FDCA monomer from MMF results in lower formation of humins, there are other side products such as ML coming from the YXY technology (Scheme 5).^[72] Nevertheless, the production of ML as side product in this process may

create new opportunities, two of which will be described in detail in the following sections.

1.2.2. Synthesis and applications of levulinic acid esters

As already mentioned, levulinic acid (LA) is a high-potential platform chemical (Figure 1) that can be obtained from lignocellulosic biomass by treatment with dilute acids at high temperatures.^[73] Also known as 4-oxopentanoic acid or gamma ketovaleric acid, LA is a short chain acid with molecular formula $C_5H_8O_3$.^[73] The presence of two carbonyl groups, a ketone function ($C=O$) and an acidic carboxyl group ($COOH$) impart the ability to react with many different reagents to form a wide range of products.

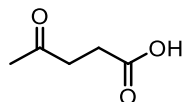


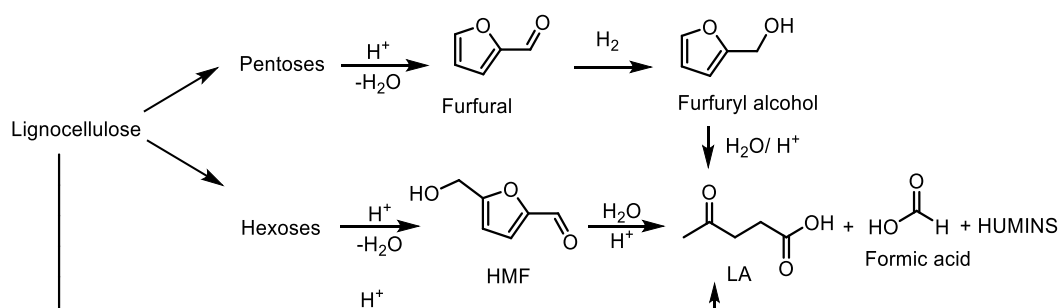
Figure 1. Levulinic acid (LA).

Already in 1840, the formation of LA was observed by Mulder during the heating of a mixture of sucrose with mineral acids.^[74] 100 years later it was found that cellulose can be used for the production of LA.^[75] Recently, the company Biofine developed a two-stage process for the production of levulinic acid from biomass.^[74] Although the company ran two pilot plants over the course of several years this process has never reached commercial stage. A demonstration size plant was built in Caserta, Italy, but this plant never produced a single gram of levulinic acid because of flaws in the process.^[76] In addition, the chosen raw material, waste tobacco leaves, had rather high calcium content, leading to calcium sulfate formation with sulfuric acid, the catalyst used in the process.^[76] In the meantime, a new process was developed by the company GFBiochemicals, which is expected to reach commercial stage in the near future.^[77]

There is an inherent problem in the commercialization of these new processes. Since there is not yet a well-developed market for products that can be produced from LA the initial market demand is rather small, justifying only a relatively small-scale LA plant. This leads to an LA price that is much higher than it would have been if the plant size was 100 000 Ton/year, a usual size for a bulk chemical plant (Economy of Scale). In turn, this high price hinders the development of further follow-on products. This phenomenon is called the Valley of Death. This vicious circle can only be broken if a company decides to invest in a large-scale plant in spite of the fact that it may not be profitable for many years to come.

Examples of how LA can be produced from renewable feedstocks are presented in Table 1. Rice husk, sugars, 5-HMF (derived from glucose) or furfuryl alcohol can all be used to synthesize LA. Typically, an affordable acid catalyst is sufficient to catalyze

these transformations, giving over 90% yields of the desired product in some cases (Scheme 6 and Table 1).



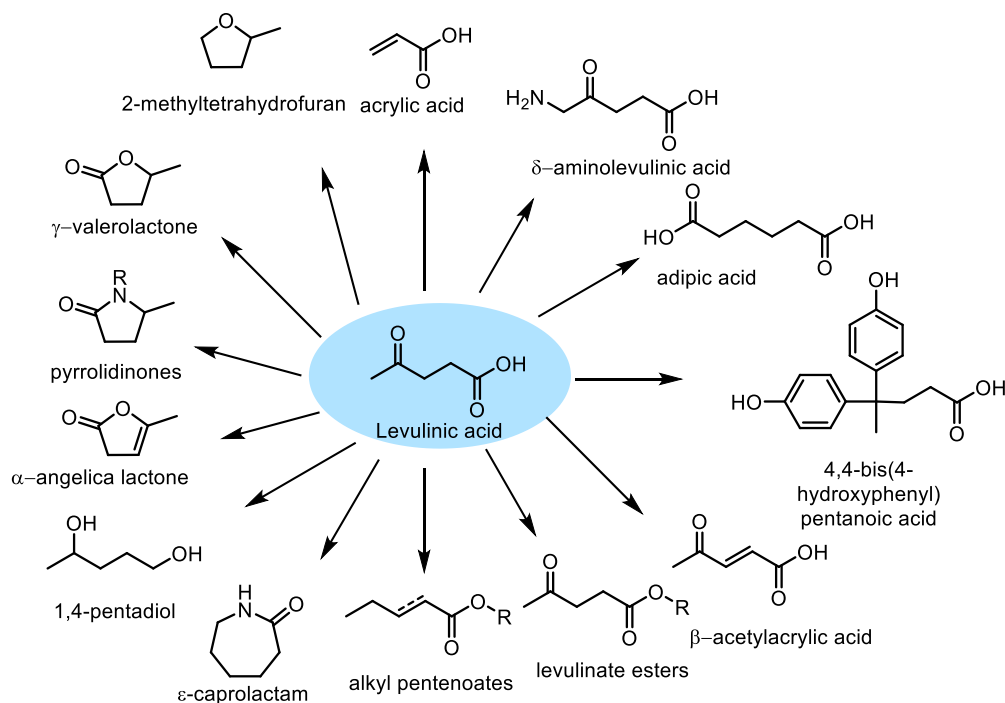
Scheme 6. Synthesis of LA from lignocellulose.

Table 1. Selected examples of sources used for the LA production.

Starting material	Conditions	Catalyst ^a	LA yield	References
Rice husk	60 °C, 56 bar and 70 min	4.5% (v/v) HCl	55%	[78]
Cellulose	150 °C, 2 h	1 M aq. H ₂ SO ₄	54 mol%	[79]
Fructose	140 °C, 8 h	6.7% Amberlyst 15	56 mol%	[80]
Fructose	Flow, 100 – 120 °C, 3h	H ₂ SO ₄ (96-98%)	94	[81]
Glucose	155 °C, 5 h	IL-SO ₃ H-NiSO ₄	56	[82]
5-HMF	170 °C, 5h	IL - [C ₃ SO ₃ Hmim]HSO ₄ + H ₂ O	93	[83]
5-HMF	98 °C, 180 min	1 M aq. H ₂ SO ₄	94 mol%	[84]
Furfuryl alcohol	120 °C, 2h	3 wt% ArSO ₃ H-Et-HNS	83	[85]

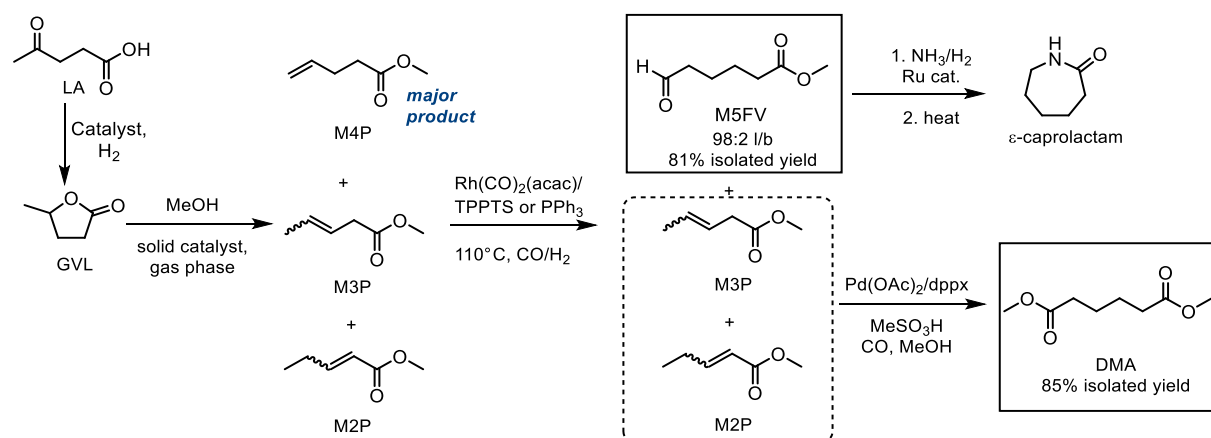
^a IL-SO₃H-NiSO₄: sulfonic acid functionalized ionic liquid with nickel sulfate. IL-[C₃SO₃Hmim]HSO₄: 1-methyl-3-(3-sulfopropyl)-imidazolium hydrogen sulfate, ArSO₃H-Et-HNS: arenesulfonic acid functionalized ethyl-bridged organosilica hollow nanospheres

Numerous compounds can be prepared from LA, the most relevant among those are presented in Scheme 7.



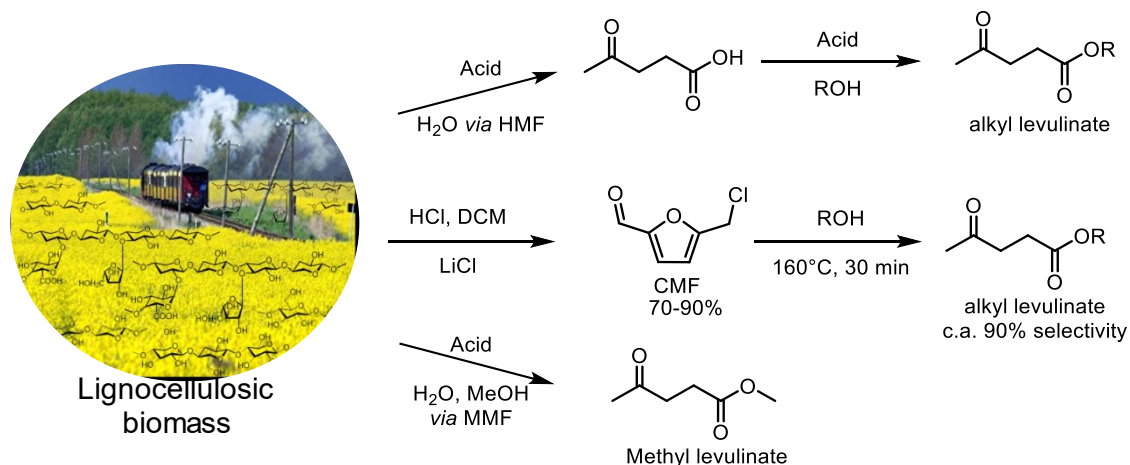
Scheme 7. Selected compounds that can be synthesized from levulinic acid.

Alkyl pentenoates can be prepared in two steps from LA: first, LA is hydrogenated to γ -valerolactone (GVL)^[86-89] and then GVL is converted to a mixture of methyl 2-, 3- and 4-pentenoates in the gas phase in the presence of MeOH and acidic or basic catalyst.^[90-95] These methyl pentenoates can be further converted into nylon precursors such as adipic acid (ref to chemical record paper) and Caprolactam. The most recent example of the conversion of GVL to methyl pentenoates, and the subsequent catalytic preparation of nylon precursors was published recently in our group by Marckwordt *et al.* The conversion of GVL to a mixture of methyl pentenoates in 95% selectivity using a zirconium oxide catalyst was achieved. Remarkably, in contrast to the previous work with acidic catalysts, we were able to produce a mixture consisting of 81% of methyl 4-pentenoate (M4P) along with methyl 3-pentenoate (M3P) and methyl 2-pentenoate (M2P) making up the remainder. This mixture was subjected to a selective hydroformylation of the terminal alkene M4P using Rh/TPPTS (TPPTS=tris-sulfonated triphenylphosphine) as catalyst, leaving the internal pentenoates almost intact. The resulting methyl 5-formylvalerate, which was obtained in 81% yield (L/B ratio = 97:3) can be converted to caprolactam by reductive amination and ring-closure in good yield. The remaining M3P and M2P isomers were then converted to dimethyl adipate (DMA) through an isomerising methoxycarbonylation in 85% yield (Scheme 8).^{[14],[96]}



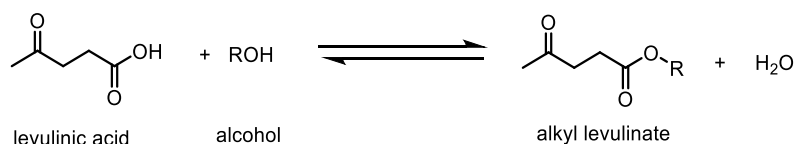
Scheme 8. Catalytic preparation of nylon monomer precursors from Levulinic acid

Other important LA derivatives are alkyl levulinates. There are three ways to prepare levulinate esters from biomass in high selectivity; (I) the esterification of LA^[97-98], (II) the alcoholysis of 5-(chloromethyl)furfural (CMF)^[99] and (III) the direct alcoholysis of biomass (Scheme 9).^[100-102] In industry, the production of levulinate esters has been mainly achieved directly from the acid catalyzed esterification of LA with alcohols. Because of the higher stability of CMF compared to HMF, the formation of alkyl levulinates from its alcoholysis leads to selectivities of about 90%.^[97]



Scheme 9. Possible ways for the conversion of biomass to alkyl levulinates.

The reaction of LA with primary alcohols in solution occurs in the presence of an acidic catalyst (Scheme 10). Ester formation is an equilibrium reaction and, therefore, requires constant removal of water from the reaction mixture.



Scheme 10. Synthesis of alkyl levulinates from levulinic acid.

The esterification of LA to methyl levulinate (ML) and ethyl levulinate (EL) in the presence of sulfuric acid, solid-phase acid catalysts or enzymes, has been reported elsewhere.^[103-104]

Of the alkyl levulinates, EL is the most used one because of its extensive applications in medicines, as solvent, in organic chemistry, in the fragrance industry etc. Furthermore, it can be directly used as an additive for gasoline and diesel.^[105] On the other hand, ML could also be another interesting alkyl levulinate. Although quite a number of excellent synthetic procedures for the synthesis of ML have been found (Table 2), so far, to the best of our knowledge, only very limited applications of ML exist at the moment (such as its use as a solvent or as a food additive).^[106]

Table 2. Some selected examples of homogeneous and heterogeneous catalysts employed in methyl levulinate production.

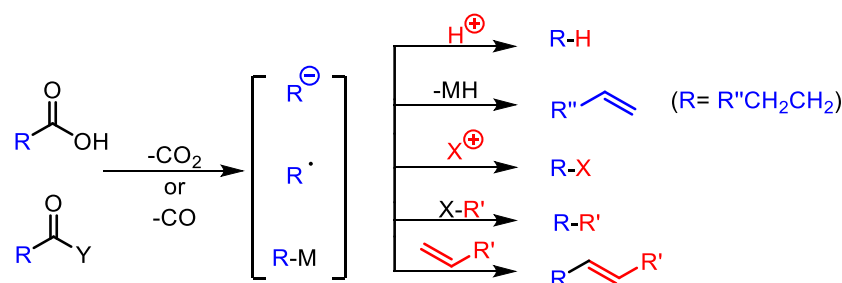
Starting material	Conditions	Catalyst ^a	ML yield%	References
Cellulose	Microwave, 180 °C, MeOH, 40 min.	1.2 mmol Al ₂ (SO ₃) ₄	71	[107]
Fructose	MeOH, 130 °C, 2MPa, 2h	0.48g Fe-HPW-1	73	[108]
Cellulose	180 °C, MeOH, 5h	In(OTf) ₃ + 2-NSA (0.02 mmol LA, 0.20 mmol BA)	75	[109]
Levulinic acid	65 °C, 5h, 1:20 MeOH:LA	30% Amberlyst- 15	82	[110]
Furfuryl alcohol	MeOH; 130; 2 h	(0.6 mol%) [BMIM -SH][H ₂ SO ₄]	94	[111],[112]

^a HPW-1: Phosphotungstic acid, 2-NSA: 2-naphthalenesulfonic acid, [BMIM -SH][H₂SO₄]: mixture of 1-methyl-3-(4-sulfobutyl)-1H-imidazol-3-ium ionic liquid and sulfuric acid.

1.3. Deoxygenation of biomass-derived feedstocks to chemicals via decarbonylation and decarboxylation

The production of renewable materials from biomass still presents a variety of drawbacks because of the presence of functional groups in biomass compared to fossil fuels. In many cases prior defunctionalization is needed. More concretely, due to the high oxygen content in the constituent C₆ and C₅ sugars that form the building blocks of cellulose and hemicellulose, at least some deoxygenation is generally required. Catalytic deoxygenation can be performed in various ways. The deoxygenation process entails the removal of oxygen, for example by elimination of water, carbon monoxide, or carbon dioxide. For instance, the hydrodeoxygenation reaction,^[113] dehydration, decarbonylation or decarboxylation are examples of deoxygenation reactions that are already being applied in biomass conversion.^[114]

In this thesis, the decarboxylation and decarbonylation reactions are described, which are well-known and very important transformations in synthetic organic chemistry. The loss of carbon dioxide (CO₂) or carbon monoxide (CO) from a carboxylic acid (R-COOH) or its derivatives (R-COY) formally generates a reactive intermediate (e.g. a carbocation, carbanion, radical, or organometallic species) of the R fragment, which can undergo subsequent transformations, including protonation, elimination, electrophilic halogenation, cross-coupling, and Heck-type reactions (Scheme 11). There are several classes of catalysts such as heterogeneous, homogeneous, bio- and organocatalysts that can be effectively used for these types of transformations.

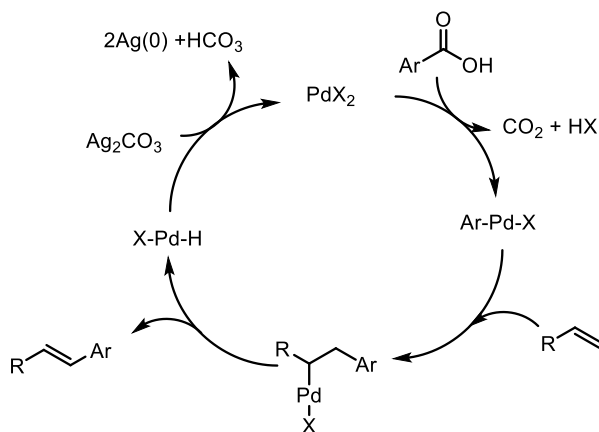


Scheme 11. Decarboxylation/decarbonylation reactions followed by other transformations.^[115]

1.3.1. Decarboxylation and decarbonylation of carboxylic acids.

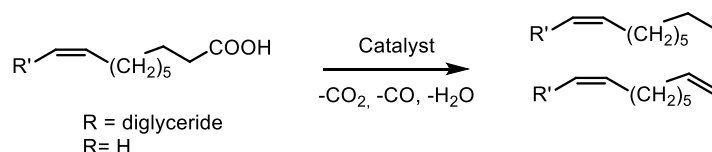
Decarboxylation is a widely investigated organic reaction, since it often takes place during pyrolysis, and the volatile products are distilled directly from the reactor. High temperatures are often required in this process due to the high activation energy barriers. The thermal decarboxylation can proceed *via* a unimolecular mechanism (S_E1) or a bimolecular mechanism (S_E2).^[116]

The ability of transition metals to promote the decarboxylation was first observed in 1930, when Shepard and co-workers found that furan-2-carboxylic acid derivatives were more prone to undergo protodecarboxylation in the presence of a copper catalyst rather than simple heating under catalyst-free conditions.^[117] An important example of such a catalytic conversion is the palladium-catalyzed decarboxylative and decarbonylative cross-couplings reactions of activated carboxylic acids to form new C-C and C-heteroatom bonds. In 2005 Meyers *et al.* described the mechanism of decarboxylative cross-coupling reaction (Scheme 12).



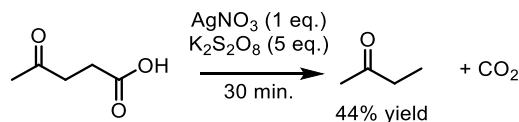
Scheme 12. Pd-catalyzed decarboxylative cross-coupling mechanism.^[118-119]

There are many examples of decarboxylation of bio-based carboxylic acids with heterogeneous catalysts. Fatty acids, found mainly as constituent of fats, can be converted to olefins *via* decarboxylation in the presence of heavy metals.^[120] In particular, using catalytic quantities of silver and copper salts, it was shown that several saturated (stearic and palmitic acid) and unsaturated (oleic, ricinoleic, elaidic, linoleic, linolenic) fatty acids are able to undergo oxidative decarboxylation to form alkenes (Scheme 13).^[121]



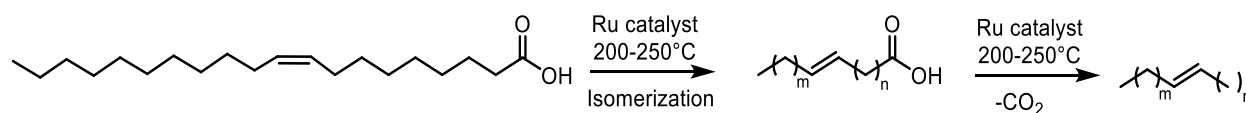
Scheme 13. Decarboxylation of (unsaturated) vegetable oils or fatty acids.^[121]

The same strategy has been applied in the oxidative decarboxylation of amino acids. Bio-derived glutamic acid was first dehydrated to pyroglutamic acid which could be oxidatively decarboxylated in aqueous solution at room temperature to succinimide in 96% yield.^[122] Levulinic acid can also decarboxylate to form the ketone which was already reported in 1983 by Chum *et al.* using undoped platinized n-titanium dioxide powders through a photoelectrochemical process.^[123] LA was transformed to methyl ethyl ketone (MEK), propionic acid, acetic acid, acetone and acetaldehyde as major products. Nevertheless, the butanone yield was not satisfactory (~ 1%). More recently, Gong *et al.* reported that use of cupric oxides in this reaction, which was performed in a buffer solution with pH of 3.2 as the solvent afforded up to 67.5% yield of butanone.^[124] Later on, the same authors described the oxidative decarboxylation of LA to afford 44.2% yield of butanone in the gas phase, using silver (I) salts under milder conditions (Scheme 14).^[125]



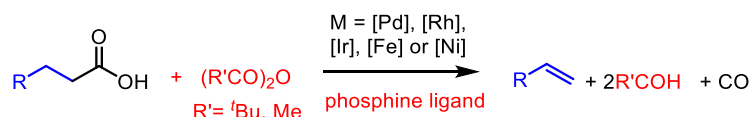
Scheme 14. Levulinic acid decarboxylation to MEK.^[125]

While this approach shows promising MEK yields, the stoichiometric amounts of silver and 5 eq. of potassium peroxodisulfate ($\text{K}_2\text{S}_2\text{O}_8$) required makes its implementation on an industrial scale unfeasible. To overcome this issue, a ruthenium-based catalytic system has been used for the tandem isomerization-decarboxylation of unsaturated fatty acids into alkenes by the group of Murray.^[126] Temperatures between 200-250°C were used for the conversion of long chain unsaturated carboxylic acid such as oleic acid to the corresponding unsaturated hydrocarbon using triruthenium dodecacarbonyl and prepared $[\text{Ru}(\text{CO})(\text{RCO}_2)]_n$ complex as *in situ* pre-catalysts (Scheme 15). The proximity of the double bond to the carbonyl group is essential for the decarboxylation to occur. Only the isomers with the double bond in the 2-, 3- or 4-position could be decarboxylated.



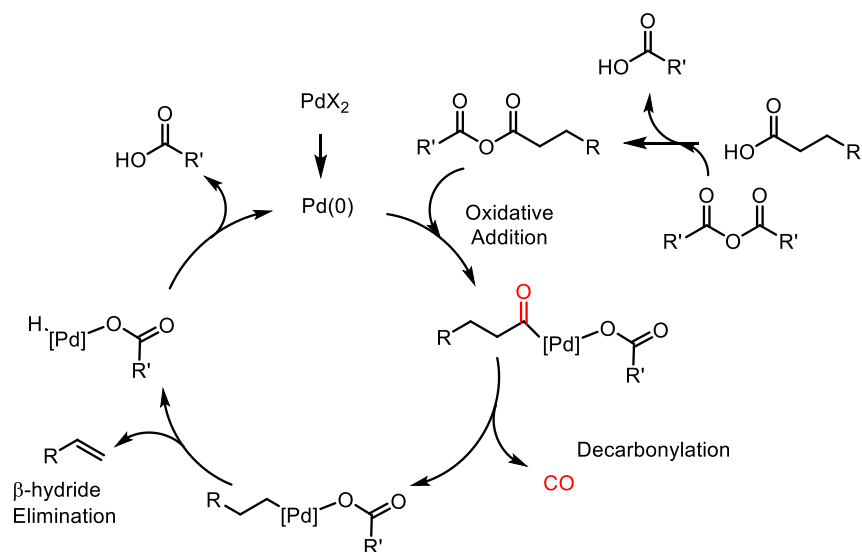
Scheme 15. Ru-catalyzed tandem isomerization-decarboxylation of oleic acid.^[126]

Carboxylic acids can also undergo decarbonylation reactions in the presence of a catalyst. The opposite reaction, known as carbonylation (usually hydroxycarbonylation or alkoxy carbonylation) is widely used on industrial scale.^[127] When it comes to decarbonylation of aldehydes such as furfural, palladium-based catalysts show high activity. However, when the same strategy is applied on the carboxylic acids with the aim to make olefins, the decarbonylation requires either high temperature or high catalyst loading. Therefore, the decarbonylation of, for example, aliphatic fatty acids under mild conditions and low catalyst loadings only takes place after converting the acid to the anhydride. Metals such as Pd, Rh, Ir and more recently base metals like Ni and Fe are able to catalyze such conversions (Scheme 16).



Scheme 16. Metal-catalyzed decarbonylation of acids.^[127]

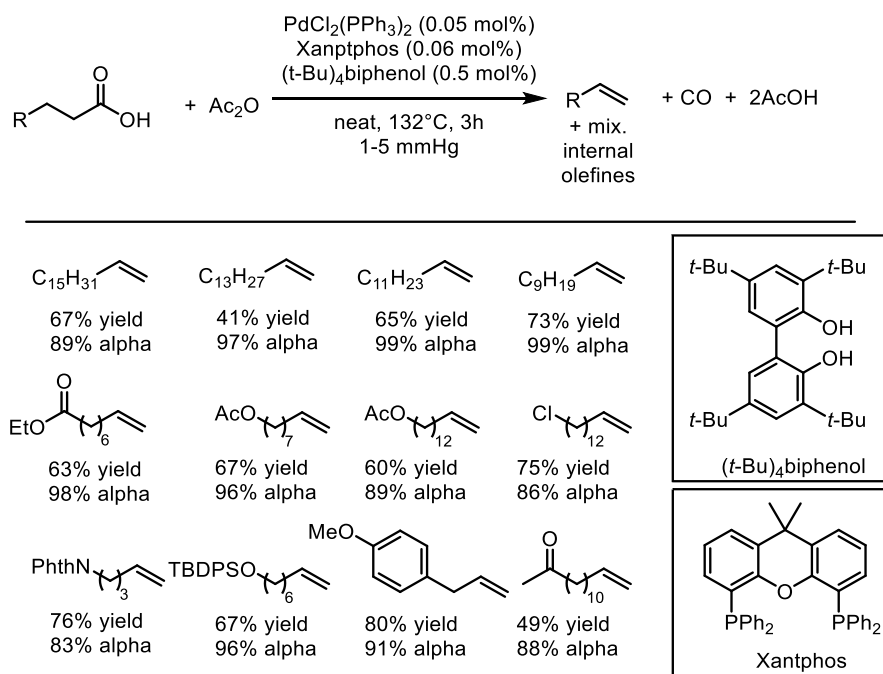
The report by Miller and co-workers described the preparation of terminal alkenes from long chain fatty acids under neat conditions at 250 °C in the presence of one equivalent of acetic anhydride. The reaction proceeds through decarbonylation of the *in situ* prepared anhydride derivative in the presence of 0.01 mol% of a Pd- or Rh-based catalyst and 0.5 mol% of triphenylphosphine.^[128] In 2004 Gooßen *et al.* reported the decarbonylation of fatty acids *via* anhydride formation in the presence of PdCl₂–DPEPhos (Dichlorobis(diphenylphosphinophenyl)ether palladium (II)), as catalyst (Scheme 17).^[129]



Scheme 17. Mechanism of the Pd-catalyzed decarbonylation of acids via anhydride formation.^[129]

The catalytic reaction mechanism starts with the anhydride (generated in situ) undergoing an oxidative addition onto a Pd(0) species to yield an acyl complex. Then decarbonylation takes place releasing one equivalent of CO. Subsequent β -hydride elimination affords the corresponding olefin along with an equivalent of R'OOH (Scheme 14). It was found that the use of other phosphorus-based ligands leads to rapid isomerization and loss of the selectivity towards terminal alkene. The best ligand was DPEPhos which improved the activity and selectivity in the transformation of phenylbutanoic acid.

Maetani *et al.* also showed that the same catalytic decarbonylation reaction can be performed in the presence of an iron(II) chloride catalyst using DPPent as ligand.^[130] Using the same strategy, the group of Stoltz^[131] published in 2014 the palladium-catalyzed decarbonylative dehydration of fatty acids to olefins of different lengths and bearing distinct functional groups (Scheme 18). During the optimization of the reaction conditions they found that the (t-Bu)₄biphenol was the best protic additive as it was observed that addition of acid improved the product yield.



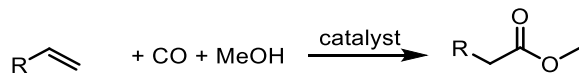
Scheme 18. Pd-catalyzed decarbonylative dehydration of fatty acids for the synthesis of linear alpha olefins.^[131]

In 2016, Cramer and co-workers described the mechanism of the Pd-catalyzed decarbonylation of biomass-derived activated anhydrides from hydrocinnamic acid to styrene.^[132]

The above described reactions show the potential of the decarbonylation reaction in the conversion of bio-based carboxylic acids to produce highly valuable olefins for further applications.

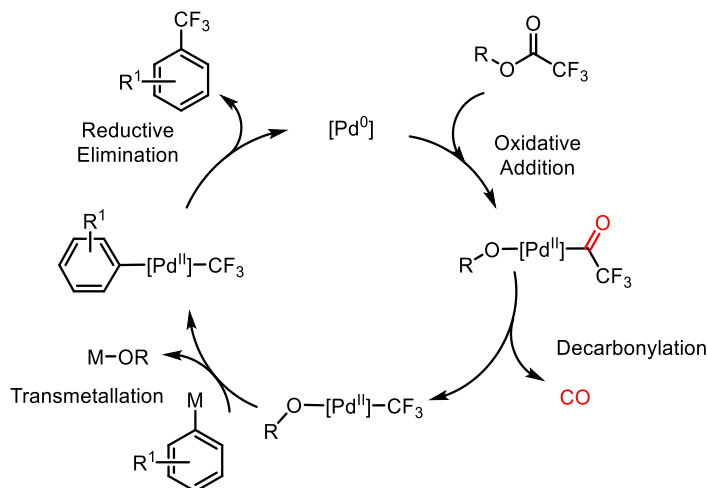
1.3.2. Decarbonylation and dealkoxycarbonylation of esters

The metal-catalyzed alkoxy carbonylation reaction is well known and has been reviewed extensively.^[133] For this conversion, the best catalysts have been shown to be palladium-phosphine,^[134] cobalt^[135] or ruthenium^[136] carbonyl complexes (an example of methoxycarbonylation reaction is shown in Scheme 19). The methoxycarbonylation of ethylene to methyl propionate has been commercialized by Lucite as part of their methyl methacrylate process.^[137]



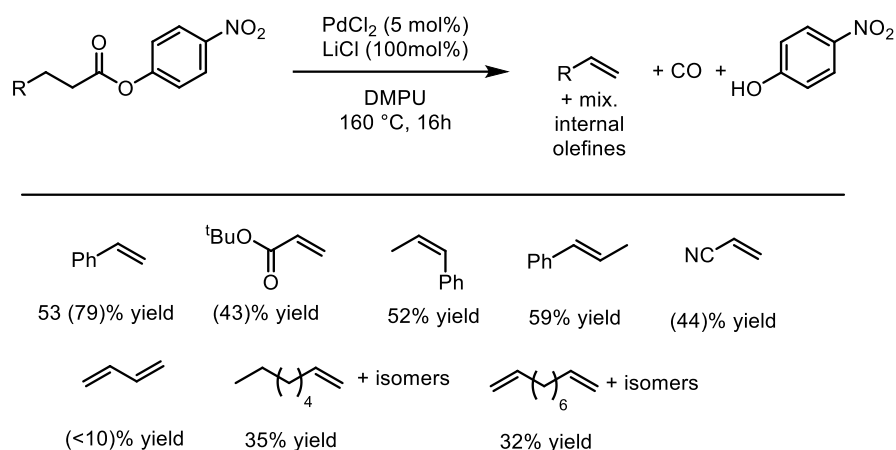
Scheme 19. General methoxycarbonylation reaction.

Conversely, paraffins and olefins can be formed by the decarboxylation or decarbonylation of activated carboxylic acids (and esters), respectively.^[127] The decarbonylation of methyl esters to form alkenes and alcohols, or dealkoxycarbonylation, remains a challenging reaction. As a consequence of the high acyl bond energy, the activation *via* introduction of electron-withdrawing substituent to the acyl C=O moiety prior to the decarbonylation is often required.^{[138],[139-141]} That is the reason for a limited number of reports which describe the decarbonylation of esters. Sanford *et al.* reported the metal-catalyzed decarbonylative trifluoromethylation using trifluoroacetic acid esters. The trifluoroacetic acid ester undergoes oxidative addition to the metal center followed by the loss of a CO molecule (decarbonylation). The last two steps of the catalytic cycle, transmetalation and reductive elimination, deliver the aryl-CF₃ compound (Scheme 20).^{[142],[143]} Later work by these authors describes the mechanism of the decarbonylation of trifluoroacetic acid esters by the preparation and characterization of a series of fluoroalkyl palladium(II) and nickel(II) complexes *via* decarbonylation of the corresponding acyl metal species.



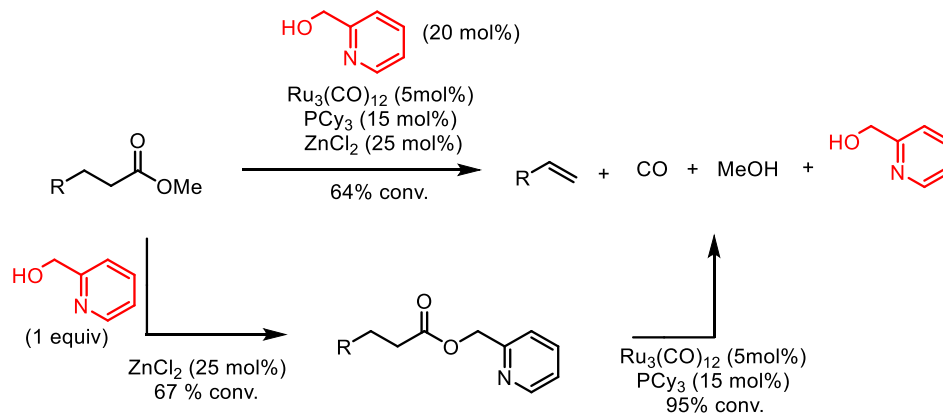
Scheme 20. Palladium-catalyzed decarbonylative trifluoromethylation using trifluoroacetic acid esters.

Tolman and co-workers described the decarbonylation of *p*-nitrophenyl esters using PdCl₂ in the presence of alkali/alkaline-earth metal halides (Scheme 21).^[144] Later on, they reported the selective decarbonylation of *p*-nitrophenol esters from fatty acids to form linear α -olefins achieving high ester conversions (>98% selectivity, >90% conversion) at 190 °C.^[145]



Scheme 21. Tolman's Pd-catalyzed decarbonylation of *p*-nitrophenyl esters to olefins.

In 2018, the same authors reported the homogeneous ruthenium catalyzed dehydrative decarbonylation of fatty acid methyl esters (FAME) in order to form olefins. Their strategy relies on an initial catalytic transesterification that converts FAME to alkyl esters that contain an appended directing group, namely a pyridyl moiety (Scheme 22).^[146]



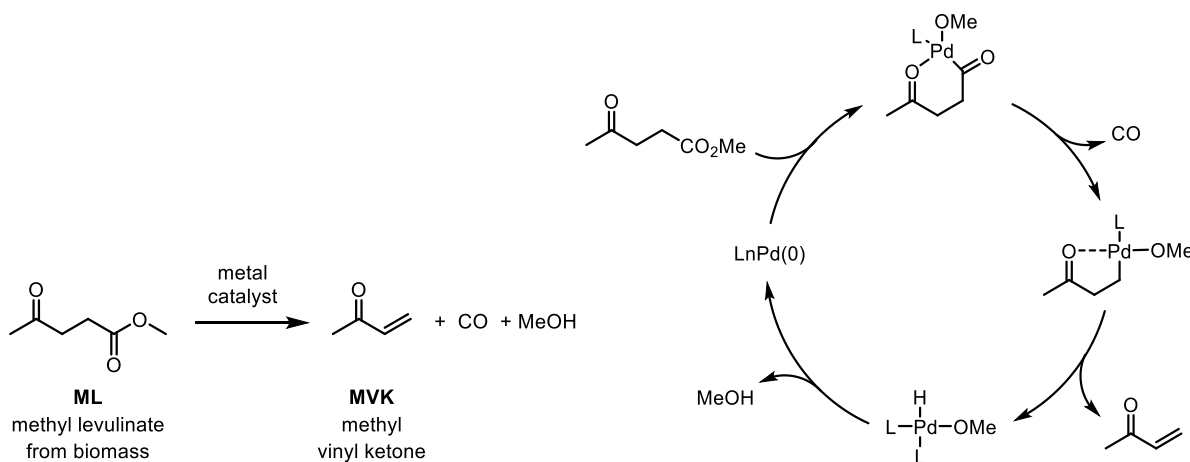
Scheme 22. Tolman Ru-catalyzed dehydrative decarbonylation of fatty acid methyl esters.

In conclusion, both Sanford's and Tolman's studies give us insights on the need of the prior methyl ester activation.

1.4. Goal of the research described in this thesis

1.4.1. Methyl vinyl ketone

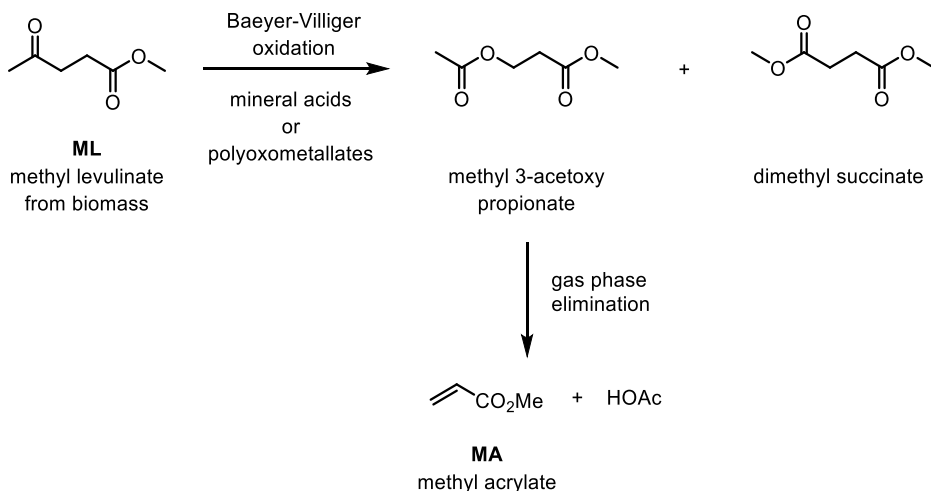
As a result of the interest in converting biomass into platform chemicals, an example would be the conversion of an attractive side stream of Avantium's YXY Technology, i.e. ML into commercially relevant olefins such as methyl vinyl ketone, a building block for vitamins and methyl acrylate. ML can be produced through esterification of LA; the latter can, in turn, be produced by treating lignocellulose with dilute acids at high temperatures. Although potential applications of LA have been found, so far limited applications have been found in the case of ML. This study shows the conversion of ML into two important existing chemicals (drop-ins). The first of these, MVK is an important intermediate for the production of Vitamin A and E. It has a quite elevated market price and is currently prepared starting from fossil-derived acetone via its condensation with formaldehyde.^[147] The proposed route towards this compound is shown in Scheme 23.



Scheme 23. Demethoxycarbonylation of ML to MVK.

1.4.2. Methyl acrylate

The second aim of the project was to obtain methyl acrylate (MA) from methyl levulinate in two steps: the conversion of ML to methyl 3-acetoxy propionate by Baeyer-Villiger oxidation and subsequent gas phase elimination of acetic acid (Scheme 24).

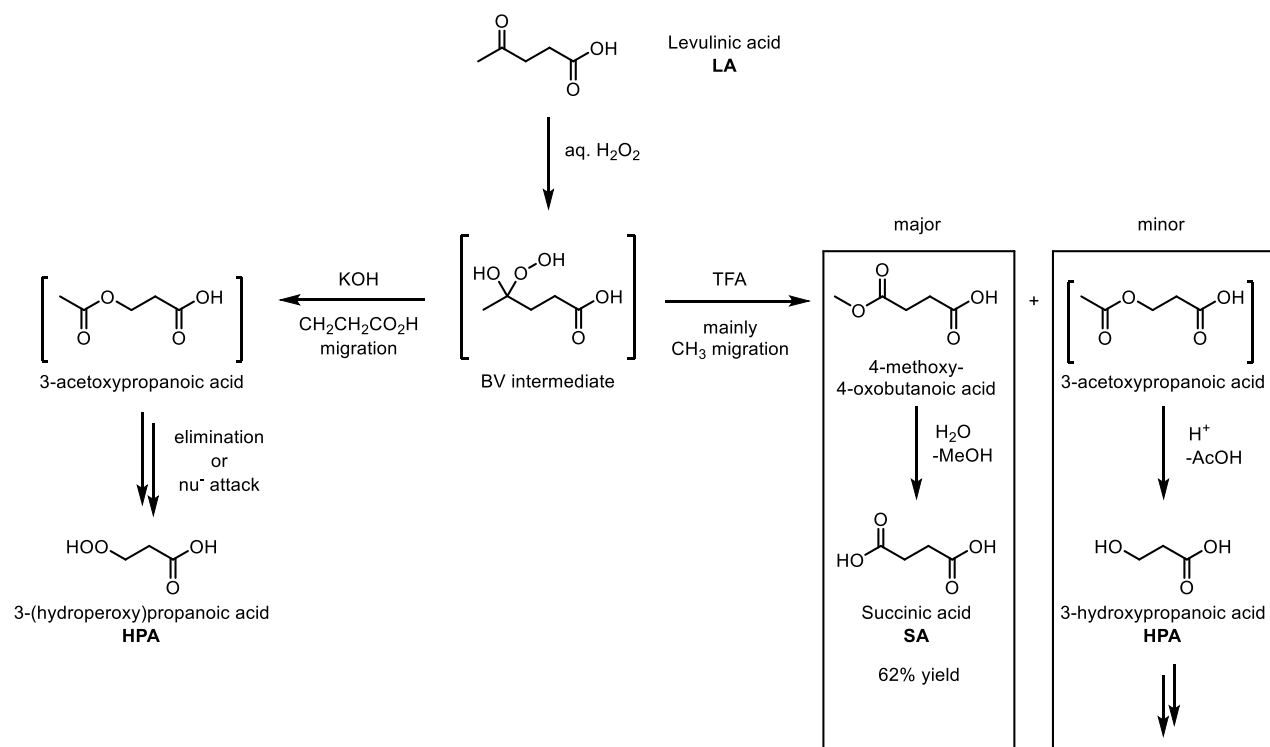


Scheme 24. Baeyer-Villiger oxidation of ML followed by elimination to MA.

The Baeyer-Villiger oxidation was already discovered in 1899.^[148] Hence, it is a well described and understood reaction.^[149-150] Peracids (e.g. meta-chloroperoxybenzoic acid, *m*-CPBA) can be employed as oxidants in the Baeyer-Villiger conversion. Solid supported peracids were also developed for this transformation. Alkyl peroxides and hydrogen peroxide require the presence of either an organic acid or a catalyst to promote the oxidation. For the latter case, methyltrioxorhenium (MTO) or platinum complexes were reported.^[151-153] Other catalytic systems utilize oxygen as an oxidizing agent in the presence of a sacrificial aldehyde, and complexes based on nickel, iron, ruthenium, as well as manganese oxides or heteropolyoxometallates. Sn-MCM-41 is an efficient heterogeneous catalyst in this respect. Another option to perform this reaction is the activation of the carbonyl group for the oxidation by Lewis acids.^[151-153]

These selected examples represent a plethora of possibilities to approach the Baeyer-Villiger oxidation of methyl levulinate. In 1975, the oxidation of the benzyl ester of LA has been reported using a 4.4 fold excess of pertrifluoroacetic acid delivering the corresponding acetate with a maximum yield of 65%.^[154] Mascal and co-workers focused on the metal free Baeyer-Villiger oxidation of LA. They found trifluoroacetic acid (TFA) to be more efficient acid catalyst for the oxidation of LA to succinic acid (SA). Next to 4-methoxy-4-oxobutanoic acid, minor amounts of 3-acetoxypyranoic acid were observed. Moreover, they also showed that TFA can be fully recycled. SA could be isolated through distillation of TFA and byproducts, and 62% isolated yield was obtained at 90°C for 6 h. (Scheme 25).^[155-156] Very recently, Mihovilovic and co-workers reported

an enzymatic approach to the Baeyer-Villiger oxidation of ML. Using monooxygenases CPMO_{Coma}, 80% yield of the corresponding methyl 3-acetoxy propionate was achieved.^[157]



Scheme 25. Baeyer-Villiger oxidation of LA.

Initially, one of the aims of this doctoral research was to explore the Baeyer-Villiger oxidation of ML to 3-acetoxypropanoic acid in order to search for a more efficient process compared to the ones already reported. Following the enzymatic Baeyer-Villiger oxidation reported by Mihovilovic and co-workers, the present study shows MA synthesis from the 3-acetoxy propionate through a gas-phase elimination of acetic acid using a continuous flow system.

2. Chapter 1: Liquid phase conversion of methyl levulinate and levulinic acid to methyl vinyl ketone

2.1. Introduction

As mentioned in Section 1 of the introduction, this study focuses on the catalytic conversion of ML to MVK. The envisaged reaction is in essence the reverse of a methoxycarbonylation reaction.^[158-160] The metal-catalyzed alkoxycarbonylation reaction is well known and has been reviewed extensively,^[133, 161] where the key catalysts are the palladium-phosphine,^[134] cobalt^[135] or ruthenium^[136] carbonyl complexes. Inversely, olefins can be formed by the decarboxylation or decarbonylation of activated carboxylic acids and esters respectively.^[127] The decarbonylation of methyl esters to alkenes and alcohols is called a *dealkoxycarbonylation* reaction, which however still remains a highly challenging reaction of which few examples have been reported.

2.2. Objectives

The first aim of this research was to investigate if the decarbonylation of ML in the liquid phase would be feasible applying several approaches found in the literature. It was proposed to start off attempting the demethoxycarbonylation of ML via activation of the ester functionality in a homogenous fashion. If that approach would not work, the decarbonylation of ML could be tested using supported heterogeneous catalyst at higher temperatures.

2.3. Results and discussion

Pd-catalyzed demethoxycarbonylation of ML

A range of homogeneous palladium catalysts, made *in situ* by combining the ligand with Pd₂(dba)₃ as the metal precursor, were screened. A number of ligands as well as an NHC-Pd complex were selected (Figure 2), since they were used in the past for the alkoxycarbonylation of olefins.^{[134],[162],[163]}

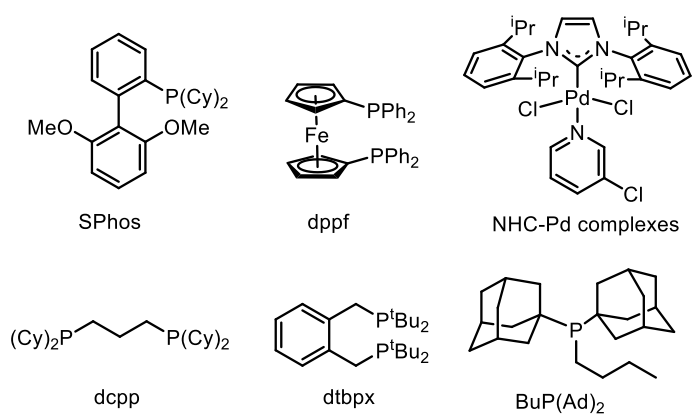
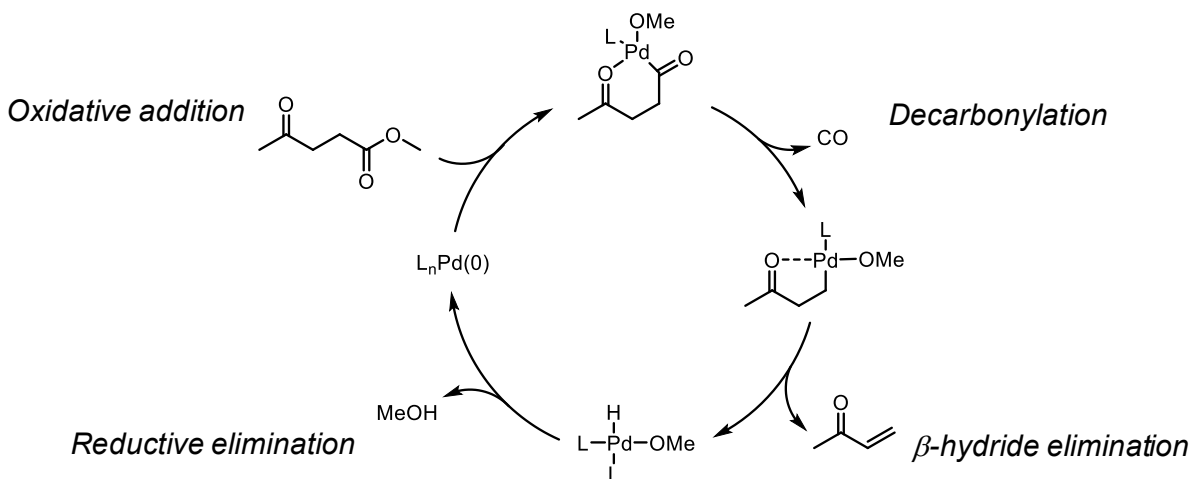


Figure 2. Selected ligands and a NHC-Pd complex for the Pd-catalyzed demethoxycarbonylation of ML.

The catalytic cycle is proposed based on the studies performed by the groups of Sanford and Cramer (Scheme 26).^[143, 164] In the first step, ML undergoes an oxidative addition to Pd(0) center. Then decarbonylation takes place forming an alkyl-Pd species which undergoes β -hydride elimination to form the alkene, resulting in a hydridometal alkoxy species. A reductive elimination of methanol regenerates the initially catalytically active Pd(0) intermediate.

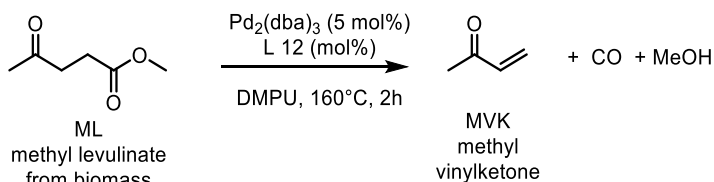


Scheme 26. Proposed mechanism for the Pd-catalyzed demethoxycarbonylation of ML.

The initial approach to the demethoxycarbonylation reaction of ML using homogeneous catalysts was not successful (Table 3). The starting ester remained unconverted. At the end of each reaction palladium black was formed. Furthermore, It was not possible to isolate or observe any Pd-acyl complex. This suggests that the first step of the envisioned catalytic cycle, namely the oxidative addition of the ester C-O bond to Pd,

did not occur. This hypothesis is supported by the scarce literature examples of oxidative addition of the ester C-O bond to the metal, which only works when electron-poor esters (such as perfluorinated aromatic or *p*-nitrophenol esters) are used. Sanford *et al.* noted that the use of Buchwald-type bulky monophosphine ligands should enhance the decarbonylation reaction.^[143-146, 165] However, use of S-PHOS as ligand was unsuccessful in the decarbonylation of ML

Table 3. Ligand screening in the Pd-catalyzed decarbonylation of ML.



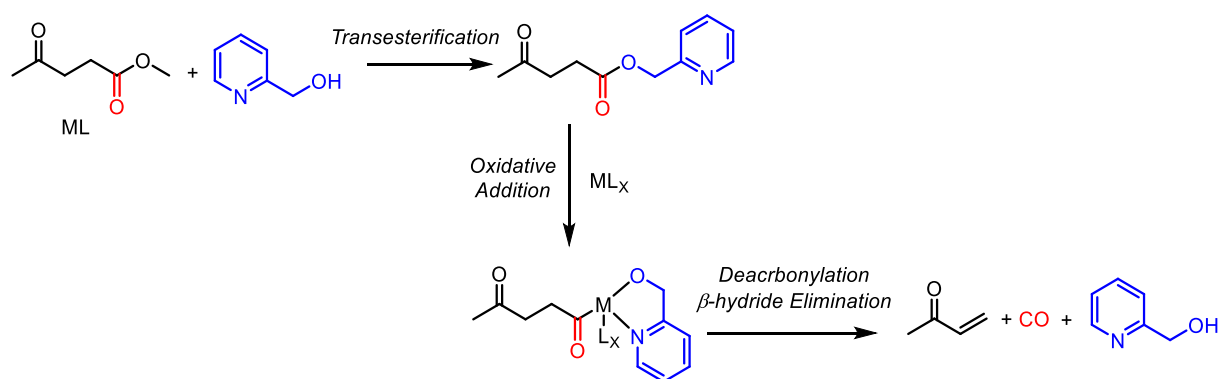
Entry ^a	Ligand	X _{ML} [%] ^c	Observations
1	SPhos	0	Pd black, yellow solution
2	Dppf	0	Dark red solution, Pd Black
3	BuP(Ad) ₂	0	Pd Black, yellow solution
4	dtbpx	0	Pd Black, yellow solution
5	dcpp	0	Dark red solution, Pd Black
6	NHC-IPr ^b	0	Dark green solution, Pd Black

^a Conditions: 0.4 mmol of ML, 0.02 mmol of Pd₂(dba)₃, 0.048 mmol of ligand, DMPU: N,N'-dimethylpropyleneurea. ^b 0.02 mmol of NHC-Pd complex was used. ^c Determined by ¹H NMR spectroscopy and Gas Chromatography.

Ruthenium-catalyzed reductive decarbonylation of pyridyl esters

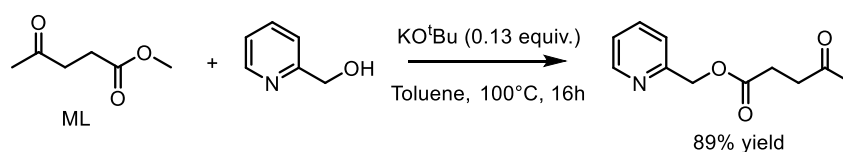
It was then decided to attempt the reaction with chelating esters instead. The Ru-catalyzed decarbonylation of 2-pyridylmethyl esters has been reported to benefit from a chelate effect.^[166-167]

Based on the work of Murai and co-workers as well as from the recent work of Tolman *et al.*^[146] a plausible reaction pathway for the formation of MVK from 2-pyridylmethyl levulinate was proposed (as shown in Scheme 27).



Scheme 27. Proposed reaction pathway for the Ru-catalyzed decarbonylation of ML.

The 2-pyridylmethyl ester was prepared by a straightforward base-catalyzed transesterification in 89% yield (Scheme 28).



Scheme 28. Synthesis of 2-pyridylmethyl levulinate from ML.

The next step was the decarbonylation reaction which was then attempted with the 2-pyridylmethyl in the presence of triruthenium dodecacarbonyl ($\text{Ru}_3(\text{CO})_{12}$) catalyst. The results are illustrated in Table 4. Furthermore palladium-NHC and nickel-phosphine catalysts did not show any activity in this conversion (Table 4, entries 2 and 3). MVK was not observed in any of the attempts. Mainly starting material was observed in the GC-MS.

Table 4. Reductive decarbonylation of 2-pyridylmethyl ester using different metal precursors.

CC(=O)CCC(=O)OCc1ccncc1 $\xrightarrow{\text{cat. (5 mol%)}}$ CC(=O)C=C + O=C=O + Oc1ccncc1
MVK

Entry ^a	Catalyst	Solvent	T (°C)	Observations ^b
1	$\text{Ru}_3(\text{CO})_{12}$	1,4-Dioxane	160	no MVK detected
2	Pd PEPPSI	NMP	180-200	no MVK detected
3	Ni(dppb)	NMP	180-200	no MVK detected

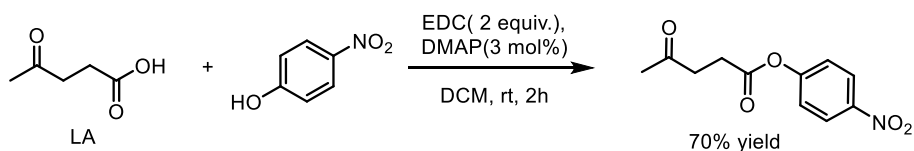
^aConditions: 0.18 mmol of pyridin-2-ylmethyl 4-oxopentanoate, 0.01 mmol of catalyst, 0.6 mL of solvent, 16 h. NMP: N-methyl-2-pyrrolidon. ^cDetermined by ^1H NMR spectroscopy and Gas Chromatography.

While this approach was unsuccessful in our case, recently the same strategy was applied by Tolman and co-workers in the dual-catalytic decarbonylation of fatty acid methyl esters. First the transesterification reaction in the presence of a Lewis acid catalyst (ZnCl_2) and a chelating alcohol (2-pyridinemethanol) converted methyl palmitate to the corresponding alkyl ester in up to 67%. The following decarbonylation using $\text{Ru}_3(\text{CO})_{12}$ and $\text{P}(\text{Cy})_3$ as catalyst was accomplished resulting in 95% conversion of the starting material. A one pot reaction (tandem transesterification followed by decarbonylation) resulted in 65% conversion.^[146] At this stage, it was considered that the presence of the ketone group might play an inhibiting role. Nevertheless, it was decided to test another approach by using an electron deficient ester moiety.

Synthesis of levulinic acid *p*-nitrophenyl ester and its attempted decarbonylation using transition metal catalysts

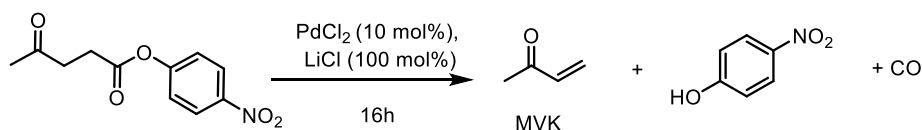
In 2015 Tolman and co-workers reported the decarbonylation of *para*-nitrophenol esters by using a ligand free PdCl_2 catalyst in the presence of alkali/alkaline-earth metal halides.^[145] This catalyst was earlier developed by de Vries and co-workers for the palladium-catalyzed decarbonylative Heck reaction of aromatic carboxylic anhydrides.^[168] The active catalyst was later shown to be halide stabilized palladium nanoparticles.^[169] Additionally, a patent from 2014 claims the use of aromatic and methyl esters of stearate for this reaction, but only a 6% yield was achieved when methyl ester was used.^[170]

Following the same strategy, the corresponding levulinic *p*-nitrophenyl ester from levulinic acid using EDC-HCl ((1-ethyl-3-(3-dimethylaminopropyl)carbodiimide) hydrochloride) and catalytic amounts of DMAP (4-(dimethylamino)pyridine) was prepared (Scheme 29).



Scheme 29. Synthesis of levulinic *p*-nitrophenyl ester from LA.

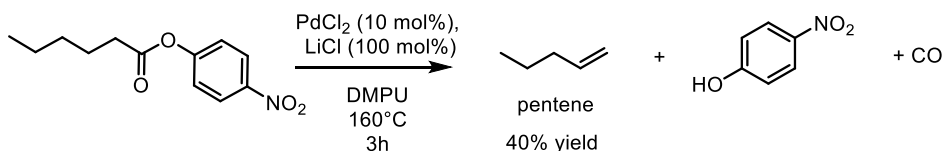
The desired ester was obtained in 70% yield. The latter was subjected to the decarbonylation reaction using PdCl_2 catalyst in the presence of LiCl . The results are shown in Table 5. Different solvents and temperatures were used for this conversion.

Table 5. Pd-catalyzed decarbonylation of *p*-nitrophenyl ester.

Entry ^a	Catalyst	Solvent	T (°C)	X _{p-NO₂ ester} [%] ^b
1	PdCl ₂	DMPU	160	0
2	PdCl ₂	NMP	160	0
3	PdCl ₂	1,4-Dioxane	160	0
4	PdCl ₂	Toluene	160	0
5 ^c	PdCl ₂	-	160-220	0

^a Conditions: 0.18 mmol of 4-nitrophenyl 4-oxopentanoate, 0.017 mmol of PdCl₂, 0.17 mmol of LiCl, 0.5 mL of solvent, 16 h. DMPU: N,N'-Dimethylpropyleneurea. NMP: N-Methyl-2-pyrrolidone. ^b Determined by ¹H NMR spectroscopy. ^c The following temperatures were tested: 160, 180, 200 and 220 °C. In all cases the results were the same.

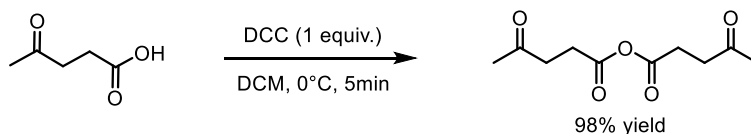
Despite the fact that high temperatures were used (up to 220 °C), no conversion of the ester group was observed by NMR. At this stage we wondered whether the ketone function might have an effect on the decarbonylation reaction, presumably by coordination to the metal center. To corroborate this suspicion, it was decided to synthesize the analogous ester without the ketone group which was subjected to the decarbonylation using similar reaction conditions (Scheme 30). 4-Nitrophenyl hexanoate was subjected to the Pd-catalyzed decarbonylation reaction resulting in a 40% yield of the corresponding pentene.

**Scheme 30.** Decarbonylation of *p*-nitrophenyl hexanoate to pentene.

From this experiment it was concluded that the ketone function has an inhibiting effect on the catalytic reaction.

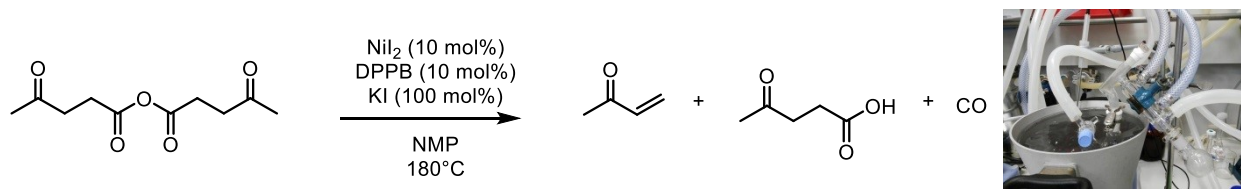
Ni-catalyzed dehydrative decarbonylation of levulinic anhydride

Not deterred by this finding, the decarbonylation of highly activated levulinic acid anhydride using nickel catalyst was examined. The anhydride was prepared using dicyclohexylcarbodiimide (DCC) as a coupling agent (Scheme 31).



Scheme 31. Preparation of levulinic acid anhydride.^[171]

It was attempted to perform the decarbonylation using nickel iodide and DPPB 1,4-Bis(diphenylphosphino)butane phosphine ligand in the presence of potassium iodide, since this catalyst was employed for this type of transformation in the past.^[172] The reaction was performed in a flask connected to a short path distillation apparatus in order to remove CO and highly volatile MVK during the course of the reaction (Scheme 32).



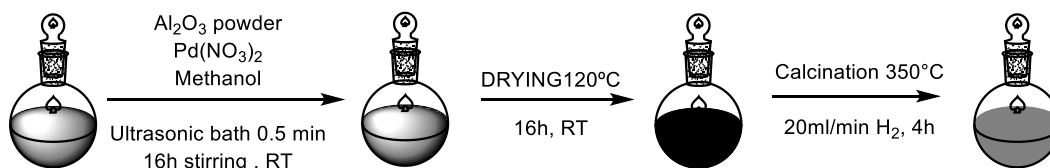
Scheme 32. Ni-catalyzed decarbonylation of levulinic anhydride.

At 180°C, only traces of MVK could be observed in the GC-MS spectra, together with angelica lactones, acetic acid and other cyclic compounds.

At this stage, it was decided to stop the homogeneous catalysis approach, and switch to the use of heterogeneous catalysts for the liquid-phase decarbonylation of ML.

Preparation and application of Pd supported NPs for the decarbonylation of ML

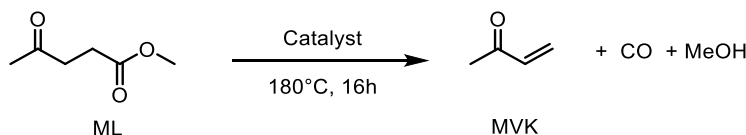
Since the desired reaction obviously requires higher temperatures, it was decided to test heterogeneous catalysts due to their higher robustness. The initial approach was the use of supported Pd nanoparticles (NPs) as catalyst for the demethoxycarbonylation. These were synthesized by the incipient wet impregnation procedure (Scheme 33). Alumina (doped or not doped with potassium), was used as the support.



Scheme 33. Procedure for the synthesis of Pd supported catalysts.

The results of the application of these supported catalysts in the conversion of ML are shown in Table 6. The reaction was attempted in various solvents, as well as under solvent free conditions. It was observed that these supported catalysts were completely inactive for the desired transformation at 180 °C.

Table 6. Heterogeneous Pd-catalyzed decarbonylation of ML using different solvents.



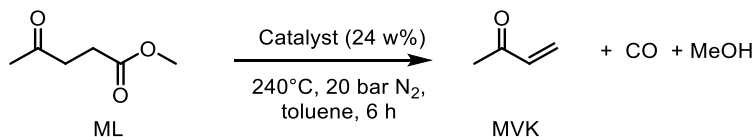
Entry ^a	Catalyst	Solvent	X _{ML} [%] ^b
1	Pd/Al ₂ O ₃	NMP	0
2	Pd/Al ₂ O ₃	DMPU	0
3	Pd/Al ₂ O ₃	1,4-Dioxane	0
4	Pd/Al ₂ O ₃	-	0
5	Pd-K/Al ₂ O ₃	NMP	0
6	Pd-K/Al ₂ O ₃	DMPU	0
7	Pd-K/Al ₂ O ₃	1,4-Dioxane	0
8	Pd-K/Al ₂ O ₃	neat	0

^a Conditions: 4 mmol ML, 0.104 g catalyst. Reactions carried out for 16 h using short path distillation apparatus at 180°C. ^b Determined by ¹H NMR spectroscopy and Gas Chromatography.

High throughput screening of supported catalysts for the decarbonylation of ML and LA

Since palladium on alumina appeared to be non-promising, a high throughput screening (HTS) experiment with other heterogeneous catalysts was carried out for the liquid-phase conversion of ML. A number of supported transition metal catalysts as well as metal oxides were screened (Table 7).

Table 7. Overview of the selected results from liquid phase conversion of ML to MVK in toluene using heterogeneous supported catalysts.



Entry ^a	Catalyst	X _{ML} [%]	Yield [%]				
			MVK	MEK	MeOH	LA	GVL
1	5 wt% Pd/charcoal	41	0	0	4.1	0.1	0.2
2	25 wt% Pd/ 2.5 wt% Pt on carbon	38	0	0.1	0.9	0.5	0
3	5 wt% Ru/ Al ₂ O ₃	41	0	0.1	1.8	1.3	0
4	60 wt% Ni/ SiO ₂ /Al ₂ O ₃	46	0	0	0.3	0.4	4.5
5	5 wt% Ru carbon	39	0	0.1	0.4	0.1	0
6	5 wt% Pt/ sulfided carbon	74	>0.1	0	0	0.1	0.2
7	CuZn/ Al ₂ O ₃	33	>0.1	0.2	0.5	0.1	0

^a Quantification by GC, acetophenone as internal standard. The following sets of conditions were tested: 123 mg of ML, 30 mg of catalyst = various commercially available supported catalysts, T= 240 °C, t = 6 h, atmosphere = N₂, P = 20 bars, solvent = toluene.

Methanol and levulinic acid (LA) were observed, which indicates hydrolysis of the starting material due to the presence of moisture in the reaction media.

MEK was observed in low yields in some cases (Table 7, entries 2, 3, 5 and 7). It could be formed either via the decarboxylation of LA or via reduction of MVK in the presence of methanol. γ-Valerolactone (GVL) was formed when a nickel catalyst was used (Table 7, entry 4) in 4.5%. Its occurrence can be explained by reduction of the ketone group in ML by methanol.

An alternative explanation for the formation of MEK could be that the catalysts tested are well known as hydrogenation catalysts, especially Pt, Ni, and Ru. That could explain the MVK reduction to MEK in the presence of MeOH as a hydrogen source. As shown

in entries 2 to 3 of Table 7, we can observe that MEK yields are higher. Since reduction of MVK to MEK may occur it is clear that MVK has to be removed from the reaction as fast as possible, which argues for a gas phase reaction.

Supported Pt and Cu catalysts were also applied under the same reaction conditions. Traces of MVK in those cases when Pt sulfided on carbon or CuZn catalysts were applied were observed (Table 7, entries 6 to 7).

In all these experiments, the formation of very small amounts of α -angelica lactone (α -AL) was found and according to Dumesic's studies, this could lead to deactivation of the catalytic system.^[173]

MVK is known to be a reactive molecule and its polymerization is exothermic in the presence of light or heat, which could be another reason for the poor mass balances. To corroborate that MVK could polymerize inside the reactor, MVK was used as starting material under the reaction conditions in the presence of the catalysts that gave higher conversions of ML. Indeed, polymerization did occur under these reaction conditions. ML, MVK and Platinum on sulfide carbon in dioxane were mixed inside the autoclave and heated to 240°C. As result, it was found that ML was converted in 23% conversion and MVK as converted in 95% conversion. MEK was formed in 24% yield, 14% yield of MeOH and 9% yield of LA were observed. These results concluded that under the reaction conditions used, MVK was polymerizing. The missing MeOH could be attributed to the hydrogen formation which hydrogenates MVK to MEK. Attempts to inhibit the polymerization step using radical scavengers such as hydroquinone and benzoquinone were unsuccessful.

Overall, this set of experiments helped us to identify Pt on sulfided carbon and CuZn as promising catalysts for the desired reaction. It is also clear that the reaction needs to be performed in a flow system in order to remove MVK as soon as it is formed.

Attempts in the decarboxylation of LA to MVK using bulk oxides

Gong and co-workers^[124] used copper oxides as catalysts for the decarboxylation of LA to MEK. The surprising MEK yield of ~ 68% was achieved at 300 °C for a reaction time of 2 h. The initial pH of the reaction was observed to be pivotal in increasing MEK yields (optimum at pH = 3.2). In following studies, other oxides and Ag₂S₂O₈^[125] were used to catalyze the same reaction giving, however, lower yields than in the case of copper oxides.

In this case it was wondered whether it was possible to achieve higher yields of MVK from LA in water in the presence of metal oxides (Table 8).

Table 8. MVK and MEK yields in the conversion of LA in H₂O using silver and copper oxides as catalysts.

LA $\xrightarrow[200\text{ }^{\circ}\text{C, 1h, 1bar Air}]{\text{Catalyst}}$ MVK + CO₂

Entry ^a	Catalyst	X _{LA} [%]	Yield [%]				
			MVK	MEK	α-AL	AcOH	GVL
1	Ag ₂ O	24.4	8.2	0.2	4.1	0.1	0.2
2	AgCl	11.4	3.1	0.3	0.9	0.5	0
3	Cu ₂ O	30.5	7.2	0.2	1.8	1.3	0
4	CuO	43.2	10.7	0.2	0.3	0.4	4.5

^a Quantification by GC, acetophenone as internal standard. In all listed cases the following conditions were used: solvent = H₂O, T = 200 °C, t = 1 h, P (@RT) = 1 bar (compressed air).

Under all experimental conditions tested, the yields of MVK are significantly higher than of MEK. As already studied by Gong and co-workers^[124], the mechanism proceeds through a radical reaction in which a facile oxidation of LA by Ag(II) in a fast follow-up step could bring about a radical anion of CH₃COCH₂CH₂CO₂^{•-}, which could be subsequently fragmented to an CH₃COCH₂CH₂[•] radical and CO₂. Depending on the reaction conditions, MEK was derived by uptake of a hydrogen atom by the CH₃COCH₂CH₂[•] from the solvent. Instead, in the presence of Cu(II), an electron and a proton could be subtracted from CH₃COCH₂CH₂⁺ delivering MVK.

In a set of experiments buffered at pH ≈ 10 (by addition of KH₂PO₄) performed in H₂O-NaOH (initial), however, higher MEK yields were obtained (up to 32% yield of MEK and 3% yield MVK). This shows the potential to shift the product slate in the desired manner by varying the pH of the reaction media or possibly the acidity and basicity of the catalyst.

It was also observed that MVK yields obtained from LA are higher than those from ML. The best experimental conditions include the use of 1 bar of air, 225°C, one hour of reaction time, and CuO as the metal oxide catalyst resulting in 10-12 % MVK yield.

2.4. Conclusion

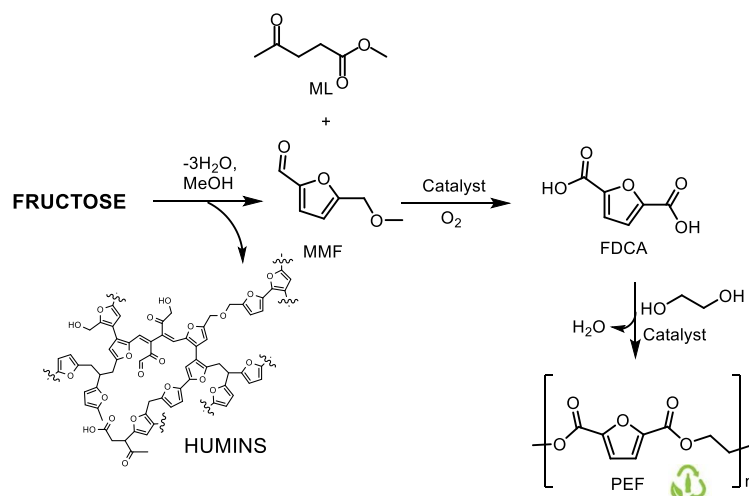
- The pursued homogenous dealkoxycarbonylation of ML was not successful using palladium-phosphine complexes. Mainly decomposition of the catalyst was observed at the conditions used. No conversion of ML was achieved in any of the attempted reactions.
- The expected beneficial effect of a chelating pyridylmethyl ester did not materialize in the case of the levulinic acid ester. While conversions were very low, only traces of MEK were observed when using a reducing agent.
- Using a more activated *p*-nitrophenyl ester in the demethoxycarbonylation reaction did not improve the results as no conversion of the starting material was observed. It was then noted that the ketone has an inhibiting effect.
- Using heterogeneous catalysts, traces of MVK were observed when using platinum on sulfided carbon and CuZn catalysts.
- When LA was used as starting material, over 10% of MVK was obtained using copper oxides as catalysts.
- The possibility of MVK polymerization as well as the need of harsher reaction conditions suggested that a gas-phase reaction may lead to better results in the demethoxycarbonylation of ML.

3. Chapter 2: Gas phase conversion of bio-based methyl levulinate to methyl vinyl ketone

3.1. Introduction

Research on the conversion of renewable feedstocks into bulk and fine chemicals has gained immense importance in the recent decades propelled by the future exhaustion of fossil resources. In particular, biomass is seen as one of the most promising alternative feedstocks for chemicals in the coming future. Catalytic conversion of bio-based materials, such as cellulose, lignin or lignocellulose has been intensively explored over the past few years.^[12]

As already mentioned in this thesis introduction, the YXY technology platform created by Avantium Chemicals B.V. and now used by Synvina, is an important example where biomass is used as a starting material for bio-based plastic production.^[21] This process deals with the production of 2,5-Furandicarboxylic acid (FDCA) from biomass derived HMF or 5-methoxymethylfurfural (MMF). FDCA is the precursor of polyethylenefuranoate (PEF) which could serve as the potential replacement polymer of the well-known and widely used polyethylene terephthalate (PET). This process consists of multiple steps which give rise to the formation of by-products such as methyl levulinate (ML) as well as a polymeric substance known as humins (Scheme 34).^[21]

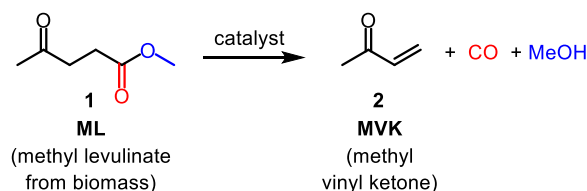


Scheme 34. FDCA synthesis from biomass derived HMF and MMF.

The valorization of these side streams is certainly of great interest. ML is a side product in the synthesis of MMF from cellulose derived fructose and methanol (MeOH).

Although several applications of levulinic acid (LA) have been found, so far, to the best of our knowledge, only very limited applications of ML are known at the moment

(such as the use of it as a solvent or food additive).^[106] Therefore there is a need to explore different possibilities to utilise these side streams for producing valuable chemicals. The direct conversion of ML to methyl vinyl ketone (MVK) is one such good option to valorise ML. The target product, MVK (shown in Scheme 35) is an important intermediate for the production of Vitamins A and E. Moreover, MVK is a relatively expensive compound which is currently made from non-renewable acetone via condensation with formaldehyde.^[174] To the best of our knowledge, there is no single source of publication in both patent and open literature on the one-step conversion of ML into MVK.



Scheme 35. General reaction for the conversion of ML to MVK.

The envisaged reaction is in essence the reverse of a methoxycarbonylation reaction.^[158-159] The metal-catalyzed alkoxycarbonylation reaction is well known and has been reviewed extensively,^[133] where the key catalysts are the palladium-phosphine^[134], cobalt^[135] or ruthenium^[136] carbonyl complexes. Inversely, olefins can be formed by the decarboxylation or decarbonylation of activated carboxylic acids and esters respectively.^[127] The decarbonylation of methyl esters to form alkenes and alcohols is named as *dealkoxycarbonylation* reaction, which however still remains a highly challenging reaction.

As consequence of the high C-O bond energy, an activation of the acyl C-O moiety prior to the decarbonylation is often required.^[138] Sanford *et al.*^[142] and Cramer *et al.*^[164] reported the catalytic cycle for palladium-catalyzed decarbonylative trifluoromethylation using trifluoroacetic esters. Cramer and co-workers described the mechanism of Pd-catalyzed decarbonylation of biomass-derived activated anhydrides from hydrocinnamic acid to styrene. Both of these studies provide us good hints to the activation of methyl esters in order to favor the decarbonylation step.

Another example described by Tolman and co-workers was the decarbonylation of *p*-nitrophenyl esters using PdCl₂ in the presence of alkali/alkaline-earth metal halides.^[144] The same authors have recently published the selective decarbonylation of *p*-nitrophenol esters from fatty acids to form linear α-olefins achieving high ester conversions (>90%) and selectivities (>98%) at 190°C.^[146]

In an attempt to deoxygenate biomass derived chemicals for its proper use, the decarboxylation reaction has been intensely reported over the past decades. The

decarboxylation of organic molecules happens by removal of a carboxyl group from the carboxylic acid, which is further replaced by a hydrogen atom.

LA is a platform chemical that results from a series of biomass lignocellulose hydrolysis reactions and is also a widely explored chemical with extensive applications.^[175]

The decarboxylation of LA has been reported not only in a homogeneous fashion^[125] but also in heterogeneous catalytic process^{[176],[177],[124, 178]} and in particularly enzymecatalyzed reactions.^[179] The expected product would be 2-butanone, also known as methyl ethyl ketone (MEK).^[114]

Relevant homogeneous catalytic systems for the decarboxylation of LA have been reported.^[125] In 2011, Lin and coworkers described a novel pathway for the oxidative decarboxylation of LA using Ag(I)/S₂O₈²⁻ system under mild conditions. Changing the pH of the solution to 5.0, using NaOH-KH₂PO₄ at 160 °C, a 44 % MEK yield at a 70% LA conversion was achieved.^[125]

Applying heterogeneous catalysts, limited examples of ester decarbonylation are reported^[124-125, 176-177] In 1945 Bremner and Jones reported the direct formation of MVK from either LA or the corresponding ester over silica chips or aluminium silicate at temperatures between 570 and 580°C.^[177]

Lin *et al.* also reported that the heterogeneously catalyzed oxidative decarboxylation of LA over CuO/CeO₂ yields only 15% MVK, while unsupported CuO gave a remarkably high yield of MEK (68%). In both cases, temperatures as high as 300°C were used.^[124] Moreover, Dumesic and West described the conversion of LA to MVK over a solid acid catalyst at temperatures above 250°C. The authors speculate that the key intermediate for the formation of MVK from LA is α -angelica lactone (α -AL), which is known to poison solid catalysts.^[178]

Recently, Wang and co-workers have reported the decarboxylation of GVL to butane using zeolites. Full GVL conversion and about 98% yield of butane could be achieved using aluminum beta zeolite with high content of Lewis acid sites.^[180]

Our initial efforts were focussed on investigating the dealkoxycarbonylation of ML using the commonly employed alkoxycarbonylation palladium catalysts with Pd(OAc)₂ and Pd₂(dba)₃ as the sources of choice. So far, a number of promising phosphine ligands was tested. However, almost no conversion under such mild reaction conditions employed (80-100°C organic solvents/neat) was achieved. However, when the reaction temperature was further increased to 220°C, the formation of black precipitate was observed, which is presumably due to formation of metallic particles (See supporting information). It is believed that the oxidative addition of the ester, which would be the first step of the putative catalytic cycle, did not take place. Obviously, this step requires the use of more severe reaction conditions, where the homogeneous metal complex does not survive. Various heterogeneous catalysts were also screened for this conversion in the liquid phase. It was observed that MVK product was polymerizing under the reaction conditions, making the process unfeasible.

3.2. Objectives

In this part of the investigation, the aim is to explore the gas phase conversion of ML in the presence of the most active catalyst (e.g. Pt on sulfided carbon) that was identified during the liquid phase experiments. The idea is to enhance the yields of the desired product MVK besides improving the long-term stability of the catalysts. In addition, a second objective is to investigate a possible reaction mechanism *via* control experiments in order to identify potential reaction intermediates. Another objective is to employ bio-based LA (C5-platform chemical, and also the intermediate in the conversion of ML) as a reactant to produce MVK in a single step in a gas phase continuous mode using a fixed bed stainless steel reactor.

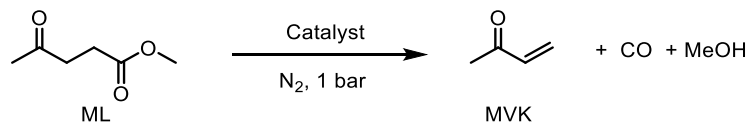
3.3. Results and discussion

It was concluded from the results obtained in the liquid phase experiments that further investigations in the gas phase mode would improve the target product yields when the contact time with the catalysts surface is minimized and also by optimizing the reaction parameters. This approach certainly helps to minimize undesired side reactions and thereby enhances the selectivity of target product, MVK.

The screening of numerous commercial catalysts for the conversion of ML in the gas-phase was possible using Avantium's high throughput flow technology, the Flowrence® equipment (See experimental section). This set-up consists of 2 HPLC pumps and various mass flow controllers (MFC). Both the liquid and the gas flow are homogeneously distributed over 64 parallel small reactors. These reactors are divided in 4 blocks of 16 reactors each and are heated independently. A series of pressure indicators are installed near the reactors in order to check the reaction pressure, leakage and/or blockage of reactor lines. Selector valves situated in an oven are responsible for selecting the stream of gas that is desired to be analyzed. A series of 2 online sequential GC devices make it possible to analyze the reaction components present in the product gas stream.

From the 64 reactors, for safety reasons only 16 were used at the same time. An overview of the results obtained is shown in Table 9.

Table 9. Overview of the results from gas phase high through put screening of various supported metal catalysts for demethoxycarbonylation of ML.



Entry ^a	Catalyst	T (°C)	Yield [%]						
			MVK	MEK	MeOH	CO	CO ₂	α-AL	GVL
1	5 wt%Pt/sulfide carbon	450	1	0	9	2	0	7	0
2 ^b	Co-Mo/Al ₂ O ₃	400	2	0	15	15	0	15	0
3 ^b	Ag/carbon	400	0	1	39	14	0	29	0
4 ^b	Cu-Zn-alumina	450	2	1	4	22	8	22	1
5 ^c	NiS	420	2	0	51	6	3	15	0
6 ^c	Cu/carbon	450	3	1	44	13	0	30	1
7 ^c	5 wt%Ru/Al ₂ O ₃	420	2	1	1	11	70	16	0
8 ^c	3 wt%Pt-0.3 wt%Cu/Carbon	420	3	2	33	17	6	10	0
9 ^c	5 wt%Pt/sulfide carbon	350	7	12	30	46	4	0	0
10 ^c	5 wt%Pt/sulfide carbon	450	10	5	4	21	48	11	1

^a α-AL: alfa angelica lactone, GVL: gamma valerolactone *in situ* pre-reduction (~10 vol% H₂) at 250°C for 2h. Catalyst: 5 wt% Pt on sulfide carbon, 150 mg. Quantification by online GC. Helium as an internal standard. Total flow: 0.4 L/h. bed volume: 0.19 cm³. GHSV: 2085 h⁻¹. 1.5 mmol/h of substrate in a stream of N₂ as a dilution gas to maintain constant GHSV. Concentration of ML: 20 vol% in N₂ stream. ^b2 vol% of H₂O. ^c ML: 1.5 %vol in N₂ stream, 20 vol% of H₂O.

The ML conversion is not shown in Table 9 due to condensation issues in the downstream of the apparatus. The addition of water to the feed mixture had also shown promotional effect on the yields of MVK (Table 9, entries 1 and 10). The presence of water can also attenuate the formation of deposits of carbonaceous compounds (coke),

and facilitate easy desorption of products thus enhancing the yield of target product MVK.^[181] It can be seen that with most catalysts very little MVK was obtained.

To conclude this part, it was found that use of 5 wt% Pt on sulfided carbon as catalyst gave the most promising results in the conversion of ML to MVK and methyl ethyl ketone (MEK) in the gas-phase. In the best experiment, an MVK yield up to 12%, and a MEK yield up to 10% could be obtained, however their distribution depends upon the reaction conditions applied (Table 9, entries 9 and 10). At 350°C, the yield of MEK is higher than that of MVK, while at a higher reaction temperature (450°C), the yield of MVK is higher than of MEK (Table 9, entries 9 and 10). This fact suggests that the temperature plays a pivotal role on the distribution of these two products. In other words, high reaction temperature favors the formation of MVK while the low temperature promotes MEK formation. This can be due to the initial hydrogenation of MVK to MEK which at higher temperatures is less predominant because of the deactivation of the corresponding active sites. It seems that at higher temperatures the decarbonylation reaction is more likely to take place.

Based on the results observed, and on the mechanism suggested by Dumesic and co-workers,^[1] a tentative reaction pathway can be suggested. According to this, the first step is the ring closure of ML to give α -AL; which is then isomerized to β -AL and finally MVK is formed via decarbonylation.

An alternative reaction pathway entails the decarboxylation of LA to give methyl ethyl ketone (MEK) and CO₂. This is also based on the observation that large amounts of CO₂ were detected in some experiments (Table 9, entries 4, 9 and 10).

As already mentioned, another possible pathway for the formation of MEK involves formation and subsequent reduction of MVK. Once again it is speculated that MeOH would act as the hydrogen source.

The deactivation behaviour of the 5 wt% Pt on sulfided carbon catalyst is illustrated in Figure 3. The reaction was carried out at varying temperatures in the range from 220 to 450°C. The product analysis was done using on-line GC and each sample was analysed for every 30 minutes. It should be noted that the results obtained from two sets of experiments carried out in the absence and presence of water vapour were compared in Fig. 2.1. Unfortunately, in all cases a fast and pronounced catalyst deactivation was observed. As can be seen, the MVK yield decreased very rapidly with time-on-stream. It is also evident from Figure 3. a, that the yield of MVK is strongly dependent on the reaction temperature. Surprisingly, raising the reaction temperature from 300 to 350°C results in a higher yield of MVK even when the catalyst is already deactivated. However, this increase in MVK yield is relatively low (4%) compared to the first cycle (Y-MVK: 7%). An attempt to reactivate the catalyst with hydrogen (ca. 10 vol%) was performed at 350°C, but the the yield was improved only to a small extent (Y-MVK: ~2%). Nevertheless, the tendency of deactivation remained more or less similar in each cycle. Another interesting observation is related to the influence of water

vapour on the yield of MVK. In the second set of experiments (Figure 3. b), water vapour was added to the reactant feed mixture at 300°C, where the yield of MVK was improved significantly from 7% (in the absence of water) to 12% (in presence of water vapour). However, the yield decreased rapidly again due to deactivation in a similar way as that of experiments carried out in the absence of water vapour. In subsequent cycles the reaction temperature was raised further in a similar manner to that of previous experiments performed in the absence of water vapour. It is notable that the yield of MVK enhanced considerably in the 2nd, 3rd and 4th cycles with rise in temperatures to 350, 400 and 450°C. Based on these results, it can be stated that admixture of water vapour to the feed along with a rise in reaction temperature can help to improve the yield of MVK even in the deactivated catalyst but it can not solve the problem of deactivation, which seems to be inevitable for the moment.

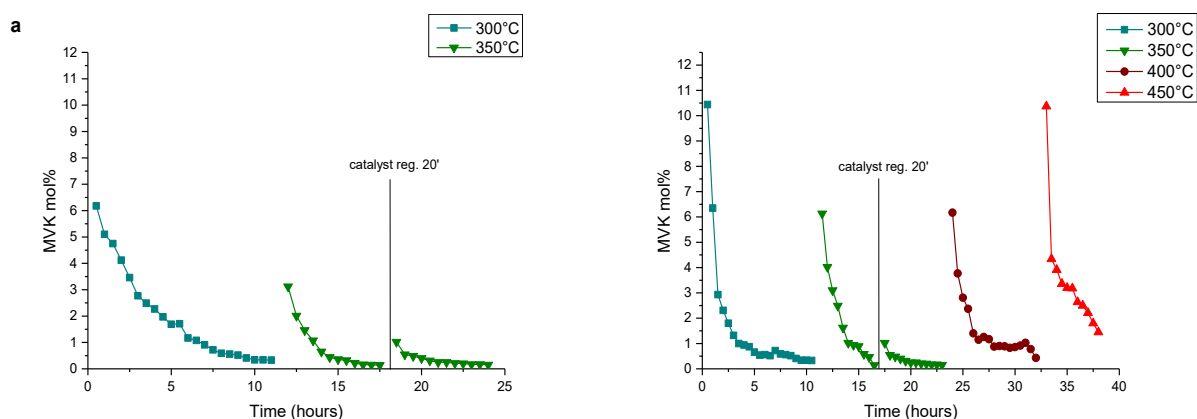
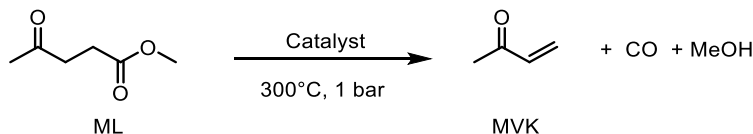


Figure 3. Deactivation curves of 5%Pt on sulfided carbon for MVK formation obtained from high throughput screening. Reaction conditions: *In situ* pre-reduction (~ 10 vol% H_2) at 250°C for 2 h. Catalyst: 5 wt% Pt on sulfide carbon, 0.19 cm³ (150 mg). Regeneration at 300°C with H_2 (~ 10 vol%) for 30 min. Two different experiments; a) pure ML feed, 1.5 %vol in N_2 stream, and b) ML 1.5 %vol in N_2 stream with 20 wt% water feed.

With the most promising catalyst in hands, a single-reactor system was built for the optimization of the reaction conditions in the gas phase. In order to gain more information about the demethoxycarbonylation of ML in the gas phase a single reactor, flow set-up adapted with an online GC was used (see experimental section). The selected results obtained from the ML conversion are shown in Table 10.

Table 10. Effect of H₂O admixture on the activity and selectivity of 5wt% Pt/sulfided Carbon catalyst tested in a single reactor system.



Entry ^a	Time (min)	X _{ML} [%]	Yield [%]						MB [%]
			MVK	MEK	MeOH	α-AL	β-AL	Others	
1	20	53	3	4	20	13	9	4	94
2	40	61	10	8	24	10	4	4	92
3	60	35	1	2	13	7	5	7	97
4 ^b	20	82	18	14	37	4	2	7	87
5 ^b	40	67	14	4	28	13	7	1	92
6 ^b	60	59	6	1	23	14	7	8	92

^a α-AL : alfa angelica lactone, β-AL : beta angelica lactone, ML: 6 mmol/h, bed volume: 2 cm³, total flow: 8.8 L/h, GHSV: 4400 h⁻¹ (Argon used as an internal standard, N₂ as a dilution gas to maintain constant GHSV, 0.65 g of 5wt% Pt on sulfided carbon catalyst. Samples were taken every 20 min. ^bin presence of water.

Apart from the desired MVK, many other compounds were also formed during the course of the reaction (Table 10). It is evident from Table 10 (entry 1) that the first sample collected after 20 min-on-stream (in absence of H₂O) has shown considerably high conversion (53%) of ML with only 3% yield of MVK, which is further increased to 10% after 40 min. However, after 60 min-on-stream, the catalyst underwent deactivation (Table 10, entry 3). An explanation for the higher initial activity of the present platinum catalyst could be due to presence of small amounts of sulfur in this Pt/C catalyst because the support is sulfided carbon. These results indicate that the presence of small amount of sulfur seems to be essential for improved activity. In general, it is known that sulfidation is one of the possible methods to reduce coke formation on the catalyst surface.^[182] In addition, the presence of sulfur may retard the reduction of MVK to MEK.

In order to improve the yield of MVK using this sulfided Pt/C catalyst, it was attempted to look for alternative ways to perform the reaction.

Subsequently, the reaction was performed in the presence of water. Interestingly, addition of water to the steam improved both the conversion of ML and the yield of the target products, MVK and MEK, significantly (Table 10, entry 4). Amazingly, the yield of MVK obtained is almost doubled in presence of H₂O steam (i.e. an increase of MVK

yield from 10% to 18%). However, the conversion of ML decreases over time even in the presence of water (Table 10, entry 4 to 6). The differences in the conversion of ML and yield of MVK between the absence and presence of water in the feed could be due to differences in the reaction pathways they follow (Scheme 36). In the absence of water, the reaction seemed to proceed via formation of α -AL, β -AL due to ring closure of ML (i.e. without LA intermediate) followed by decarbonylation (Table 10, entry 1). In the presence of water, the reaction may proceed via *in-situ* generation of LA, which undergoes either decarboxylation to MEK or dehydroxycarbonylation to MVK in subsequent steps Table 10, entry 4). Moreover, the presence of water could also facilitate easy desorption of products and thereby enhance the selectivity (as well as yield) of the targeted product MVK.^[183]

Even though water admixture improved both the yield of the target products and the conversion, it was still not possible to fully overcome the issue of catalyst deactivation. As a result, after 60 minutes of reaction, the catalyst again suffers from deactivation (Table 10, entry 6). In order to understand possible reasons for such deactivation, the spent catalysts were characterized by various techniques. For instance, XPS analysis has shown that the atomic quantity of platinum on the surface decreases from 1.1% in the fresh catalyst to 0.64% in the spent catalyst. This indicates that coke formation is taking place. Interestingly, in the presence of water, the decrease of platinum in the spent catalyst is much lower (0.88%) (see experimental section, Table 18). The BET surface area analysis of spent catalyst has shown that the surface area has been decreased dramatically from 736 m²/g (fresh catalyst) to 225 m²/g in the absence of water and to 455 m²/g in the presence of water (see experimental section, Table 17). This fact suggests that the addition of water also slows down the rapid decrease of surface area of the spent catalyst. In addition, sintering of the platinum particles was also observed. The crystallite size of Pt (estimated from XRD) has been increased significantly from 2 nm (fresh catalyst) to 8 nm in the spent catalyst (see experimental section, Table 20). In order to check the particle size, the fresh and spent catalysts were characterized by TEM analysis (Figure 4). The agglomeration of the particles can easily be seen in picture b corresponding to the spent catalyst.

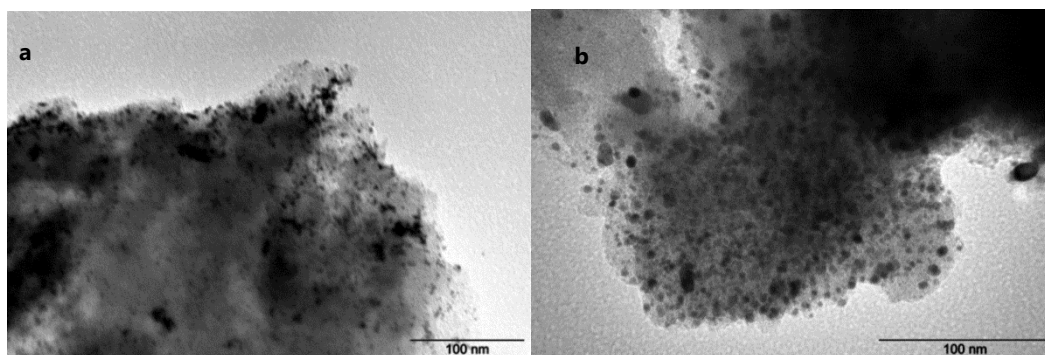


Figure 4. TEM pictures: a) fresh 5 wt% Pt on sulfide carbon b) spent 5 wt% Pt on sulfided carbon.

On the whole, it can be stated that in the spent catalyst

- i) surface area is decreased
- ii) sintering of platinum particles occurred

It was noticed that besides MVK, various other products such as MEK, α -AL, β -AL etc. were also formed in considerable amounts in most of the experiments (Table 10). Based on the products observed in the present study and also based on the proposal of Dumesic and co-workers,^[178] it was decided to investigate all other possible reaction pathways that could possibly be involved during the conversion of ML into MVK. Based on this, a reaction network is proposed as shown in Scheme 36. The first reaction considered is the direct demethoxycarbonylation of ML to MVK, MeOH and CO (Scheme 36, A). This reaction remains until now unreported. However, the catalytic demethoxycarbonylation of p-nitrophenyl esters^[145] and pyridyl esters^[146] as well as the decarbonylation of anhydrides^[144] have been reported and therefore the demethoxycarbonylation seems a feasible reaction.

It is likely that in the presence of water, ML is converted to LA and MeOH (Scheme 36, B) through a known hydrolysis reaction. The formed MeOH can be easily dehydrogenated into first formaldehyde and H₂ and then formaldehyde can be further CO and H₂ as shown in step C of Scheme 36.^[184-185] The catalytic methanol conversion to formaldehyde and H₂ as well as the direct conversion of methanol to CO and two molecules of H₂ has been extensively studied by the group of Beller.^[186-187]

As discussed earlier, LA can be converted to MVK presumably through a dehydroxycarbonylation reaction by removing a molecule of CO and H₂O (Scheme 36, D). An oxidative decarboxylation of LA is not considered in this case because of the absence of oxidant in the reaction media.

The conversion of LA directly to MEK can take place *via* decarboxylation (Scheme 2.3, E).^[125]

In addition, LA can undergo ring-closure to α -AL at elevated temperatures (Scheme 36, F).^[188] At the same time, it is also possible that α -AL can form directly from ML in the presence of H₂ and H₂O (Scheme 36, G).^[189] Furthermore, α -AL can isomerize to β -AL (step H). This isomerization is often a base-catalyzed reaction.^[190]

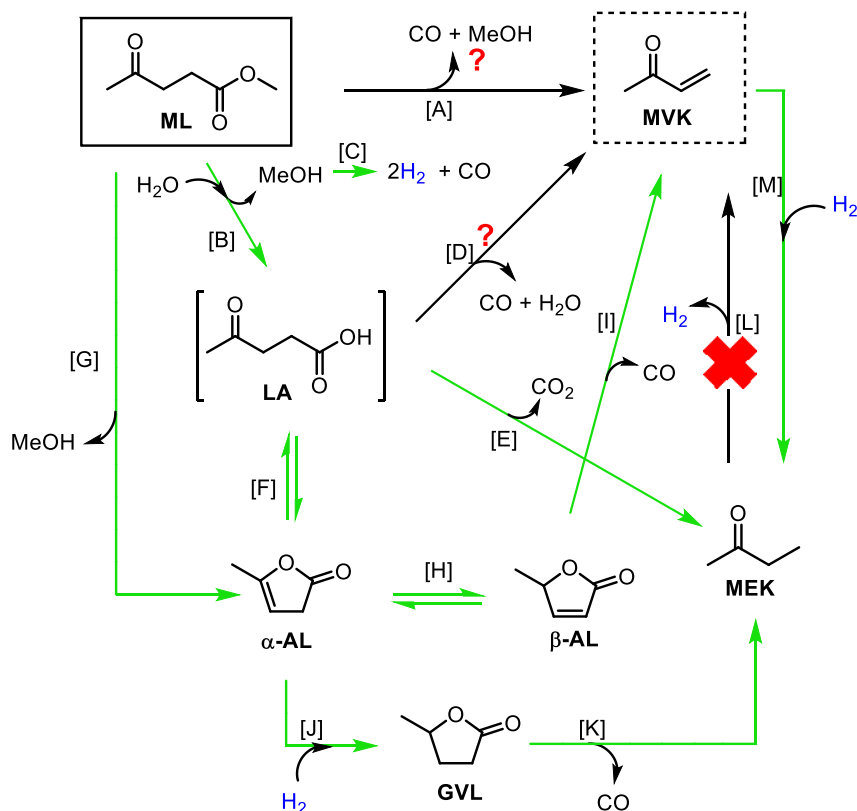
Based on Dumesic's and also earlier work, β -AL undergoes decarbonylation to MVK (Scheme 36, I).^[178]

The decomposition of furanone rings forming CO and corresponding unsaturated carbonyl compounds is reported to happen at high temperatures (>600°C).^[191-193] The authors believe that the mechanism of the ALs decarbonylation proceeds *via* alpha to beta isomerization at 450°C and further decarbonylation at 600°C delivering CO and MVK. Already in the 1975, Skorianetz and co-workers reported the decarbonylation of

α -AL achieving 75% yield of MVK at lower temperatures (475°C) applying a vacuum of 15 Torr.^[191]

In the presence of H₂ (i.e. expected from the decomposition of formed methanol (Scheme 36, C)), α -AL can also partly convert into GVL by hydrogenation (Scheme 36, J), which then undergoes decarbonylation to form MEK (Scheme 36, K). The thermal decomposition of GVL is known to give trace amounts of MVK.^[194] Although it seems not likely, it is speculated that dehydrogenation of MEK can lead to the formation of MVK (Scheme 36, L). At the same time, MVK can also convert back into MEK (Scheme 36, M) under hydrogenation conditions.

To get reliable and corroborative evidence to the above-described reaction network, preliminary experiments were carried out using some putative intermediates as reactants. In particular, α -AL, GVL, and LA were tested as reactants under similar reaction conditions. The results are illustrated in Table 11. At first, the direct decarbonylation of α -AL in the absence and presence of hydrogen in the feed was tested (Table 11, entries 1-3). As expected, in the absence of hydrogen in the feed, the isomerization reaction dominates and as a result β -AL forms as a major product with a yield of 20% at 33% conversion of α -AL (Table 11, entry 1). Additionally, a small amount of MVK (3%) is also formed. However, neither MEK nor GVL are formed, as expected. The addition of hydrogen to the feed completely changed the direction of the reaction giving GVL and MEK as major products with 37% and 46% yields, respectively. In principle, α -AL is hydrogenated first to GVL which is then decarbonylated to MEK (Table 11, entry 2). In addition, the conversion is also enhanced remarkably from 33% (in the absence of H₂) to 94% (in the presence of H₂ in the feed). It is also obvious from entry 3 in Table 11 that a MVK yield of 38% could be obtained along with 16% yield of MEK at a conversion of 84%. The formation of MVK is also expected from the initial isomerization of α -AL to β -AL, which then undergoes decarbonylation to MVK. An explanation for the poor MVK yield at the very beginning of the reaction (Table 11 entry 1) could be attributed to the rapid deactivation of the catalyst in the presence of α -AL.

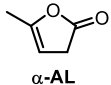
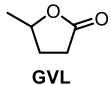
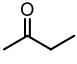
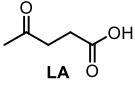


Scheme 36. Proposed reaction pathways for the conversion of ML to MVK. Lines with a red question mark refer to reaction pathways that are not proven experimentally, neither supported by the literature. Lines in green are either experimentally proven and/or known reactions in the literature.

In order to validate the pathway K of Scheme 36, the decarbonylation of GVL under similar reaction conditions was also investigated. It is quite evident from Table 11, entry 4 that GVL can be easily converted to MEK by decarbonylation, which is evidenced from 44% yield of MEK at 64% conversion of GVL. MEK was also used as reactant in order to find whether possible dehydrogenation to MVK takes place. From the results obtained (Table 11, entry 5), it is clear that MEK remained unreacted.

Furthermore, LA as a reactant was also investigated. LA could not be fed in its pure form, because LA is a solid at room temperature. Therefore, LA was dissolved in water and fed to the reactor using an HPLC pump. It was confirmed that LA converts to MVK and to MEK (see Scheme 36, steps D and E). It is also evidenced from this experiment that 35% yield of MVK and 27% yield MEK could be successfully achieved at a LA conversion of 96%. As shown in Scheme 36, LA can be converted to MVK directly through a dehydroxycarbonylation reaction or LA can be first ring-closed to α -AL and further decarbonylated to MVK. MEK can be either coming from the direct decarboxylation of LA or *via* the hydrogenation of MVK.

Table 11. Control experiments for the gas phase conversion of ML.

Entry ^a	Substrate	X [%]	Yield [%]					
			MVK	MEK	α -AL	β -AL	GVL	Others
1	 α -AL	33	3	1	-	20	0	9
2 ^b		94	0	46	6	4	37	1
3 ^c		84	38	16	16	11	0	3
4	 GVL	64	3	44	0	0	-	17
5	 MEK	0	0	-	0	0	0	0
6 ^d	 LA	96	32	26	18	21	0	3

^aSamples taken after 1h. Total flow: 8.8L/h. bed volume: 2 cm³. GHSV: 4400 h⁻¹. 6 mmol/h of substrate in a stream of N₂ as a dilution gas to maintain constant GHSV, 0.65 g of 5wt% Pt on sulfided carbon catalyst. Samples were taken every 20 min. p: 1 bar, Argon as internal standard. p: 1 bar, Temperature 300°C. ^bAfter 4h of reaction, catalyst reactivation with H₂ for 4h. ^cAfter ceasing H₂ flow. ^d50 wt% solution of LA in H₂O. After 4h of reaction.

Based on the results obtained from Table 11 (entry 6), it was realized that the addition of water has a beneficial effect on the formation of LA as a useful intermediate for improving the yield of the desired product, MVK. In view of this, it was decided to further explore the long-term stability of the catalyst using LA as a starting material.

The long-term stability of Pt/C (sulfided) catalyst was investigated for 7 hours-on-stream and the results obtained are depicted in Figure 5. The catalytic test was performed at ambient pressure and at a reaction temperature of 250°C. Interestingly, the conversion of LA achieved was $\geq 90\%$ throughout. However, the product distribution is observed to change considerably with time. It is evident from Figure 5 that MEK was the major product initially, which, however, decreases over time. MEK yields up to 60% could be achieved initially. Quite interestingly, the yield of MVK is increasing with time at the expense of MEK reaching approximately a 1:1 ratio after 4 hours-on-stream. The hydrogenation of MVK to MEK in the first instance can be the explanation for the initial MEK formation. In this case the hydrogen can be formed from CO and water *via* the water-gas shift (WGS) reaction .^[195]

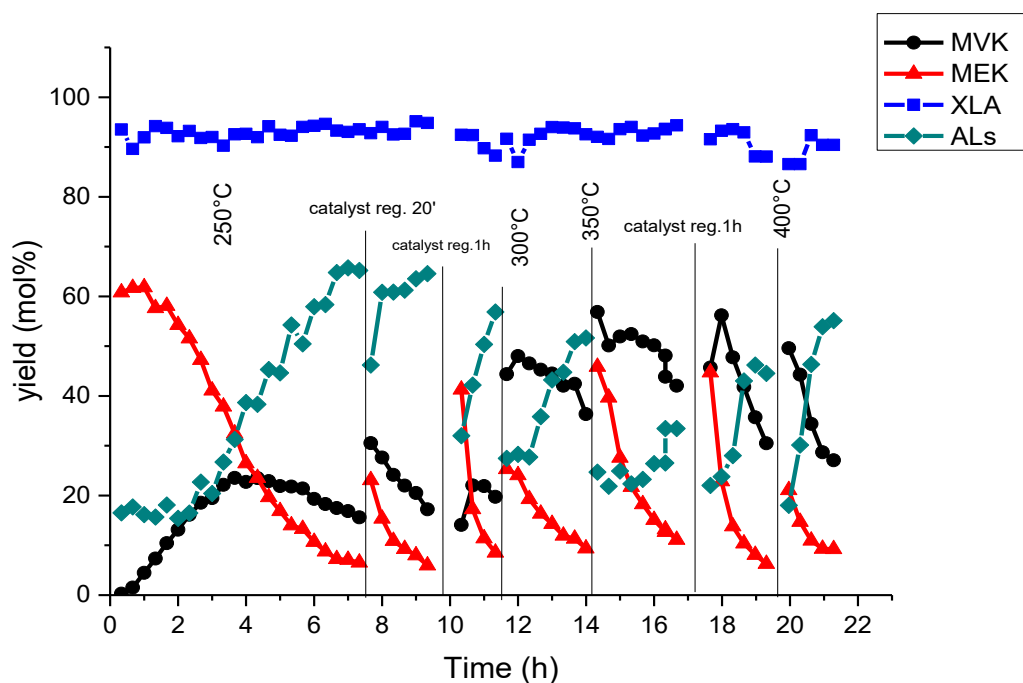


Figure 5. Time-on-stream behavior of Pt/C catalyst and the effect of reactivation on the yields of MVK and MEK from LA. (LA: 6 mmol/h, Total flow: 8.8L/h, cat. bed volume: 2 cm³, GHSV: 4400 h⁻¹, Argon was used as an internal standard, p: 1 bar)

It is notable that the yield of MVK remained more or less the same (over 20%) from 3 hours to nearly 6 hours-on-stream. The probable reason for this behaviour is the deactivation of the active sites able to perform the WGS reaction or those responsible for the hydrogenation of MVK to MEK. After that, the ring closure of LA to ALs takes place mainly.^[188] Once the catalyst is deactivated, the decarbonylation of ALs is no longer occurring and ALs yields start increasing while MVK and MEK yields decrease. It is clear from Figure 5, that over time the active sites responsible for the conversion of LA to MVK/MEK seemed to become inactive and hence the only reaction that takes place at this stage is the ring closing of LA to ALs. Once the yields of target product (MVK) reduced and ALs became predominant after 7 hours-on-stream, the reaction was stopped, and the catalyst was reactivated in a stream of hydrogen for 20 min in the first cycle at 250°C. The idea was to reactivate the catalyst in order to modify the product distribution in a desired way. It should be noted that the spent catalyst (after 7 hours-on-stream) was re-activated without unloading it from the reactor in a stream of hydrogen and continued testing at the same temperature (250°C). It was indeed interesting to examine the behaviour of this reactivated catalyst in hydrogen stream. To our surprise, the yields of both MVK and MEK improved to a large extent initially. At this stage, the MVK yield increased from 16% to over 30% while the MEK yield enhanced from 7% to 23%, respectively. Nevertheless, this improvement in initial yields could not be

maintained for longer times. In other words, the improved yields of MVK and MEK after reactivation decreased rapidly within one hour. After we found this rapid decrease in yields of target products, one more effort to reactivate the catalyst with H₂ was made. However, in this effort, the reactivation time was prolonged for a period of 1 hour instead of earlier 20 min, but the temperature was again 250°C. The idea of reactivation worked well to a considerable extent to modify the product distribution in a desired way.

It was observed that after 1 h of reactivation, the catalyst behaviour was exactly the same as 4 h after the start of the reaction. This means that the hydrogen is able to reactivate the catalyst presumably by partial removing coke deposits from the catalyst surface.^[196]

Another idea was to increase the reaction temperature from 250 to 300°C and check its influence on the product distribution. Such rise in reaction temperature has shown highly pronounced promotional effect on the yield of MVK, which has been increased to 45%. However, such rise in temperature has not shown any beneficial effect on the yield of MEK, which remained more or less the same. In any case, the yields of both products were observed to decrease again in a similar manner. When it was realized that there is a clear beneficial effect of temperature on the yield of MVK in particular, the reaction temperature was again raised to 350°C and the reaction was continued. Amazingly, the yield of MVK enhanced to 54%, while only a slight increase in the yield of MEK was detected. This result prompted us to raise the reaction temperature further to 400°C from 350°C. Unfortunately, this rise in reaction temperature to 400°C did not improve the yields of the target products. It rather caused a significant decrease in the yield of MVK. Based on these results, it appears that a reaction temperature of 350°C is optimum for obtaining higher yields of MVK. It is notable that such an increase in the yield of MVK is limited to initially one or two hours and after that the reaction is moving in an unwanted direction where ALs are the major products due to ring closure of LA.

It was decided then to study the activity of the catalyst starting at higher temperature (350°C) under the same reaction conditions. Time-on-stream behaviour of the Pt/C catalyst tested at 350°C is portrayed in Figure 6.

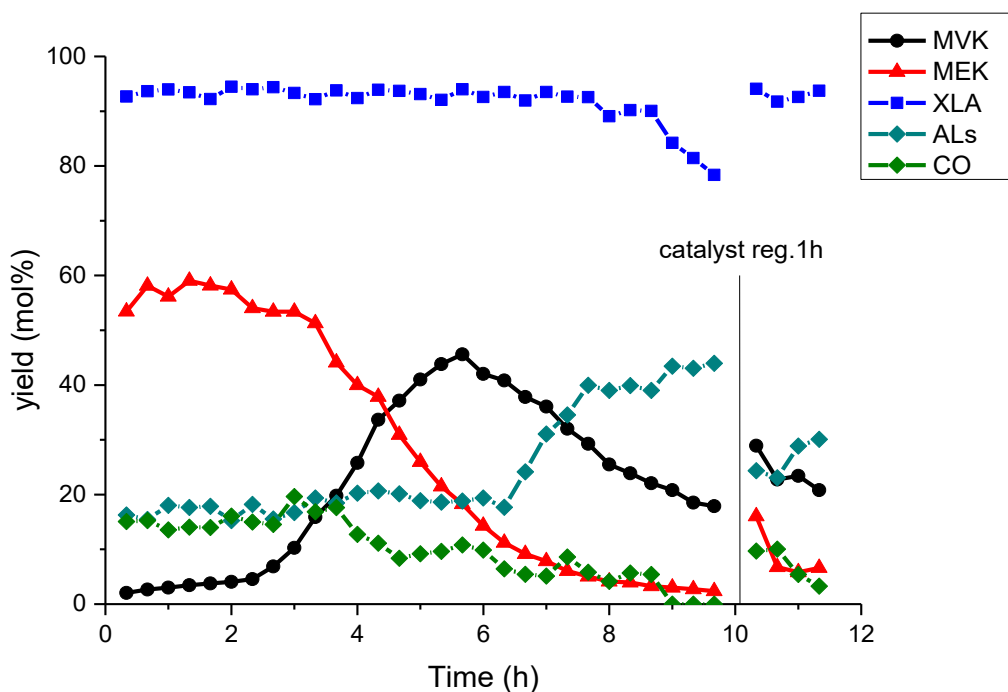


Figure 6. Time-on-stream stability of Pt/C catalyst and the effect of temperature on the yields of MVK and MEK from LA at 350°C.

At 350°C, it was observed that within the first 4 hours-on-stream, the catalyst behaviour was very similar to the results that were observed at 250°C. In this case, the yield of MVK was very low in the first 2 hours-on-stream, which then increased progressively, reaching a maximum of nearly 50% after 6 hours-on-stream. On the other hand, the yield of MEK was very high initially (i.e. for the first two hours), and then decreased continuously over time. In any case, the yields of both MVK and MEK decreased at the end. At this point, it was observed that the yields of angelica lactones started increasing, meaning that the ring closure of LA to angelica lactones becomes predominant. After 8 hours on stream, the conversion of LA was observed to decrease from 93% to 74% (Figure 6). During this experiment the analysis and quantification of CO was also carried out. It was noticed that the CO was formed at the beginning of the reaction in about 20% yield and over the period, it was observed to decrease slowly.

An attempt to reactivate the catalyst in a H₂ stream was done for a period of 1h. After that a slight increase in the yields of MVK and MEK was observed. Again, the yields of target products decreased while the yields of angelica lactones began to increase.

It is clear that no fast catalyst deactivation occurred when LA was used as the substrate compared to ML. The absence of methanol formation when LA was used as reactant could be one possible explanation for the relatively better stability of the catalyst. In fact, methanol could be a potential source of CO and at the same time CO can also form from the decarbonylation of ALs. Both ALs and CO formation can poison the catalyst

and causes deactivation as in the case where ML was used as a reactant (cf. Table 10). In all the cases, MVK polymerization can take place and contribute to the coke formation. The temperature effect also shows an important trend. The higher the temperature, the higher the desired product yields especially in the case of LA as a feedstock.

3.4. Conclusion

- This study has shown the possibility of the valorisation of ML to MVK for the first time. A yield of the desired product (MVK) of up to 18% could be achieved from ML using 5wt% Pt on sulfided carbon as catalyst in a gas phase continuous reaction. However, the yield of MVK could not be sustained for more than a few hours because of catalyst deactivation.
- MEK was another product which could be made from ML in up to 15% yield. To the best of our knowledge, this is the first study concerning the production of MVK and MEK from ML.
- Results revealed strong evidence that the formation of MVK from ML is occurring by means of three different reactions such as demethoxycarbonylation of ML, dehydroxycarbonylation of LA and ALs decarbonylation.
- The reaction temperature was found to play a key role in the product distribution. Higher reaction temperatures favour the formation of MVK while lower temperatures promote the formation of MEK.
- In order to improve the yield of MVK, the effect of H₂O-admixture was explored. This study revealed that in the presence of water the reaction may run *via* formation of LA as an intermediate. LA ring-closing to ALs has been observed and the catalytic decarbonylation of the latest leads to the formation of MVK.
- During the long-term experiments, MEK was formed in higher amounts at the beginning of the reaction, while MVK yields started increasing over the time. This indicated that MEK is most likely to be formed from the *in-situ* hydrogenation of MVK.
- At 350°C, up to 57% yield of MVK was successfully obtained from LA. This is indeed a remarkable outcome of this study. The hydrogenated product MEK was

formed in 62% yield at 250°C. It is believed that the presence of H₂ coming from methanol decomposition (when ML is used as reactant), or from the WGS reaction in the case of LA, could cause the hydrogenation of MVK to MEK.

- The characterization of the spent catalyst revealed a decrease of the surface area presumably due to coke formation and an increase of particle size due to sintering of the metal particles. The deactivation of the catalyst took place rather fast, more likely due to side products, such as MVK polymers or carbon monoxide, known to poison the catalyst's active sites.
- Even though considerably high yields of MVK and MEK from ML for the first time were achieved, there is still a lot to be done to improve yields and enhance long-term activity of the catalysts.

4. Chapter 3: Preparation of methyl acrylate from biomass-derived methyl levulinate

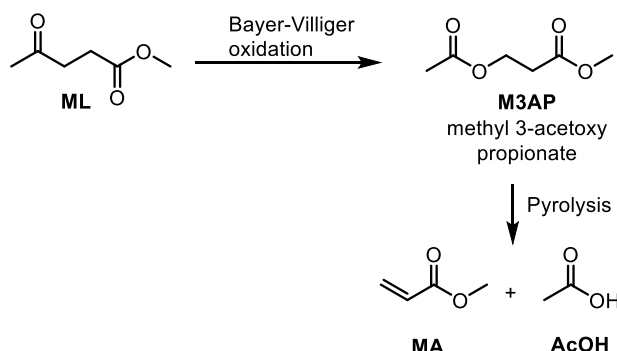
4.1. Introduction

Acrylates are well-known monomers with a wide range of applications. In particular, methyl acrylate (MA) is known to be used, apart from chemical synthesis, in the production of adhesives, inks, coatings and plastics among others. The industrial production of MA follows the one step aldol condensation of methyl acetate and formaldehyde.^[197]

Starting from renewable sources, various methods for the synthesis of MA have been reported.^[198] For example, MA can be directly prepared from 3-hydroxypropionic acid, obtained by fermentation, and methanol.^[199] Another route towards MA synthesis is the reaction of acrolein, obtained from glycerol,^[200-202] with methanol in the presence of an oxidant to form the desired compound.^[203] A direct synthesis of MA can be achieved starting from 3-hydroxypropionic acid (which is prepared by fermentation) and methanol.^[199] An alternative pathway is the dehydration of 3-hydroxypropionic acid to acrylic acid (AA) first,^[199, 204-205] following esterification to afford MA. From renewable methyl lactate, MA can be achieved in 2 steps, but this conversion suffers from poor yields due to competitive side reactions during the catalytic dehydrogenation step.^{[206],[207],[208]} Another example of renewable MA preparation is the condensation of methyl acetate with formaldehyde.^[209] In fact, acetic acid itself can be converted to AA via the reaction with formaldehyde,^[210] which can be esterified afterwards. So far none of these processes have been implemented on large scale.

4.2. Objectives

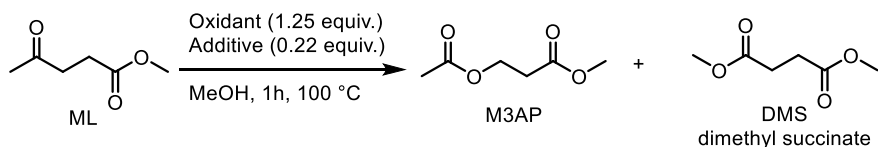
The aim of this part of the investigation was to explore the Baeyer-Villiger (BV) oxidation ^[151-153] of methyl levulinate (ML), which is a side stream of Avantium's 2,5-furandicarboxylic acid process, to methyl 3-acetoxypropionate (M3AP) followed by acetic acid elimination in the gas phase to form MA and AcOH (Scheme 37).



Scheme 37. MA and AcOH from bio-based ML.

4.3. Results and discussion

The conversion of ML to M3AP through a well-known BV oxidation was the starting point of this project. Based on the literature, oxidants such as *meta*-chloroperoxybenzoic acid or simple aqueous H₂O₂ in the presence of additives as for example Lewis acids are able to oxidize methyl ketones to the corresponding acetates. Although the BV oxidation (using H₂O₂/trifluoroacetic anhydride) of benzyl levulinate to benzyl 3-acetoxypropionate was reported to proceed in 63% isolated yield,^[211] in the attempted BV oxidation of ML, only mixtures of compounds with *meta*-chloroperoxybenzoic acid (*m*CPBA) or H₂O₂ catalysed by acids were obtained (Table 12).

Table 12. BV oxidation of ML using peroxides.

Entry ^a	Oxidant	Additive	[X] _{ML} %	Yield [%]				
				DMS	M3AP	α-AL	LA	AcOH
1	<i>m</i> CPBA	—	18	0.4	0	19	4.7	2
2	<i>m</i> CPBA	NaHCO ₃ buffered	9	0.1	0	4	0.1	2
3	<i>m</i> CPBA	AlCl ₃	10	0.2	0	0	1.8	6
4	<i>m</i> CPBA	NaHCO ₃ buffered/AlCl ₃	2	0.1	0	4	0	1
5	<i>m</i> CPBA	NaHCO ₃ buffered/AlCl ₃ /BF ₃ on silica	2	0.1	0	3	0.1	0
6	H ₂ O ₂ (30% aq)	AlCl ₃	11	0.2	0	7	0.3	1
7	H ₂ O ₂ (30% aq)	2Na ₂ CO ₃ . 3H ₂ O ₂	9	0.2	0	5	0.1	1
8	H ₂ O ₂ (30% aq)	AlCl ₃	20	0.1	0	4	0.3	0
9	H ₂ O ₂ (30% aq)	BF ₃ on silica	8	0.1	0	3	0.2	2
10	H ₂ O ₂ (30% aq)	AlCl ₃	12	0.2	0	0	0.2	1

^a α-AL: alfa angelica lactone, LA: Levulinic acid, AcOH: Acetic acid. General conditions: 0.4 mmol ML, 0.5 mmol of oxidant, 0.1 mmol of additive. Reactions carried out for 1 h at 100°C under 20 bars of synthetic air. Determined by gas and liquid chromatography (dioxane and pyroglutamic acid as respective external standards).

It was found that Mascall and co-workers reported that the BV oxidation reaction of levulinic acid gives mixtures of succinic acid and 3-hydroxypropionic acid, but the later undergoes a retro-aldol reaction to finally form AcOH and formaldehyde.^[156]

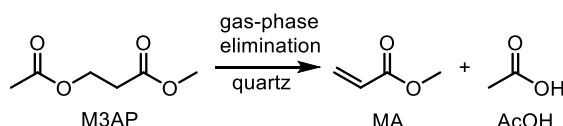
Recently a good enzymatic procedure was published by Fink and Mihovilovic. The authors were able to perform the BV oxidation of ML to (M3AP in 80% yield using a Bayer-Villiger monooxygenase.^[157] The fact that this procedure uses

oxygen instead of hydrogen peroxide as oxidant, makes this process a potential scalable chemistry.

While ML to M3AP route is established, it was decided to explore the gas-phase pyrolysis of M3AP to MA (Scheme 37). The reaction did not require any catalyst – it was performed by flowing gasified M3AP (diluted with nitrogen) through a quartz tube at various temperatures (300-600 °C).

The results of the gas-phase elimination of acetic acid from M3AP are shown in Table 13.

Table 13. Gas-phase elimination of acetic acid from methyl 3-acetoxypropanoate.



Entry ^a	T, °C	[X] _{M3AP} % ^b	Yield [%]	
			MA	AcOH
1	300	0	-	-
2	400	0	-	-
3	500	49	46	46
4	550	58	58	56
5	600	99	98	97

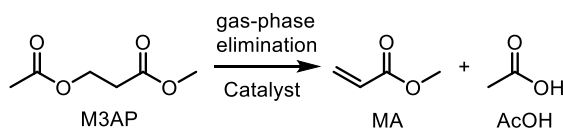
^a General condition: continuous flow of the gas-phase M3AP (0.5 ml h⁻¹, 3.8 mmol h⁻¹) and N₂ gas (20 ml min⁻¹) through a quartz tube filled with 7 cm³ quartz pieces at the reaction temperature. Total flow: 1.3 L h⁻¹. M3AP:N₂ molar ratio was 1:13. The GHSV was 183 h⁻¹. Contact time 20 s. The resulting conversions and yields were calculated by GC and ¹H-NMR.

At 400 °C or lower temperatures, the reaction did not work (Table 13, entries 1 and 2). Partial conversion of M3AP occurred at 500 °C and 550 °C (Table 13, entries 3 and 4). When the temperature was raised to 600 °C, 99% of M3AP was converted. Under these reaction conditions MA and AcOH were obtained in almost quantitative yields (98% and 97% respectively) (Table 13, entry 5). Furthermore, all these experiments have shown clean spectra with no other side products. Both products, MA and AcOH, are easily separable by distillation.^[212]

Catalytic attempts to eliminate acetic acid from M3AP

Aiming to lower the reaction temperature, catalytic tests were performed. For that, 1 wt% Pd on Al₂O₃ and Amberlyst 15 were tested under the same flow rates at temperatures between 300 °C and 500 °C. The results are shown in Table 3.3.

Table 14. Catalytic elimination of acetic acid from methyl 3-acetoxypropanoate.



Entry ^a	Catalyst	T, °C	[X] _{M3AP} % ^b	Yield [%]	
				MA	AcOH
1	1 wt% Pd /Al ₂ O ₃	300	24	20	19
2	1 wt% Pd /Al ₂ O ₃	400	49	40	31
3	1 wt% Pd /Al ₂ O ₃	500	89	48	35
4	Amberlyst 15	300	47	13	15

^a General conditions: continuous flow of the gas-phase M3AP (0.5 ml h⁻¹, 3.8 mmol h⁻¹) and N₂ gas (20 ml min⁻¹) through a tube filled with 1 cm³ bed volume (200 mg) of the corresponding catalyst at the reaction temperature. Total flow: 1.3 L/h. M3AP:N₂ molar ratio was 1:13. The GHSV was 1284 h⁻¹. Contact time 3 s. The resulting conversions and yields were calculated by GC.

The use of 1 wt% Pd /Al₂O₃ resulted in 24 % conversion of M3AP at 300 °C. Under these conditions, up to 20% yield of MA and 19% yield of AcOH were obtained (Table 14, entry 1). However, unlike in the pyrolysis experiments, side products were already detected. When the temperature was raised to 400°C, using the same catalyst, the conversion was increased to 49% achieving 40% yield of MA and 31% yield of AcOH (Table 14, entry 2). At 500°C, although 89% conversion of M3AP was obtained, the yields of MA and AcOH were 48% and 35% respectively (Table 14, entry 3).

The acidic catalyst Amberlyst 15 has shown higher activity than 1 wt% Pd /Al₂O₃ catalyst (Table 14, entry 4) at 300°C, nevertheless the yields of the desired products MA and AcOH were lower. In all catalytic experiments, the main side product is methyl acetate (determined by GC-MS). The conversion of acetic acid to CO₂ and methane can be the explanation for the low acetic acid selectivity.

4.4. Conclusion

- The Baeyer-Villiger oxidation of ML using peroxides and acids was unsuccessful resulting in mixtures of compounds.
- The gas-phase pyrolysis of methyl 3-acetoxypropionate results in almost quantitative yields of methyl acrylate (98%) and acetic acid (97%). No other side products were detected by GC analysis.
- Catalytic experiments afforded the desired products already at 300°C. However, even at lower temperature methyl acetate side product was detected. None of the catalytic attempts delivered MA and AcOH in high selectivity at high conversion of M3AP.
- This study allows the simultaneous production of these two industrially important molecules via a two-steps process starting from methyl levulinate. Hence, this is a green and 100% atom efficient way to utilise this side stream compound to useful chemicals.

5. Thesis summary

This work aimed at the valorization of bio-refinery side stream methyl levulinate (ML) to methyl vinyl ketone (MVK) and methyl acrylate (MA) monomers (as shown in Figure 7).

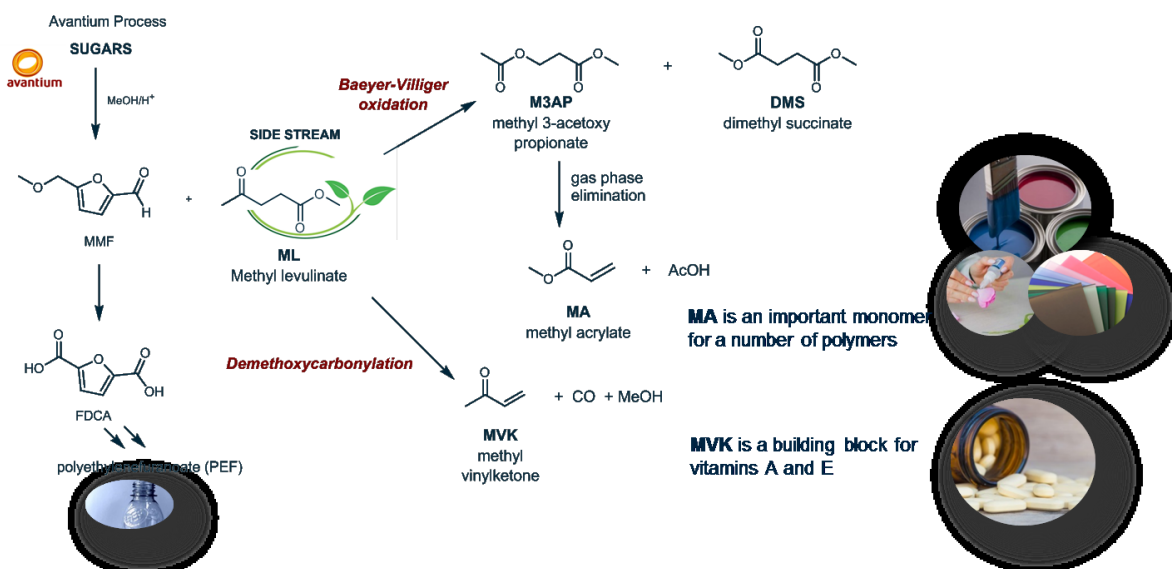


Figure 7. The overview of the project.

The catalytic demethoxycarbonylation of ML using palladium-phosphine based catalyst system was proposed as a promising reaction to convert ML to MVK, methanol (MeOH) and carbon monoxide (CO) in the liquid phase.

It was observed that the reaction does not take place under mild reaction conditions. Harsher reaction conditions were attempted at which mainly catalyst decomposition took place. Attempts to activate the methyl ester moiety have also been carried out. Upon further derivatization of ML to the corresponding *para*-nitrophenyl ester, pyridyl ester and to levulinic anhydride, the corresponding catalytic transformation starting from each ML derivative did not deliver more than traces of MVK. It was found that the ketone function present in the molecule plays an important role in the catalyst deactivation. It was decided to switch from homogeneous to heterogeneous catalysis in order to be able to increase the reaction temperature. High throughput screening of several heterogeneous catalysts on the demethoxycarbonylation of ML was executed. It was found that MVK polymerizes in the liquid phase for which reason a gas-phase reaction was established. After promising results were obtained during the high throughput screening it was found that the best catalyst (5 wt% platinum on sulfide

carbon) did show the desired activity and some selectivity to MVK. Although the catalyst is able to convert ML to MVK, only 18% yield was obtained and this could not be further improved due to side reactions that resulted in catalyst deactivation (for example, the MeOH formed in the reaction was dehydrogenated to formaldehyde and hydrogen). To have a better understanding of the reaction mechanism, side products were fed as reactants. This study revealed that in the presence of water the reaction may run *via* formation of levulinic (LA) as an intermediate. LA ring-closing to angelica lactones has been observed and the catalytic decarbonylation of the latest leads to the formation of MVK. Starting from LA, at 350°C, up to 54% yield of MVK was successfully obtained.

The second aim of this project was the conversion of ML to MA. Initially, Baeyer-Villiger (BV) oxidation was attempted using the established procedure. This resulted in mixtures of undesired compounds. Fortunately, the enzymatic BV oxidation of ML to M3AP has been reported occur in 80% yield. With the route from ML to M3AP secured the gas-phase pyrolysis of M3AP was examined. This reaction delivered MA in 98% yield and acetic acid in 97% yield at 600°C. The use of acidic catalysts in the gas-phase pyrolysis of M3AP resulted in higher yields at lower temperatures but the reaction suffered from poor selectivity.

In conclusion, although the direct gas-phase conversion of ML in the presence of water delivered MVK in up 18% yield for the first time, deeper studies on the catalyst nature and *in situ* characterization must be carried out in order to gain deeper understanding on the reaction mechanism and catalyst deactivation. On the other hand, the study on the conversion of ML to MA allows the production of MA and acetic acid *via* a two-steps process. Hence, this is a green and 100% atom efficient way to utilize this side stream compound to prepare these useful chemicals.

6. Experimental work and data analysis

6.1. Chapter 1

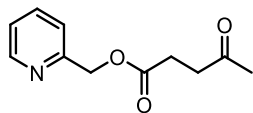
6.1.1. General considerations

All reactions were carried out in dried glassware with magnetic stirring under argon atmosphere, unless otherwise stated. Reaction solvents (Toluene and DCM) were obtained from a solvent purification system (SPS) and stored under argon. Dry and degassed DMPU and NMP solvents were purchased from sigma Aldrich. Commercially available chemicals were purchased from Sigma, Alfa, Strem, Abcr and TCI. Starting material ML was purchased from Sigma Aldrich and purified by distillation from PPh_3 in order to remove peroxides and other impurities. LA was purchased from Sigma Aldrich and used without further purification. NMR spectra were recorded on Bruker AV 300 MHz and Bruker AV 400 MHz spectrometers. ^1H and ^{13}C -NMR spectra were referenced to residual solvent peaks of chloroform-*d* (7.26 ppm 77.1 ppm respectively). All chemical shifts are reported in ppm, coupling constants in Hz. Abbreviations are s: singlet, d: doublet, t: triplet, q: quadruplet, quin: quintuplet, m: multiplet, br: broad. GC-FID analyses were carried out on an Agilent 7890B GC system with a HP-5 normal-phase silica column, using He as a carrier gas and dodecane as internal standard. GC-MS spectra were recorded with a combination of an Agilent Technologies GC Mass 5973 Network MSD and an Agilent Technology 6890N Network GC System. HR-MS measurements were recorded on an Agilent 6210 time-of-flight LC/MS (ESI) or on Thermo Electron MAT 95-XP (EI, 70 eV). Peaks as listed correspond to the highest abundant peak and are of the expected isotope pattern.

6.1.2. Experimental procedures and analytical data

Substrate syntheses

Pyridin-2-ylmethyl 4-oxopentanoate

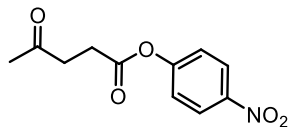


In a flame-dried Schlenck flask equipped with distillation setup, ML (5.0 mL, 4.7 g, 36.0 mmol) and 2-hydroxymethylpyridine (5.5 mL, 6.2 g, 56.0 mmol) were added to a suspension of KO^tBu (450.0 mg, 4.0 mmol) in toluene (30 mL) under argon atmosphere. The orange reaction mixture was heated to 100 °C overnight, after which the solvent was removed under reduced pressure, and the residue was purified by column

chromatography (EtOAc/heptane 1:2 on SiO₂), yielding the desired compound (6.6 g, 32.0 mmol, 89 %) as a colorless oil; ¹H-NMR (CDCl₃, 300 MHz): δ 8.54 (d, 1H, ²J = 4.5 Hz), 7.65 (t, 1H, ³J = 7.7 Hz), 7.30 (d, 1H, ²J = 7.8 Hz), 7.17 (m, 1H), 5.19 (s, 2H), 2.84-2.68 (m, 4H), 2.18 (s, 3H); ¹³C-NMR (CDCl₃) δ 173.7, 156.3, 149.3, 136.2, 122.4, 127.1, 79.4, 67.4, 58.5, 40.7, 28.2;

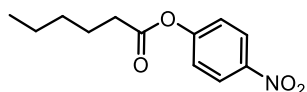
ESIHRMS for C₁₄H₁₇NO₃: calculated 247.1209 Found: 247.1215.

4-nitrophenyl 4-oxopentanoate



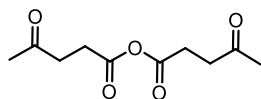
LA (200.0 mg, 1.7 mmol) and *p*-nitrophenol (240.0 mg, 1.2 equiv.) were dissolved in DCM (5 mL). Then the reaction was cooled to 0°C. EDC-HCl (396.0 g, 1.2 equiv.) and DMAP (6.0 mg, 3.0 mol%) were added slowly to the solution. The reaction was left stirring at room temperature for 2h. After completion of the reaction was confirmed by TLC (EtOAc/heptane 1:1), the mixture was quenched using a 5% NaH₂PO₄ solution and the product was extracted with ethyl acetate. 285 mg of a bright yellow liquid was obtained (1.2 mmol, 70% yield). ¹H-NMR (CDCl₃, 400 MHz): δ 8.24 (d, 2H, ²J = 6.5 Hz), 7.55 (d, 2H, ²J = 7.0 Hz), 2.89 (m, 2H), 2.82 (m, 2H) 2.23 (s, 3H); ¹³C-NMR (CDCl₃) δ 207.7, 201.7, 170.1, 156.4, 145.7, 122.5, 122.3, 39.5, 37.6, 27.3. ESIHRMS for C₁₁H₁₁NO₅: calculated 237.2087, found: 237.2091.

4-nitrophenyl hexanoate



The same procedure as described above was applied using hexanoic acid (1.7 mmol) instead of LA. 321.0 mg of a yellow liquid was obtained. (1.4 mmol, 79% yield). ¹H-NMR (400 MHz, CDCl₃): δ 8.00 (dd, ³J = 8.0, 2.0 Hz, 1H), 7.57 (ddd, ⁴J = 8.0, 2.0 Hz, 1H), 7.31 (ddd, J = 7.5, 1.3 Hz, 1H), 7.15 (dd, ³J = 8.0, 1.3 Hz, 1H), 2.56 (t, ³J = 7.5 Hz, 2H), 1.73-1.66 (m, 2H), 1.38-1.25 (m, 4H), 0.85 (t, ³J = 7.0 Hz, 3H). ¹³C-NMR (CDCl₃): δ 171.3, 144.1, 141.8, 134.7, 126.5, 125.7, 125.2, 77.5, 77.1, 76.8, 33.9, 31.1, 24.1, 22.3, 13.9. ESIHRMS for C₁₂H₁₆NO₄: calculated 238.2641 found: 238.2665.

4-oxopentanoic anhydride



LA (881.0 mg, 7.6 mmol) was added at 0°C to a solution of DCC (888.0 mg, 4.3 mmol) in DCM (20 mL). After stirring for 5 min at room temperature, the mixture was cooled (0°C) and filtered, and the urea precipitate was washed three times with DCM (4 mL)

under argon to give 32 mL of a 0.2M Levulinic anhydride solution. After solvent evaporation, the material left was isolated in near quantitative yield (1.3 mg, 6 mmol, 78% yield) and was immediately used in the decarbonylation reaction. $^1\text{H-NMR}$ (400 MHz, CDCl_3): δ 2.68 (t, $^3J = 8.0, 2.0$ Hz, 4H), 2.59 (t, $^3J = 8.0, 2.0$ Hz, 4H), 2.12 (s, 6H)

Catalytic experimental procedures

General procedure for the catalytic demethoxycarbonylation of ML

In a flame dried Schlenk flask, $\text{Pd}_2(\text{dba})_3$ (18.0 mg, 0.02 mmol) or NHC-Pd (69.0 mg, 0.1 mmol), the corresponding ligand (0.048 mmol) and ML (52 mg, 0.4 mmol) were dissolved in DMPU (5 mL). Dodecane (150 μL) was added as internal standard. The reaction mixture was heated to 160 $^\circ\text{C}$ and stirred over magnetic stirring for 2h. The reaction was monitored by TLC.

General procedure for the catalytic reductive decarboxylation of pyridyl esters

Pyridin-2-ylmethyl 4-oxopentanoate (44.0 mg, 0.2 mmol) was added in a flame dried Schlenk tube. A solution of 5 mol% catalyst ($\text{Ru}_3(\text{CO})_{12}$, Pd PEPPSI or $\text{Ni}(\text{dppb})$) in the corresponding solvent (1,4-Dioxane or NMP) (1 mL) was added to the substrate. The reaction was heated to 160 $^\circ\text{C}$ in an oil bath and left stirring for 16h while monitoring by TLC (thin layer chromatography). The composition of the reaction mixture was analyzed by ^1H NMR spectroscopy and Gas Chromatography.

General procedure for the catalytic decarbonylation *p*-nitrophenyl esters

In a flame-dried Schlenk flask, 4-nitrophenyl 4-oxopentanoate, (42.0 mg, 0.2 mmol) was added. A solution of PdCl_2 (3.0 mg, 0.02 mmol) and LiCl (7.0 mg, 0.2 mmol) in NMP (1 mL) was added. The reaction was heated to 160 $^\circ\text{C}$ and left stirring for 16 h. The composition of the reaction mixture was analyzed by $^1\text{H-NMR}$ spectroscopy and GC.

Decarbonylation of levulinic anhydride

Levulinic anhydride (1.2 mg, 6 mmol) was added to a solution of NiI_2 (186.0 mg, 0.59 mmol) and DPPB ligand (252.0 mg, 0.59 mmol) in NMP (10 mL). KI (989 mg, 5.96 mmol) was added later next to the mixture. The Schlenk was then connected to a short distillation pathway set under argon. A collecting flask was installed at the end of the distillation set-up and was cooled below 0 $^\circ\text{C}$. The reaction mixture was heated to 180 $^\circ\text{C}$ in an oil bath. After 2h under stirring conditions, no products were observed in the collection flask. The reaction mixture was analyzed by GC-MS.

Preparation and application of Pd supported NPs for the decarbonylation of ML

Preparation of 1% PdNP (1.0%)/Al₂O₃ and 1% PdNP (1.0%)/Al₂O₃ with 8% K

Palladium (II) nitrate (240.0 mg) was dissolved in methanol (10 mL) of (in the case of 8% potassium doped catalyst, 143.0 mg of potassium carbonate were added). Mesoporous gamma alumina powder (γ -Al₂O₃) was added. The mixture was submerged in an ultrasonic bath for 30 min. Excess of methanol solvent was evaporated on oil bath at 120 °C and then the mixture was left drying at room temperature during 16h. The material was calcined inside a calcination oven at 450°C for 4h under 20 ml/min flow of hydrogen.

General procedure for the heterogeneous Pd-catalyzed decarbonylation of ML

In a glass pressure tube, the corresponding catalyst (104,0 mg), ML (525,0 mg, 4.0 mmol) and solvent (3mL) were added. The reaction was heated to 180°C and left stirring for 16h. The composition of the reaction mixture was analyzed by ¹H-NMR spectroscopy and GC

High throughput screening of supported catalysts for the decarbonylation of ML and LA.

Quick catalyst screening set-up considerations

The Avantium's quick catalyst screening apparatus consists of stainless-steel blocks with up to 12 reactors (Figure 8, a), equipped with Teflon liners and magnetic stirrings. The maximum pressure the block can reach is 100 bars. The temperature is controlled by a heating box adapted with heat controllers (Figure 8, b) with a maximum temperature of 250°C. A range of gases can be used (N₂, CO, O₂). Up to 72 parallel reactions can be performed simultaneously.



Figure 8. QCS equipment. a) Reactor block, b) heating box.

General procedure for the heterogeneous Pd-catalyzed decarbonylation of ML

In a reactor block containing 12 consecutive 4 mL stainless-steel reactors (Figure 8, a), 30 mg of catalyst, 123 mg of ML and 3mL of toluene were added in each reactor. The reactor block was then sealed with screws, flushed three times with 5 bars of nitrogen and finally pressurized with 20 bars of nitrogen. The reactor block was subsequently placed in the pre-heated heating block (Figure 8, b). The reaction was left stirring for 6h with the stirring speed of 1000 rpm. The block was then cooled in an ice bucket and the gas pressure was released. After that, the reactor block was slowly opened and the samples from the reactors were filtered through a membrane filter into glass vial. The clear liquid was used for GC analysis. The external standard (acetophenone) was added. All standards and samples were analyzed by gas chromatography using a Trace 1310 GC-FID system. A total of 192 reactions were performed, including blanks, duplicates and repeats.

6.2. Chapter 2

6.2.1. Experimental procedures and analytical data

Avantium's gas-phase high throughput equipment

A Flowrance set-up was adapted for the gas-phase demethoxycarbonylation of ML under the desired reaction conditions and taking into account safety considerations (Figure 9). Two consecutive GCs equipped with FID and TCD detectors were installed. The calibration of the gaseous components such as CO, CO₂, He and CH₄ were done using a calibration bottle (Table 15). The liquid substances, ML, LA, lactones, methanol, MVK and MEK were calibrated and the corresponding response factors were calculated based on heptane carbon response factor (Table 15). The unit is equipped with mass flow controllers (MFC) for feeding N₂, He and H₂. Two HPLC pumps are used to pump the liquid through the reactors. Glass chips are small glass plates with little holes that distribute the gas and the liquid homogenously through the reactors. The flowrance unit has 4 reactor blocks which are independently heated to a maximum temperature of 500°C. Each reactor block contains 16 parallel stainless-steel reactors (2 mm diameter and 12 cm length). One of the reactors is used for blank and by-pass during pre-treatment, heating and stabilization of the system.

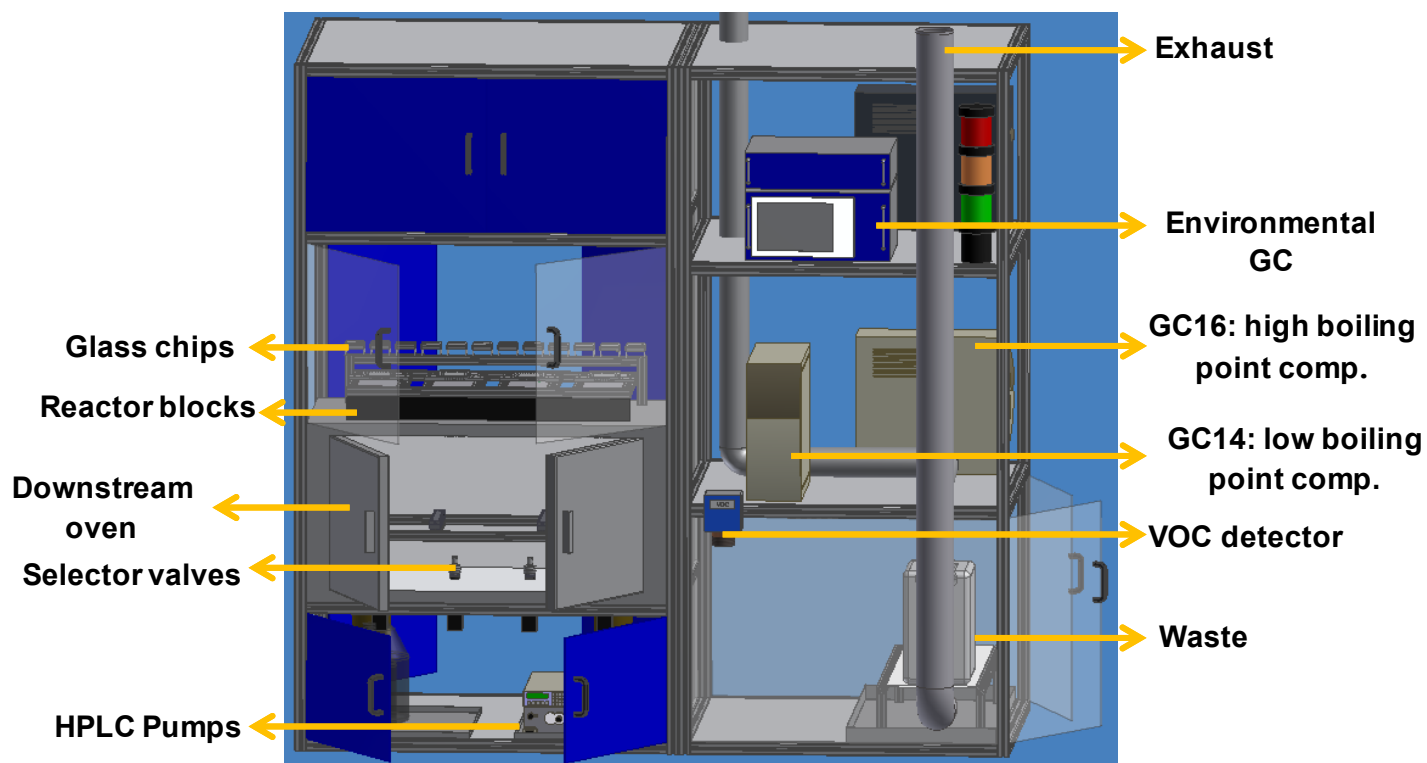


Figure 9. Reaction scheme of Flowrence set-up.

Each reactor is connected to a selector valve in the effluent line (heated by an oven) used to select the desired stream to the GC. The desired stream of gas is first flown through GC14 (Figure 9) and passed through Mol Sieve 5A PLOT Capillary GC Column which is connected to the TCD detector in order to analyze gaseous components. Since the sample is not destroyed, the same sample is conducted through a DBWAX Capillary GC Column for separating low boiling point components such as MEK, MVK and MeOH. In the second GC (Figure 9) the same sample is passed through a HP PLOT Capillary GC Column, which is able to separate high boiling point substances (ML, LA and lactones). The compounds are then detected by an FID detector.

Temperature indicators and pressure indicators are installed in different sections of the unit in order to control the temperature and the pressure online during the reaction.

Finally, a volatile organic compound detector (VOC) as well as an environmental GC and a CO detector are installed in the room for safety reasons.

Table 15. GC (TDC and FID) response factors 1.

Gas mixture:

(Gas composition: 1 vol% CO₂, 1 vol% CH₄, 1 vol% CO, 1 vol% He in N₂)

N ₂	CO ₂	CH ₄	CO	He
8808	185807	447227	157144	67231

Liquid mixture:

MEK	MVK	ML	AAL	GVL	MeOH	AcA
428812	388574	434740	182598	456778	66596	132844

General procedure for the gas-phase high throughput screening reactions

Prior starting the reaction, a safety protocol must be followed in order to avoid potential leaks or/and blockages in each unit section. Considering that MVK is highly toxic and can be deadly by inhalation, only 16 (15+1 blank) reactors out of 64 were used. Each reactor was filled with catalyst to a 30-60 mm length. The bed volumes tested were 0.094 cm³ and 0.188 cm³. The reactors were placed inside the reactor block and heated to temperatures between 250 and 450°C. A pre-treatment using 20 vol% of H₂ was conducted to reduce the metal. The HPLC pump was set to flows between 100 and 200 µl/min. The Helium flow was set to 23 ml/min. The nitrogen diluent flow was set to 2000 ml/min and the nitrogen flow was set to 400 ml/min. The concentration of in the gas stream was between 1.5 – 20 vol%. Helium was set to 1 vol%. Samples were taken every 30 min. The GHSV was kept to 5500 h⁻¹.

Conversion yield and selectivity were calculated using the following equations:

$$\text{Conversion}(\%) = \frac{\left(\text{Number of } \frac{\text{moles}}{\text{min}} \text{ ML.} \right)_{\text{in}} - \left(\text{Number of moles/min ML} \right)_{\text{out}}}{\left(\text{Number of moles/min ML.} \right)_{\text{in}}} \cdot 100$$
$$\text{Yield}(\%) = \frac{\left(\text{Number of } \frac{\text{moles}}{\text{min}} \text{ Prod.} \right)_{\text{out}}}{\left(\text{Number of moles/min ML} \right)_{\text{in}}} \cdot 100$$
$$\text{Selectivity}(\%) = \frac{\text{Yield}}{\text{Conversion}} \cdot 100$$

PFR reactor set-up

Looking into gaining more information about the demethoxycarbonylation of ML in the gas phase a single reactor flow set-up adapted with an online GC was built (Figure 10). This unit has two HPLC pumps used to pump the liquids to the reactor. The gas flow rates are controlled using MFC. Gases such as Argon (internal standard), N₂ and H₂ were installed for the further use. To control the pressure, a manometer was installed on the top of the reactor, prior to the heating chamber. To avoid condensation of liquids, all pipes through which the gas mixture flows are kept at 250 °C using heating wires. The liquid and the gas stream are combined in a pre-heated chamber in order to bring the liquid to the gas phase and subsequent dilute it in N₂ gas. The gas mixture is then flown through a stainless-steel plug flow reactor (PFR) which containing the catalyst bed fixed using Quartz wool. The reactor is surrounded by a 3-zone heating oven able to reach temperatures up to 1000K.

The downstream is then split to optimum flow that the GC can handle (20-40 ml/min). Inside the (Shimadzu 2010 Plus, Japan) equipped with a flame ionization detector (FID-2010 Plus) and capillary column (DBWAX; 15 m length, 0.53 mm internal diameter, and 0.5 µm film thickness), the flow is then split inside a 10-port gas sampling valve and each stream is sent to different GC columns and analyzed by a FID and TCD detector respectively. The calibration of the gaseous components such as CO, CO₂, He and CH₄ were done using a calibration bottle. The liquid substances, ML, LA, lactones, methanol, MVK and MEK were calibrated and the corresponding response factors were calculated based on heptane carbon response factor (Table 16).

The gas stream that is not analyzed is sent to waste bottle that contains an aqueous 10w% sodium persulfate solution used to quench the MVK formed. All outlets are connected to the exhaust. A VOC and a CO detector were also installed to detect possible leaking of dangerous volatiles.

A P&ID diagram of the unit built is shown in Figure 11.

Table 16. GC (TDC and FID) response factors 2.

Gas mixture:

(Gas composition: 1 vol% CO₂, 1 vol% CH₄, 1 vol% CO, 1 vol% He in N₂)

N ₂	CO ₂	CH ₄	CO	Ar
39242	524694	97731	157144	38692

Liquid mixture:

MEK	MVK	ML	α-AL	GVL	MeOH	LA	β-AL
300477	265095	371371	293684	417286	77291	269126	321838

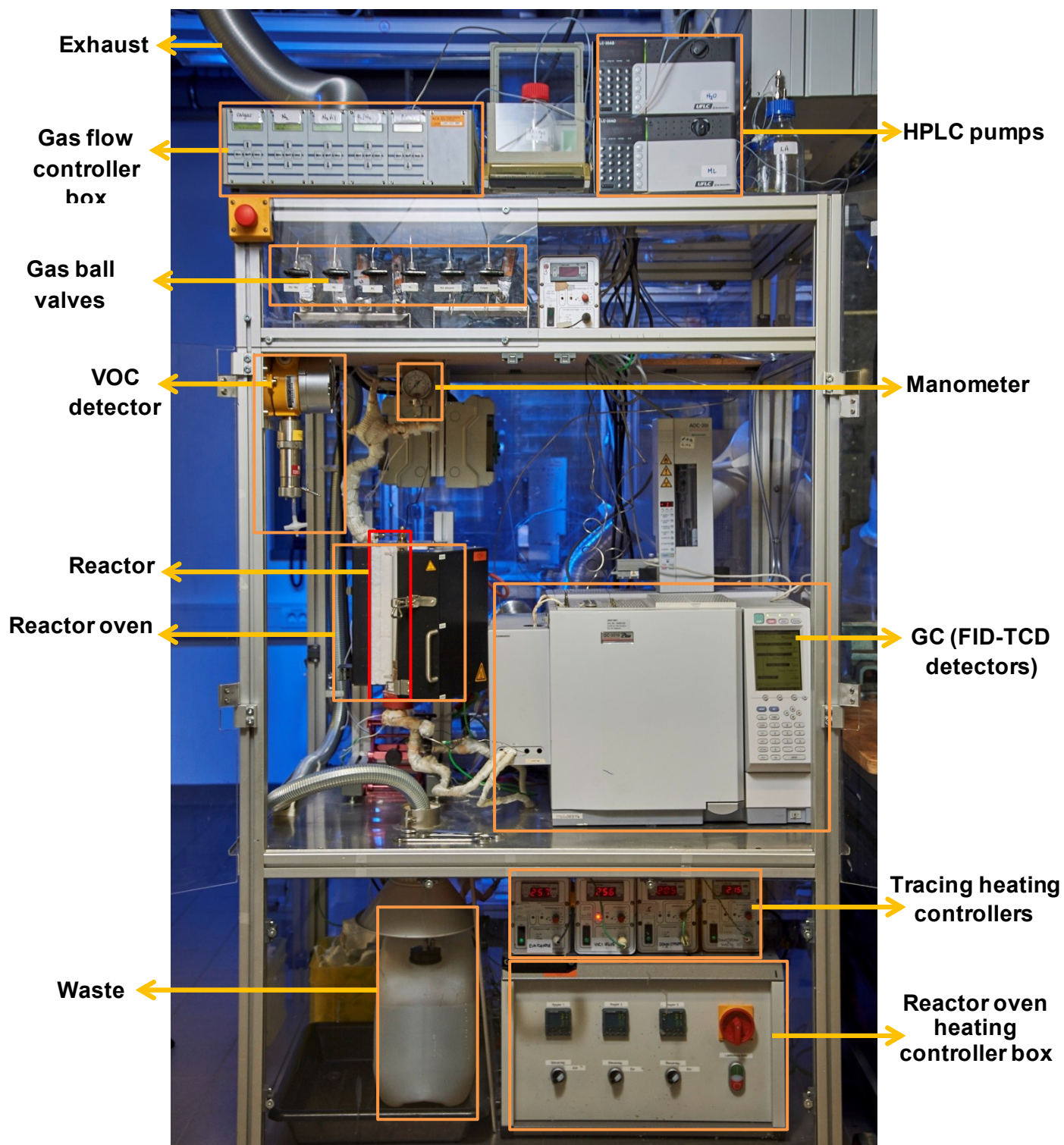


Figure 10. PFR flow set-up.

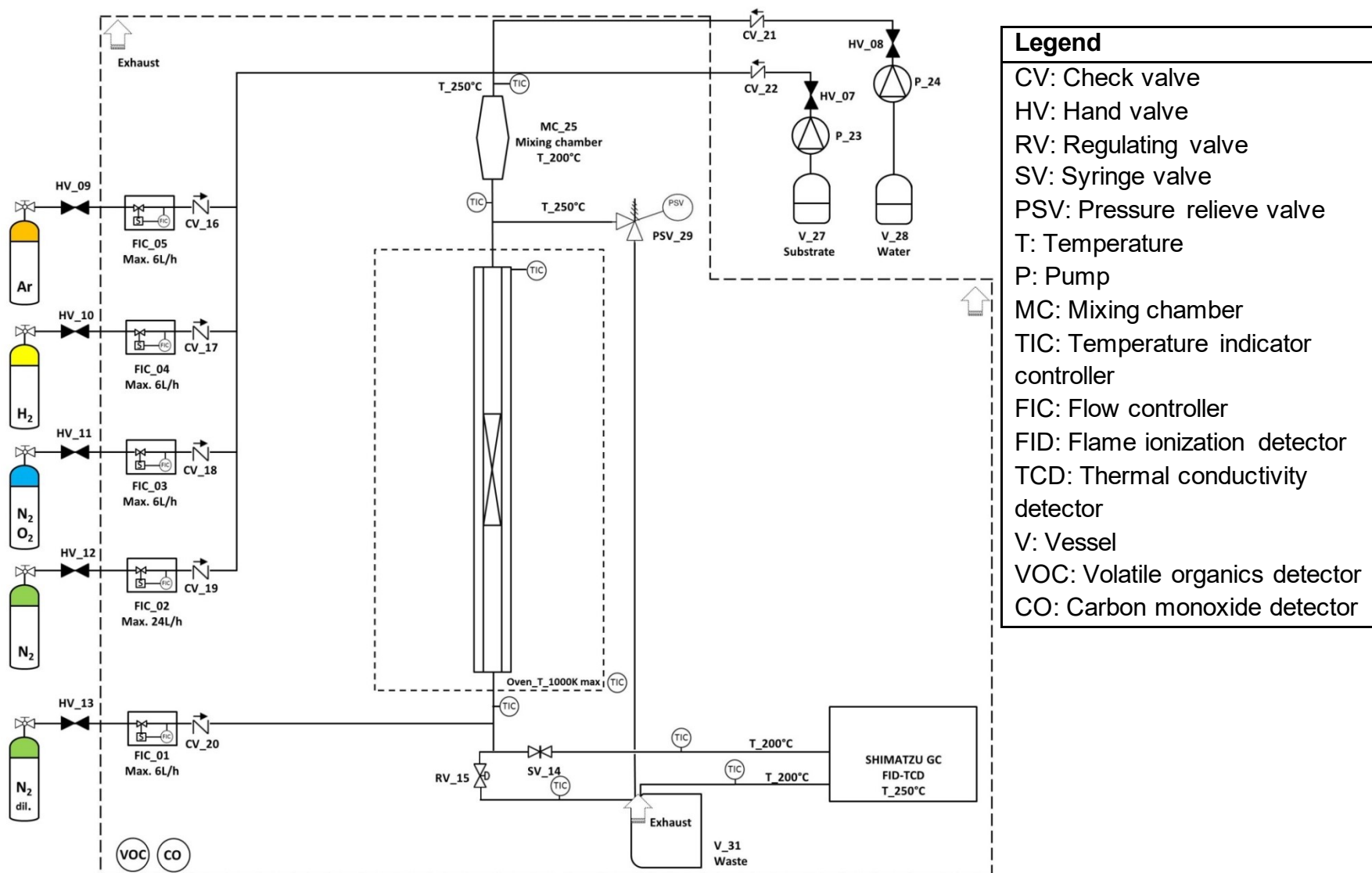


Figure 11. PFR set-up P&ID diagram.

Procedure for the gas-phase decarbonylation reaction in a single flow reactor

The decarbonylation reaction was conducted in a fixed bed stainless-steel reactor (i.d. length 27 cm, diameter 10.5/12.8 mm) at ambient pressure and temperatures ranging from 250 to 450 °C. The reactant (10-20 $\mu\text{l/min}$) was diluted with N_2 (125 ml/min), pre-heated and injected in the reactor. The flow rate of nitrogen gas was controlled using a mass flow controller. The reactor was surrounded by the oven and located in the heat box to keep the temperature stable around it. Two thermocouples were placed; one at the center of the oven to monitor the outside temperature of the reactor and the other at the middle of catalyst bed to indicate the temperature of the reaction. The reactor was charged with 1 g of catalyst particles (0.5-0.8 mm fraction) and the remaining space was filled with quartz (particles 1-1.25 mm fraction) to keep the flow in the reactor constant. The reactant feed was then introduced into the reactor and the reaction was performed, at a constant residence time of ~ 1.7 to 2.7 s and a gas hourly space velocity (GHSV) of ~ 4400 L/kgCat/h. After the set time, the mixture of products and reactant was collected in cooling traps and was analyzed by gas chromatography (Shimadzu 2010 Plus, Japan) equipped with a flame ionization detector (FID-2010 Plus) and capillary column (Agilent; 15 m length, 0.53 mm internal diameter, and 0.5 μm film thickness). The column temperature varied from 110 °C to 190 °C (10 min) at 10 °C min^{-1} ramp. The FID and injection temperature were set at 220 and 250 °C, respectively. Helium was used as the carrier gas. Also, the carbon balance was calculated based on ML concentration before and after reaction and for all samples in the range of 80-100%. Conversion, yield and selectivity were calculated using the following equations:

6.2.2. Catalyst characterization

The total surface area, pore volume, and average pore diameter of the synthesized catalysts were evaluated using the nitrogen adsorption–desorption isotherms at -197 °C via the Brunauer–Emmet–Teller (BET) method using a NOVA 4200e device (Quantachrome Instruments) by N_2 adsorption at -196 °C. Prior to the measurement, the samples were evacuated for 1 h at 120 °C and 2 h at 220 °C to remove physisorbed water. The elemental compositions were determined by ICP-OES using a Varian 715-ES ICP-emission spectrometer, which is a highly sensitive analytical technique for elemental determination and based on the principles of atomic emission. X-ray diffraction (XRD) patterns were obtained using $\text{Cu K}\alpha$ radiation ($\lambda = 1.5406$ Å) in the 2θ range of 10-60° (step width: 0.25°, 25 sec. per step) on a Stoe STADI P diffractometer and Powder Diffraction File (PDF) database of the International Centre of Diffraction Data (ICDD) software was used to analyze the data. Transmission electron microscopy (TEM) is useful for indicating the size of the supported metal crystallites in nm scale and it provides the information related to the morphology, composition and distribution. X-ray photoelectron spectroscopy (XPS) is performed to gain information about the oxidation state, surface composition, as well as atomic

ratios of the elements present in the near-surface-region of the catalysts due to shifts in the binding energies. XPS analysis was carried out using a VG ESCALAB 220iXL instrument with AlK α radiation ($E = 1486.6$ eV). The samples were fixed by using a double adhesive carbon tape on a stainless-steel sample holder. The peaks were fitted by Gaussian-Lorentzian curves following a Shirley background subtraction.

Table 17. Brunauer–Emmet–Teller (BET) fresh and spent catalyst.

Catalysts	BET surface area (m ² g ⁻¹)	Total Pore volume (cm ³ g ⁻¹)
Fresh 5 wt%Pt/SC	736.3	0.31
Spent 5 wt%Pt/SC ML	225.1	0.11
Spent 5 wt%Pt/SC ML/H ₂ O	455.8	0.28
Spent 5 wt%Pt/SC aAL	229.7	0.11
Spent 5 wt%Pt/SC LA	151.1	0.07

Table 18. X-ray photoelectron spectroscopy (XPS).

Catalysts	Pt(4f)/S(2p)	Surface characterization			
	atomic ratio (XPS)	Binding energy (eV)			
		Pt (4f)	S (2p)	Quant./at. Pt%	Quant./at. S%
Fresh 5 wt% Pt/SC	3.24	72	168.40	1.07	0.33
Spent 5 wt% Pt/SC	3.76	71.61	168.28	0.64	0.17
Spent ML/H ₂ O ^a	17.6	71.51	168.50	0.88	0.05

Table 19. Elemental compositions were determined by ICP-OES.

Catalysts	Metal content (wt%)	Sulfur content (wt%)
Fresh 5 wt%Pt/SC	4.22	0.35
Spent 5 wt%Pt/SC ML	3.42	>0.01
Spent 5 wt%Pt/SC ML/H ₂ O	3.94	>0.01
Spent 5 wt%Pt/SC aAL	3.03	>0.01
Spent 5 wt%Pt/SC LA	3.38	>0.01

Table 20. X-ray diffraction (XRD).

Catalysts	h k l	size [nm]
Fresh 5 wt%Pt/SC	1 1 1	2.1
Spent 5 wt%Pt/SC ML	1 1 1	7.6

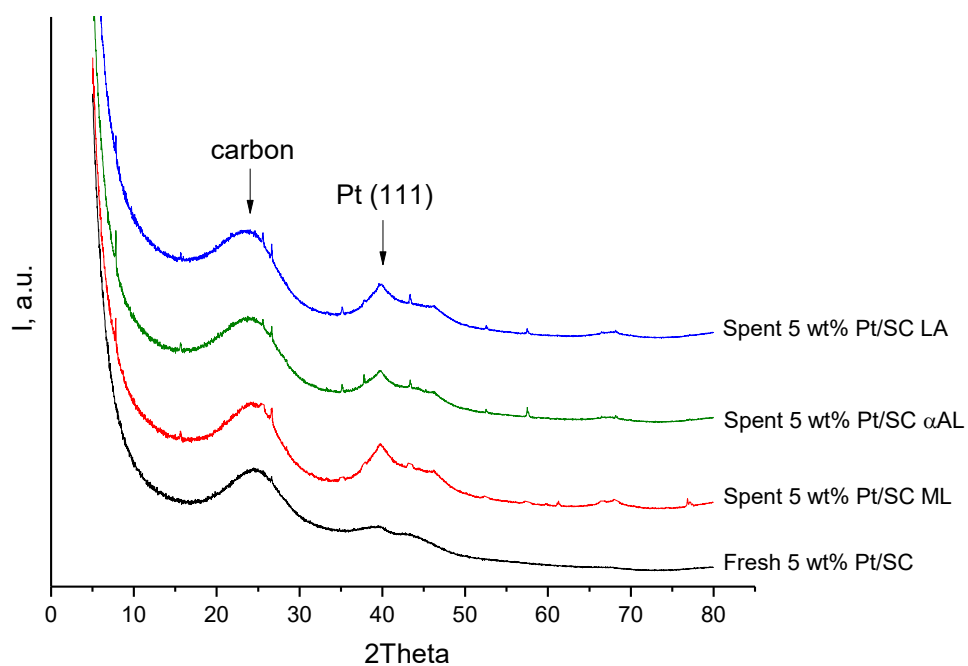


Figure 12. X-ray diffraction (XRD) fresh and spent catalyst.

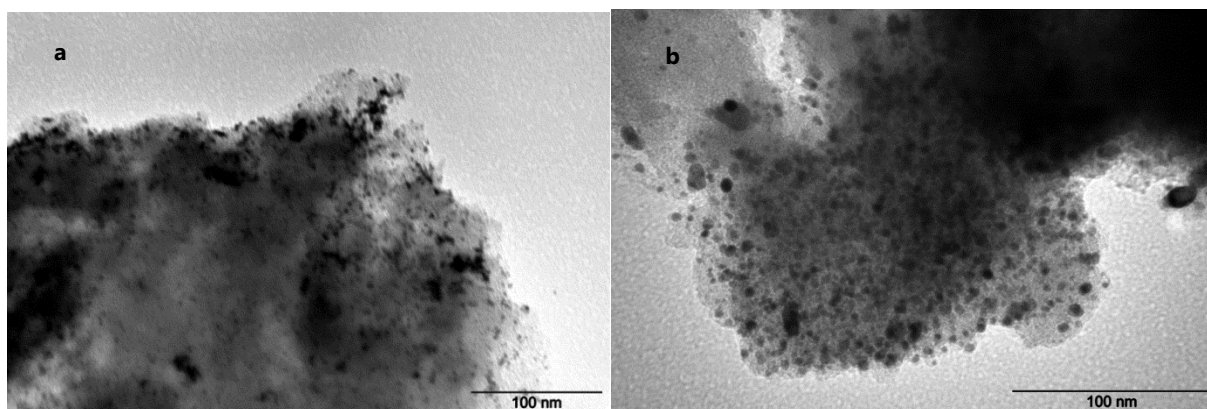


Figure 4. TEM pictures: a) fresh 5 wt% Pt on sulfide carbon b) spent 5 wt% Pt on sulfided carbon.

6.3. Chapter 3

6.3.1. Experimental procedures and analytical data

General considerations

Commercially available chemicals were purchased from Sigma Aldrich. NMR spectra were recorded on Bruker AV 300 MHz and Bruker AV 400 MHz spectrometers. ^1H - and ^{13}C -NMR spectra were referenced to residual solvent peaks of Chloroform-*d* (7.26 ppm 77.16 ppm respectively). All chemical shifts are reported in ppm, coupling constants in Hz. Abbreviations are s: singlet, d: doublet, t: triplet, q: quadruplet, quin: quintuplet, m: multiplet, br: broad. GC-FID analysis was carried out on a Shimadzu (2010 Plus, Japan) apparatus equipped with a flame ionization detector (FID-2010 Plus) and capillary column (DBWAX 15 m length, 0.53 mm internal diameter, and film thickness of 1.0 μm). Helium was used as the carrier gas.

General procedure for Baeyer-Villiger oxidation of ML

In a QCS reactor block (Figure 8, a), each 4 mL autoclave was filled with the corresponding oxidant (0.5 mmol), the additive (0.1 mmol) and 50 μL of ML (50 mg 0.4 mmol). The reactor block was pressurized with 20 bars of synthetic air and then heated to 100°C. The reactor block was subsequently placed in the pre-heated heating block (Figure 8, b). The reaction was left stirring for 6h with a stirring speed of 1000 rpm. The block was then cooled in an ice bucket and the gas pressure was released. After that, the reactor block was slowly opened and the samples from the reactors were filtered through a membrane filter into glass vial. The clear liquid was used for GC analysis (dioxane and pyroglutamic acid as respective external standards).

Pyrolysis set-up

The set-up used for the pyrolysis reaction is placed inside a ventilated fume hood. The unit is composed by a liquid feed section, gas feed section, reactor section and a collecting section (Figure 13). The liquid is fed using a syringe pump equipped with a 5 ml syringe. The N_2 gas flow is controlled by a mass flow controller (MFC). All pipes are heated above the boiling point of the liquid, using tracing wires controlled by a heating box. The gas mixture is flown through a 7 cm^3 plug-flow reactor (PFR) surrounded by an oven. The downstream is connected to a cold trap placed in an ethanol bath cooled to -20°C using liquid nitrogen.

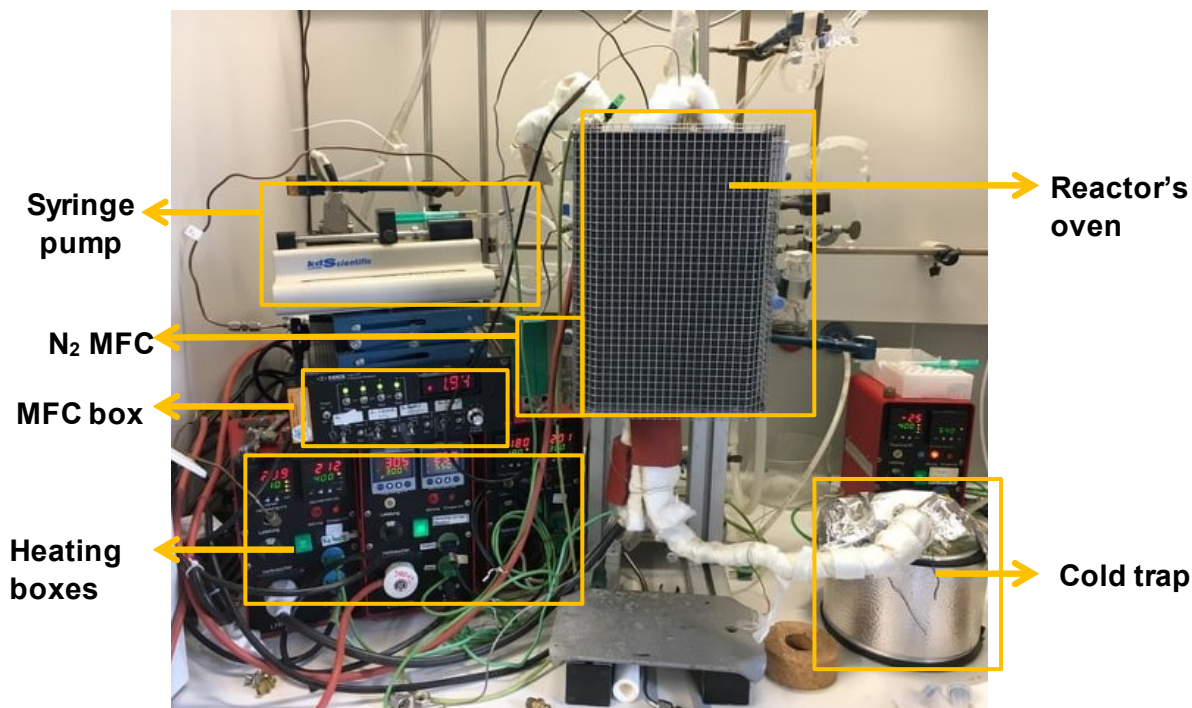


Figure 13. Pyrolysis set-up.

General procedure for the pyrolysis of M3AP

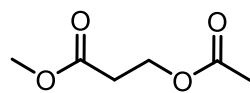
M3AP was synthesized and isolated in 86% yield following a common acetylation procedure reported in the literature.^[213] M3AP was injected into the gas-phase set-up using a 5 ml syringe pump. The flow was set to 0.5 ml/h and diluted to a N₂ stream of 1200 ml/h above the starting material boiling point (180 °C). A quartz plug-flow reactor (PFR) of 7 cm³ volume and packed with quartz powder was used. The molar ratio M3AP:N₂ was 1:13. The contact time was 20 s. The out stream was bubbled into 5 ml of acetone cooled at -20 °C. The reaction time was 1 hour. Temperatures between 300 °C and 600 °C were tested. After the set time, the mixture of products and reactant was collected in the cold trap and was analyzed by gas chromatography.

General procedure for the catalytic elimination of acetic acid from M3AP

M3AP was injected into the gas-phase set-up using a 5 ml syringe pump. The flow was set to 0.5 ml/h and diluted to a N₂ stream of 1200 ml/h at 180 °C. 200 mg (1 cm³ bed volume) of catalyst were placed inside a quartz plug-flow reactor (PFR). The molar ratio M3AP:N₂ was 1:13. The GHSV was 1284 h⁻¹. The contact time was 3 s. The out stream was bubbled into 5 ml of methanol cooled at -20 °C. The reaction time was 1 hour. Temperatures between 300 °C and 500 °C were tested. After the set time, the mixture of products and reactant was collected in the cold trap and was analyzed by gas chromatography. Dimethyl formamide (DMF) was used as external standard.

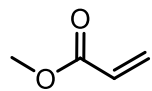
Analytical data

Methyl 3-acetoxypropionate (M3AP)

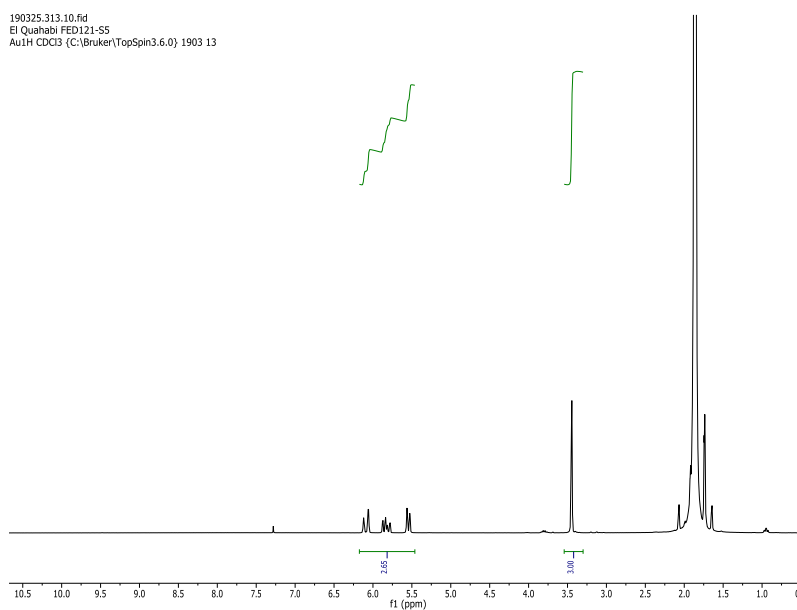


$^1\text{H-NMR}$ (300 MHz, Chloroform- d) δ 4.27 (t, $^3J_{\text{HH}} = 6.3$ Hz, 2H), 3.65 (s, 3H), 2.59 (t, $^3J_{\text{HH}} = 6.3$ Hz, 2H), 1.98 (s, 3H). $^{13}\text{C-NMR}$ (75 MHz, CDCl_3) δ 171.1, 170.8, 59.8, 51.9, 33.7, 20.9. The spectral data were in accord with those published in the literature.^[157]

Methyl acrylate (MA)

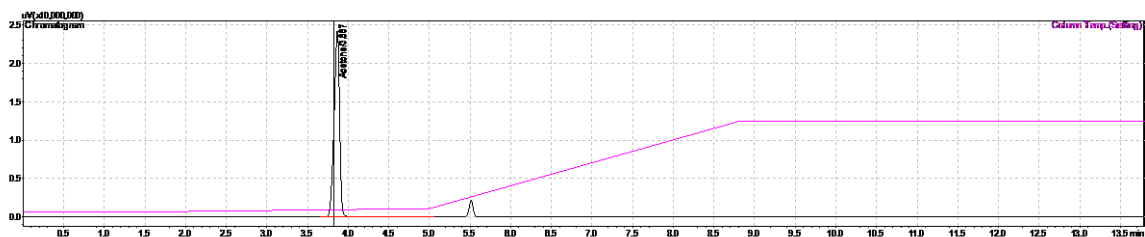


$^1\text{H-NMR}$ (300 MHz, Chloroform- d) δ 5.82 (m 3H), 3.55 (s, 3H).



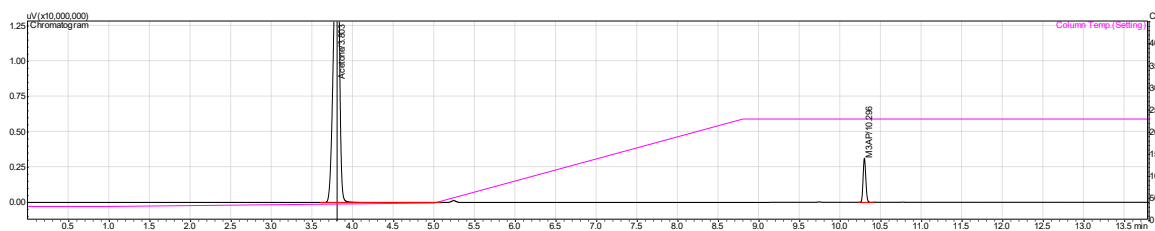
GC data

Acetone blank

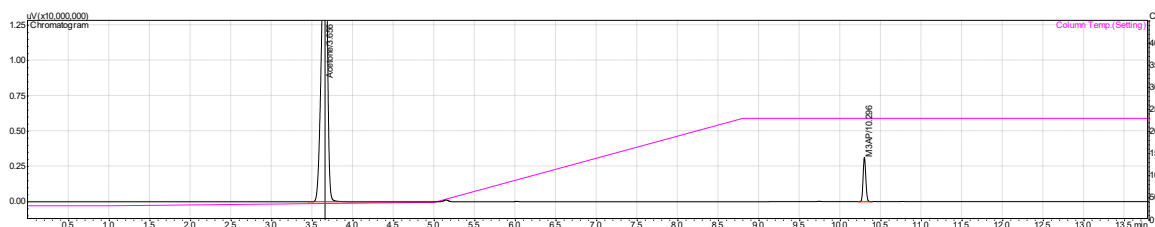


Pyrolysis experiments

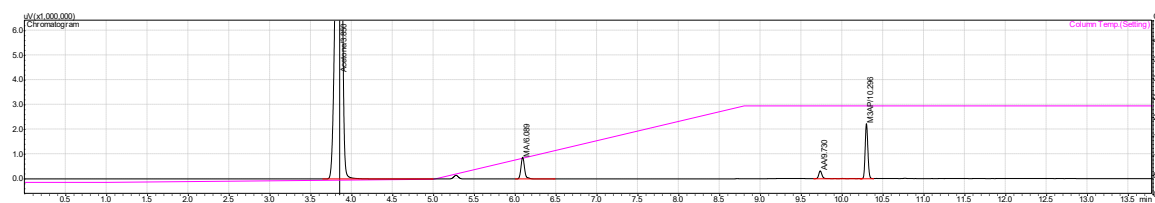
Pyrolysis at 300°C



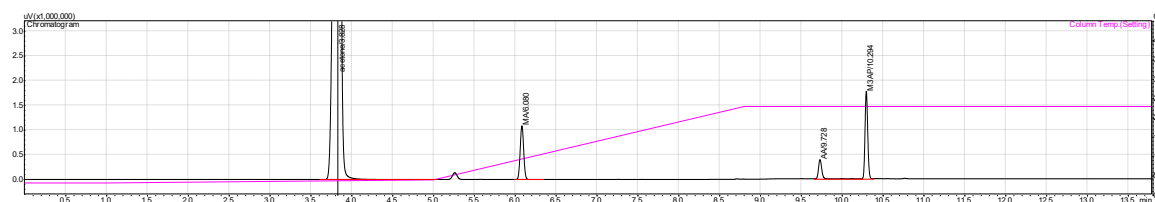
Pyrolysis at 400°C



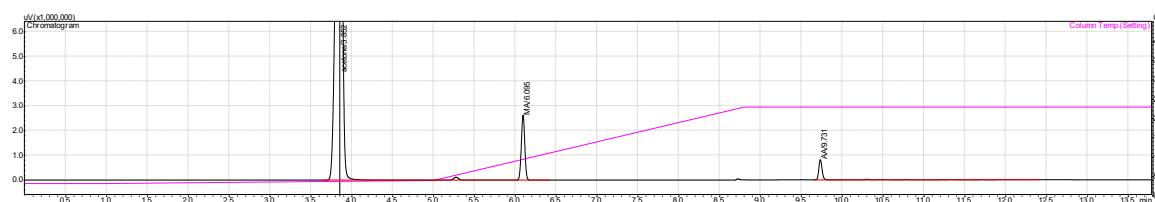
Pyrolysis at 500°C



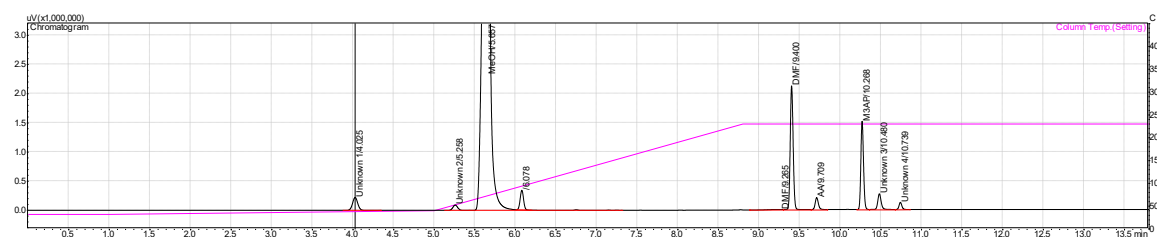
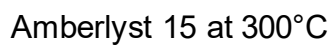
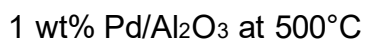
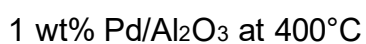
Pyrolysis at 550°C



Pyrolysis at 600°C



1 wt% Pd/Al₂O₃ at 300°C



7. Statement: Scientific Independence

Universität Rostock
Dezernat 1
Referat 1.2

Doktorandinnen/Doktoranden-Erklärung gemäß § 4 Absatz 1 Buchstaben g und h der Promotionsordnung der Mathematisch-Naturwissenschaftlichen Fakultät der Universität Rostock

Name Fatima El Ouahabi
(Name, Vorname)

Anschrift Am Vögenteich 13, 18057 Rostock
(Straße, PLZ, Wohnort)

Ich habe eine Dissertation zum Thema

From side streams to building blocks: gas phase conversion of biomass-derived feedstocks to valuable monomers

an der Mathematisch-Naturwissenschaftlichen Fakultät der Universität Rostock
angefertigt. Dabei wurde ich von Frau/Herrn

Prof. Dr. Johannes G. de Vries

betreut.

Ich gebe folgende Erklärung ab:

1. Die Gelegenheit zum vorliegenden Promotionsvorhaben ist mir nicht kommerziell vermittelt worden. Insbesondere habe ich keine Organisation eingeschaltet, die gegen Entgelt Betreuerinnen/Betreuer für die Anfertigung von Dissertationen sucht oder die mir obliegenden Pflichten hinsichtlich der Prüfungsleistungen für mich ganz oder teilweise erledigt.
2. Ich versichere hiermit an Eides statt, dass ich die vorliegende Arbeit selbstständig angefertigt und ohne fremde Hilfe verfasst habe. Dazu habe ich keine außer den von mir angegebenen Hilfsmitteln und Quellen verwendet und die den benutzten Werken inhaltlich und wörtlich entnommenen Stellen habe ich als solche kenntlich gemacht.

Rostock, den 19.08.2019


(Unterschrift)

8. Curriculum Vitae

FATIMA EL OUAHABI

Date of birth: September 18, 1992

Nationality: Spanish

Address: Am Vögenteich, 13 18057 Rostock, Germany

Telephone: +49 152 27586441

Email: fatima.elouahabi@catalysis.de

Web page: <http://www.uco.es/hugs/>

EDUCATION

- 05/2016-Present **Marie Skłodowska-Curie European Industrial PhD (Chemistry)** in the catalysis with renewable resources group, Leibniz-Institut für Katalyse (LIKAT), Germany in collaboration with Avantium, The Netherlands
- Project: *From side streams to building blocks: gas phase conversion of biomass-derived feedstocks to valuable monomers*. Supervisors: Prof. Johannes G. de Vries and Dr. Sergey Tin
- 09/2014-07/2015 **Master in Synthesis, Catalysis and Molecular Design (Chemistry)**, University Rovira y Virgili (URV) and Institute of Chemical Research of Catalonia (ICIQ), Spain
- Master Thesis: *Synthesis of isoflavanones by asymmetric palladium-Catalyzed decarboxylative protonation*. Supervisors: Prof. Montserrat Dièguez and Dr. Oscar Pàmies
- 09/2010-07/2014 **Bachelor's in Chemistry**, University Rovira y Virgili (URV), Spain
- Bachelor Thesis: *Synthesis and characterization of dibenzothiophene and phenothiazine derivatives for organic optoelectronic devices (OLEDs)*. Supervisors: Prof. Dr. Juozas V. Grazulevicius and Dr. Aušra Tomkevičienė

PROFESSIONAL EXPERIENCE

- 07/2015-05/2016 **Research assistant**, University Rovira y Virgili (URV) Spain
- Project: *Synthesis of pyrene-tagged and water-soluble NHC transition-metal complexes*. Department of Physical and Inorganic Chemistry. Supervisors: Prof. Dr. Carmen Claver and Dr. Cyril Godard

07/2013-09/2013

Internship, LyondellBaeIl Polyolefins Iberica, S.L. *Spain*

Design of experiments and development of new methods for the characterization of polypropylene compounds and investigation of their mechano-chemical properties

EXPERIENCE

- High throughput experimentation (HTE)
- Project leader Nanoflow team (Avantium 2017-2018)
- Development and preparation of homogeneous and heterogeneous catalysts
- Analytics: GC(-MS), LC, DSC, TGA, DMA, Rheometry, BET, XPS, TEM, SEM, ICP, IR, UV-Vis, NMR
- Commissioning of flow set-ups with automatized analytics
- Health, safety & environment (HSE) implementation: experience in hazard and operability studies (HAZOP)
- Member of the organizing committee of a session (HUGS) of *NICE Nature Inspires Creativity Engineers Conference 2018*, Nice, France

COURSES

- Specialized course on oral skills at the University of Cordoba, Spain (11/2016)
- Course on scientific writing at the University of Cordoba, Spain (11/2016)
- Heterogeneous catalysis, homogeneous catalysis and catalyst deactivation at LIKAT, Germany (09/2017)
- Specialized course on management - Project management by Avantium at the University of Nice, France (09/2017)
- (Eco)toxicity, safety aspects at the INERIS institute, France (03/2018)
- Technico-economic evaluation of new processes by Avantium at the INERIS institute, France (03/2018)
- Polymer chemistry course: crystallization and advanced thermal analysis of polymers (Flash DSC) at the University of Nice, France (10/2018)

FELLOWSHIPS/AWARDS

- **University Rovira y Virgili**
10 months research assistant scholarship from the physics and inorganic department
- **Erasmus scholarship**
2/2014-7/2014 in Kaunas University of Technology (KTU), Department of Polymer Chemistry, Kaunas (Lithuania)
- **Spanish Ministry of Science and Education**
09/2010-07/2014 bachelor's degree Scholarships

LANGUAGES

Spanish Native proficiency **Arabic** Native **German** Professional working

Catalan Native **French** Basic **English** Full professional proficiency

ADDITIONAL INFORMATION

Core competences: Highly organized, very good communication skills, strong technical and analytical skills

Computing: Microsoft Office package, Access Database, specific software - Spectrum, Opus, ChemDraw, Miner3D, Origin

Hobbies: Travelling, sports (fitness, volleyball), yoga and martial arts

REFERENCES:

- Leibniz-Institut für Katalyse, Germany
Prof. Dr. Johannes G. de Vries, Johannes.deVries@catalysis.de, +49(381)1281-384. Dr. Sergey Tin, Sergey.tin@cataysis.de, +49(381)1281-256
- TNO, The Netherlands
Dr. Jan Kees van der Waal, Jankeeswanderwaal@gmail.com
- Avantium, The Netherlands
Dr. Gerard van Klink, Gerard.vanKlink@avantium.com

PUBLICATIONS:

[1] F. El-Ouahabi, M. Polyakov, N. V. Kalevaru, S. Wohlrab, S. Tin, J. G. de Vries (2019) Conversion of biomass derived methyl levulinate to methyl vinyl ketone. Manuscript in preparation.

[2] F. El-Ouahabi, M. Polyakov, G. van Klink, S. Wohlrab, S. Tin, J.G. de Vries (2019) Highly efficient and atom economic route for the production of methyl acrylate and acetic acid from a biorefinery side stream. *Green Chem.*, Manuscript submitted.

[3] A. Marckwordt, F. El Ouahabi, Hadis Amani, S. Tin, N. V. Kalevaru, P. C. J. Kamer, S. Wohlrab, and J. G. de Vries (2019) Nylon Intermediates from Bio-Based Levulinic Acid. *Angew. Chem. Int. Ed.*, **58**, 3486 –3490. DOI: 10.1002/anie.201812954

[4] P. Puylaert, A. Dell'Acqua, F. El Ouahabi, A. Spannenberg, T. Roisnel, L. Lefort, S. Hinze, S. Tin and J. G. de Vries, (2019) Phosphine-free cobalt catalyst precursors for the selective hydrogenation of olefins, *Catal. Sci. Technol.*, **9**, 61-64. DOI: 10.1039/C8CY02218F

SELECTED PRESENTATIONS:

- May 2017, *ISGC, the International Symposium on Green Chemistry*, La Rochelle, France – Poster
- March 2018, *51. Jahrestreffen Deutscher 2018 Katalytiker*, Weimar/Germany – Oral communication and poster
- July 2018, *International Symposium on Homogeneous Catalysis*, Amsterdam, The Netherlands – Poster
- October 2018, *NICE Nature Inspires Creativity Engineers Conference 2018*, Nice, France – Oral communication
- March 2019, *51. Jahrestreffen Deutscher 2019 Katalytiker*, Weimar/Germany – Poster

9. References

- [1] M. Londo, J. van Stralen, A. Uslu, H. Mozaffarian, C. Kraan, *Biofuels, Bioprod. Biorefin.* **2018**, 12, 1065-1081.
- [2] H. Wenzl, *The Chemical Technology of Wood*, 1st ed., Academic Press New York, **1970**.
- [3] A. D. Smith, M. Landoll, M. Falls, M. T. Holtzapple, *Chem. Inform.* **2012**, 43.
- [4] E. de Jong, R. J. A. Gosselink, in *Bioenergy Research: Advances and Applications* (Eds.: V. Gupta, M. Tuohy, C. Kubicek, J. Saddler, F. Xu), Elsevier, Amsterdam, **2014**, pp. 277-313.
- [5] F. H. Isikgor, C. R. Becer, *Polym. Chem.* **2015**, 6, 4497-4559.
- [6] S. Salama el, H. C. Kim, R. A. Abou-Shanab, M. K. Ji, Y. K. Oh, S. H. Kim, B. H. Jeon, *Bioprocess Biosyst. Eng.* **2013**, 36, 827-833.
- [7] P. M. Mortensen, J. D. Grunwaldt, P. A. Jensen, K. G. Knudsen, A. D. Jensen, *Appl. Catal., A* **2011**, 407, 1-19.
- [8] J. Fu, X. Lu, P. E. Savage, *ChemSusChem* **2011**, 4, 481-486.
- [9] R. Palkovits, I. Delidovich, *Philos. Trans. A Math. Phys. Eng. Sci.* **2018**, 376.
- [10] M. Ringer, V. Putsche, J. Scahill, *Large-Scale Pyrolysis Oil Production: A Technology Assessment and Economic Analysis: Technical Report*, Washington, **2006**.
- [11] R. Rauch, J. Hrbek, H. Hofbauer, *Energy Environ.* **2014**, 3, 343-362.
- [12] P. J. Deuss, K. Barta, J. G. de Vries, *Catal. Sci. Technol.* **2014**, 4, 1174-1196.
- [13] Y.-C. Lin, G. W. Huber, *Energy Environ. Sci.* **2009**, 2, 68-80.
- [14] J. G. de Vries, *Chem. Rec.* **2016**, 16, 2783-2796.
- [15] X. Zheng, X. Gu, Y. Ren, Z. Zhi, X. Lu, *Biofuels, Bioprod. Bioref.* **2016**, 10, 917-931.
- [16] S. Jia, X. He, J. Ma, K. Wang, Z. Xu, Z. C. Zhang, *Catal. Sci. Technol.* **2018**, 8, 5526-5534.
- [17] T. Kläusli, *Green Process. Synth.* **2014**, 3, 235-236.
- [18] L. Hu, L. Lin, Z. Wu, S. Zhou, S. Liu, *Renew. Sust. Energ. Rev.* **2017**, 74, 230-257.
- [19] R. J. van Putten, J. C. van der Waal, E. de Jong, C. B. Rasrendra, H. J. Heeres, J. G. de Vries, *Chem. Rev.* **2013**, 113, 1499-1597.
- [20] J. G. d. Vries, in *Heterocyclic Chemistry in the 21st Century: A Tribute to Alan Katritzky, Vol. 121* (Eds.: E. F. V. Scriven, C. A. Ramsden), Academic Press (Elsevier), Cambridge, MA, **2017** pp. 247-293.
- [21] E. de Jong, M. A. Dam, L. Sipos, G. J. M. Gruter, in *Biobased Monomers, Polymers, and Materials, Vol. 1105* (Eds.: S. Patrick B., G. and Richard A.), American Chemical Society, **2012**, pp. 1-13.
- [22] Z. Xue, Q. Liu, J. Wang, T. Mu, *Green Chem.* **2018**, 20, 4391-4408.
- [23] J. J. Bozell, G. R. Petersen, *Green Chem.* **2010**, 12, 539.
- [24] R. Fittig, *Ber. Dtsch. Chem. Ges.* **1876**, 9, 1189-1199.
- [25] M. Sajid, X. Zhao, D. Liu, *Green Chem.* **2018**, 20, 5427-5453.
- [26] P. Verdeguer, N. Merat, A. Gaset, *J Mol. Catal.* **1993**, 85, 327-344.
- [27] S. E. Davis, L. R. Houk, E. C. Tamargo, A. K. Datye, R. J. Davis, *Catal. Today.* **2011**, 160, 55-60.
- [28] N. Mosier, C. Wyman, B. Dale, R. Elander, Y. Y. Lee, M. Holtzapple, M. Ladisch, *Bioresour. Technol.* **2005**, 96, 673-686.
- [29] B. C. Saha, in *Enzymes as Biocatalysts for Conversion of Lignocellulosic Biomass to Fermentable Sugars* (Ed.: C. T. Hou), Handbook of Industrial Biocatalysis, Boca Raton, USA, **2005**, p. 112.
- [30] M. J. Taherzadeh, K. Karimi, *Int. J. Mol. Sci.* **2008**, 9, 1621-1651

- [31] See: <https://www.avantium.com/renewable-chemistries/dawn-technology/> (visited on 05.05.2019)
- [32] F. Bergius, *Ind. Eng. Chem.* **1937**, 29, 247.
- [33] Y.-B. Huang, Y. Fu, *Green Chem.* **2013**, 15, 1095-1111.
- [34] B. F. M. Kuster, *Starch-Stärke* **1990**, 42, 314-321.
- [35] L. M. Hanover, J. S. White, *Am. J. Clin. Nutr.* **1993**, 58, 724-732.
- [36] A. Corma, S. Iborra, A. Velty, *Chem. Rev.* **2007**, 107, 2411-2502.
- [37] A. A. Rosatella, S. P. Simeonov, R. F. M. Frade, C. A. M. Afonso, *Green Chem.* **2011**, 13, 754.
- [38] E. Lam, J. H. T. Luong, *ACS Catal.* **2014**, 4, 3393-3410.
- [39] P. Maki-Arvela, I. L. Simakova, T. Salmi, D. Y. Murzin, *Chem. Rev.* **2014**, 114, 1909-1971.
- [40] H. Li, Z. Fang, J. Luo, S. Yang, *Appl. Catal., B-Environ.* **2017**, 200, 182-191.
- [41] C. A. L. de Bruyn, W. A. van Ekenstein, *Rec. Trav. Chim. Pays-Bas* **2010**, 14, 203-216.
- [42] D. M. Gao, T. Kobayashi, S. Adachi, *Biosci., Biotechnol.* **2015**, 79, 470-474.
- [43] C. A. Collyer, D. M. Blow, *Proc. Natl. Acad. Sci. USA* **1990**, 87, 1362-1366.
- [44] J. Guo, S. Zhu, Y. Cen, Z. Qin, J. Wang, W. Fan, *Appl. Catal., B-Environ.* **2017**, 200, 611-619.
- [45] I. Graça, D. Iruretagoyena, D. Chadwick, *Appl. Catal., B-Environ.* **2017**, 206, 434-443.
- [46] T. Ennaert, J. Van Aelst, J. Dijkmans, R. De Clercq, W. Schutyser, M. Dusselier, D. Verboekend, B. F. Sels, *Chem. Soc. Rev.* **2016**, 45, 584-611.
- [47] C. Liu, J. M. Carraher, J. L. Swedberg, C. R. Herndon, C. N. Fleitman, J. Tessonnier, *ACS Catal.* **2014**, 4, 4295-4298.
- [48] J. M. Carraher, C. N. Fleitman, J. Tessonnier, *ACS Catal.* **2015**, 5, 3162-3173.
- [49] I. P. Delidovich, R. , *Green Chem.* **2016**, 18, 5822-5830.
- [50] S. P. Teong, G. Yi, Y. Zhang, *Green Chem.* **2014**, 16, 2015-2026.
- [51] Y. Román-Leshkov, J. N. Chheda, J. A. Dumesic, *Science* **2006**, 312, 1933-1937.
- [52] E. Weingart, L. Teevs, R. Krieg, U. Prüße, *Energy Technol.* **2018**, 6, 432-440.
- [53] A. C. Cope, in *US 2917520, Vol. 2*, **1959**, p. 520.
- [54] B. F. M. Kuster, J. Laurens, *Starch-Stärke* **1977**, 29, 172-176.
- [55] T. Shimanouchi, Y. Kataoka, T. Tanifuji, Y. Kimura, S. Fujioka, K. Terasaka, *AIChE J.* **2016**, 62, 2135-2143.
- [56] J. Lueckgen, L. Vanoye, R. Philippe, M. Eternot, P. Fongarland, C. de Bellefon, A. Favre-Réguillon, *J. Flow Chem.* **2018**, 8, 3-9.
- [57] A. Gaset, L. Rigal, G. Paillasa, J. P. Salome, and C. Fleche: Fr.Demande FR 2, 551, 754, 15. Mar. 1985.
- [58] G.-Y. Jeong, A. K. Singh, S. Sharma, K. W. Gyak, R. A. Maurya, D.-P. Kim, *NPG Asia Mater.* **2015**, 7, e173.
- [59] M. Schön, M. Schnürch, M. D. Mihovilovic, *Mol. Divers.* **2011**, 15, 639-643.
- [60] W. Partenheimer, V. V. Grushin, *Adv. Syn. Catal.* **2001**, 343, 102-111.
- [61] N. K. Gupta, S. Nishimura, A. Takagaki, K. Ebitani, *Green Chem.* **2011**, 13, 824-827.
- [62] L. Ardemani, G. Cibir, A. J. Dent, M. A. Isaacs, G. Kyriakou, A. F. Lee, K. Wilson, *Chem. Sci.* **2015**, 6, 4940-4945.
- [63] A. Abad, A. Corma, H. García, *Chem. A Eur. J* **2008**, 14, 212-222.
- [64] X. Wan, C. Zhou, J. Chen, W. Deng, Q. Zhang, Y. Yang, Y. Wang, *ACS Catal.* **2014**, 4, 2175-2185.
- [65] X. Han, L. Geng, Y. Guo, R. Jia, X. Liu, Y. Zhang, Y. Wang, *Green Chem.* **2016**, 18, 1597-1604.
- [66] M. C. D. Diego, W. P. Schammel, M. A. Dam, G. J. M. Gruter, WO2011/043660, **2011**.
- [67] M. C. D. Diego, W. P. Schammel, M. A. Dam, G. J. M. Gruter, WO2011/043661, **2011**.
- [68] M. C. D. Diego, W. P. Schammel, M. A. Dam, G. J. M. Gruter, USPat8519167B2, **2013**.

- [69] E. Mazoyer, A. S. V. De Sousa Dias, B. McKay, H. J. Baars, V. P. C. Vreeken, G. J. M. Gruter, D. L. Sikkenga, WO2014163500, **2014**.
- [70] S. Siankevich, G. Savoglidis, Z. Fei, G. Laurenczy, D. T. L. Alexander, N. Yan, P. J. Dyson, *J. Catal.* **2014**, 315, 67–74.
- [71] See: <http://avantium.com/yxy/products-applications/fdca/PEF-bottles.html>. (visited on 05.05.2019)
- [72] L. Filiciotto, A. M. Balu, J. C. Van der Waal, R. Luque, *Catal. Today*. **2018**, 302, 2-15.
- [73] B. Girisuta, H. Jan Heeres, in *Production of Platform Chemicals from Sustainable Resources* (Eds.: Z. Fang, J. R. L. Smith, X. Qi), Springer, Singapore, **2017**, pp. 143-169.
- [74] D. J. Hayes, S. Fitzpatrick, M. H. B. Hayes, J. R. H. Ross, in *Biorefineries - Industrial Processes and Products, Vol. 5*, 1st ed. (Eds.: B. Kamm, P. R. Gruber, M. Kamm), Wiley-VCH, Weinheim, Germany, **2006**, pp. 139-164.
- [75] S. W. Fitzpatrick, in *Feedstocks for the Future-Renewables for the Production of Chemicals and Materials, Vol. 921* (Eds.: J. J. Bozell, M. K. Patel), American Chemical Society, Washington, DC, **2006**.
- [76] A. M. Raspolli-Galletti, C. Antonetti, V. De Luise, D. Licursi, N. Nassi-o-Di-Nasso, *Biores.* **2012**, 7, 1824-1835.
- [77] See: www.gfbiochemicals.com. Visited on 05.05.2019
- [78] D. B. Bevilaqua, M. K. D. Rambo, T. M. Rizzetti, A. L. Cardoso, A. F. Martins, *J Clean Prod.* **2013**, 47, 96-101.
- [79] B. Girisuta, L. P. B. M. Janssen, H. J. Heeres, *Ind. Eng. Chem. Res.* **2007**, 46, 1696-1708.
- [80] P. A. Son, S. Nishimura, K. Ebitani, *React. Kinet. Mech. Cat.* **2012**, 106, 185-192.
- [81] V. Badarinarayana, M. D. Rodwogin, B. D. Mullen, I. Purtle, E. J. Molitor, WO2014/189991, **2014**.
- [82] K. Kumar, F. Parveen, T. Patra, S. Upadhyayula, *New J Chem.* **2018**, 42, 228-236.
- [83] H. Ren, B. Girisuta, Y. Zhou, L. Liu, *Carbohydr. Polym.* **2015**, 117, 569-576.
- [84] B. Girisuta, L. P. B. M. Janssen, H. J. Heeres, *Green Chem.* **2006**, 8, 701.
- [85] S. An, D. Song, Y. Sun, Q. Zhang, P. Zhang, Y. Guo, *ACS Sustain. Chem. Eng.* **2018**, 6, 3113-3123.
- [86] D. J. Braden, C. A. Henao, J. Heltzel, C. C. Maravelias, J. A. Dumesic, *Green Chem.* **2011**, 13, 1755–1765.
- [87] L. Corbel-Demilly, B. K. Ly, D. P. Minh, B. Tapin, C. Especel, F. Epron, A. Cabiach, E. Guillon, M. Besson, C. Pinel, *ChemSusChem* **2013**, 6, 2388–2395.
- [88] W. Luo, U. Deka, A. M. Beale, E. R. van Eck, P. C. Bruijninx, B. M. Weckhuysen, *J. Catal.* **2013**, 301, 175–186.
- [89] M. G. Al-Shaal, W. R. H. Wright, R. Palkovits, *Green Chem.* **2012**, 14, 1260–1263.
- [90] W. Hoelderich, F. N-umann, R. Fischer, US5144061, **1992**.
- [91] A. M. C. F. Castelijns, US2013079548, **2013**.
- [92] L. E. Manzer, WO04007421, **2004**.
- [93] R. J. Haan, J.-P. Lange, WO2005/058793, **2005**.
- [94] J. P. Lange, J. Z. Vestering, R. J. Haan, *Chem. Comm.* **2007**, , 3488–3490.
- [95] F.-X. Zeng, H.-F. Liu, L. Deng, B. Liao, H. Pang, Q.-X. Guo, *ChemSusChem.* **2013**, 6, 600–603.
- [96] J. G. de Vries, N. Sereinig, E. W. M. van de Vondervoort, M. C. C. Janssen, WO2012/131027, **2013**.
- [97] M. Mascal, E. B. Nikitin, *Green Chem.* **2010**, 12, 370-373.
- [98] H. J. Bart, J. Reidetschlager, K. Schatka, A. Lehmann, *Ind. Eng. Chem. Res.* **1994**, 33, 21-25.
- [99] M. Mascal, *ChemSusChem* **2015**, 8, 3391-3395.
- [100] G. M. G. Maldonado, R. S. Assary, J. A. Dumesic, L. A. Curtiss, *Energy Environ. Sci.* **2012**, 5 8990 -8997.

- [101] Z. H. Zhang, K. Dong, Z. B. Zhao, *ChemSusChem* **2011**, 4, 112-118.
- [102] J.-P. Lange, W. D. v. d. Graaf, R. J. Haan, *ChemSusChem* **2009**, 2, 437-441.
- [103] X. Zhang, Y. Li, L. Xue, S. Wang, X. Wang, Z. Jiang, *ACS Sustain. Chem. Eng.* **2017**, 6, 165-176.
- [104] X. Di, Y. Zhang, J. Fu, Q. Yu, Z. Wang, Z. Yuan, *Process Biochem.* **2019**.
- [105] H. Joshi, B. R. Moser, J. Toler, W. F. Smith, T. Walker, *Biom. Bioen.* **2011**, 35, 3262-3266.
- [106] L. Yan, Q. Yao, Y. Fu, *Green Chem.* **2017**, 19, 5527-5547.
- [107] Y.-B. Huang, T. Yang, Y.-T. Lin, Y.-Z. Zhu, L.-C. Li, H. Pan, *Green Chem.* **2018**, 20, 1323-1334.
- [108] Y. Liu, C.-L. Liu, H.-Z. Wu, W.-S. Dong, *Catal. Lett.* **2013**, 143, 1346-1353.
- [109] K. Tominaga, K. Nemoto, Y. Kamimura, A. Yamada, Y. Yamamoto, K. Sato, *RSC Adv.* **2016**, 6, 65119-65124.
- [110] N. A. S. Ramli, N. H. Zaharudin, N. A. S. Amin, *J. Teknol.* **2017**, 79, 137-142.
- [111] A. M. Hengne, S. B. Kamble, C. V. Rode, *Green Chem.* **2013**, 15, 2540-2547.
- [112] M. Paniagua, J. A. Melero, J. Iglesias, G. Morales, B. Hernández, C. López-Aguado, *Appl. Catal., A* **2017**, 537, 74-82.
- [113] Y. Q. Yang, H. Luo, G. S. Tong, J. S. Kevin, C. T. Tye, *Chinese J. Chem. Eng.* **2008**, 16, 733-739.
- [114] G. J. S. Dawes, E. L. Scott, J. Le Nôtre, J. P. M. Sanders, J. H. Bitter, *Green Chem.* **2015**, 17, 3231-3250.
- [115] T. Patra, D. Maiti, *Chem. A Eur. J* **2017**, 23, 7382-7401.
- [116] B. R. Brown, *Q. Rev. Chem. Soc.* **1951**, 5, 131-146.
- [117] A. F. Shepard, N. R. Winslow, J. R. Johnson, *J. Am. Chem. Soc.* **1930**, 52, 2083-2090.
- [118] A. Hossian, M. K. Manna, K. Manna, R. Jana, *Org. Biomol. Chem.* **2017**, 15, 6592-6603.
- [119] D. Tanaka, S. P. Romeril, A. G. Myers, *J. Am. Chem. Soc.* **2005**, 127, 10323-10333.
- [120] J. K. Kochi, R. A. Sheldon, S. S. Lande, *Tetrahedron* **1969**, 25, 1197-1207.
- [121] F. van der Klis, M. H. van den Hoorn, R. Blaauw, J. van Haveren, D. S. van Es, *Eur. J. Lipid. Sci. Technol.* **2011**, 113, 562-571.
- [122] J. Deng, Q.-G. Zhang, T. Pan, Q. Xu, Q.-X. Guo, Y. Fu, *RSC Adv.* **2014**, 4, 27541-27544.
- [123] H. L. Chum, M. Ratcliff, F. L. Posey, J. A. Turner, A. J. Nozik, *J. Phys. Chem.* **1983**, 87, 3089-3093.
- [124] Y. Gong, L. Lin, J. Shi, S. Liu, *Molecules* **2010**, 15, 7946-7960.
- [125] Y. Gong, L. Lin, *Molecules* **2011**, 16, 2714-2725.
- [126] R. E. Murray, E. L. Walter, K. M. Doll, *ACS Catal.* **2014**, 4, 3517-3520.
- [127] X. Zhang, F. Jordan, M. Szostak, *Org. Chem. Front.* **2018**, 5, 2515-2521.
- [128] J. A. Miller, J. A. Nelson, M. P. Byrne, *J. Org. Chem.* **1993**, 58, 18-20.
- [129] L. J. Gooßen, N. Rodríguez, *Chem. Comm.* **2004**, 724-725.
- [130] S. Maetani, T. Fukuyama, N. Suzuki, D. Ishihara, I. Ryu, *Chem. Comm.* **2012**, 48, 2552-2554.
- [131] Y. Liu, K. E. Kim, M. B. Herbert, A. Fedorov, R. H. Grubbs, B. M. Stoltz, *Adv. Syn. Catal.* **2014**, 356, 130-136.
- [132] M. A. Ortuño, B. Dereli, C. J. Cramer, *Inorg. Chem.* **2016**, 55, 4124-4131.
- [133] S. T. Gadge, B. M. Bhanage, *RSC Adv.* **2014**, 4, 10367-10389.
- [134] K. Dong, R. Sang, X. Fang, R. Franke, A. Spannenberg, H. Neumann, R. Jackstell, M. Beller, *Angew. Chem. Int. Ed.* **2017**, 56, 5267-5271.
- [135] X. Zhang, C. Shen, C. Xia, X. Tian, L. He, *Green Chem.* **2018**, 20, 5533-5539.
- [136] L. Wu, Q. Liu, R. Jackstell, M. Beller, *Org. Chem. Front.* **2015**, 2, 771-774.
- [137] W. Clegg, G. R. Eastham, M. R. J. Elsegood, R. P. Tooze, X. L. Wang, K. Whiston, *Chem. Comm.* **1999**, 1877-1878.
- [138] L. Hie, N. F. Fine Nathel, X. Hong, Y.-F. Yang, K. N. Houk, N. K. Garg, *Angew. Chem. Int. Ed.* **2016**, 55, 2810-2814.

- [139] Y.-R. Luo, *Comprehensive Handbook of Chemical Bond Energies*, CRC Press, Florida, **2007**.
- [140] X. Pu, J. Hu, Y. Zhao, Z. Shi, *ACS Catal.* **2016**, 6, 6692.
- [141] T. B. Halima, S. G. Newman, *J. Am. Chem. Soc.* **2017**, 139, 1311.
- [142] A. Maleckis, M. S. Sanford, *Organometallics* **2014**, 33, 3831-3839.
- [143] A. Maleckis, M. S. Sanford, *Organometallics* **2014**, 33, 2653-2660.
- [144] M. O. Miranda, A. Pietrangelo, M. A. Hillmyer, W. B. Tolman, *Green Chem.* **2012**, 14, 490-494.
- [145] A. John, L. T. Hogan, M. A. Hillmyer, W. B. Tolman, *Chem. Commun.* **2015**, 51, 2731-2733.
- [146] M. E. Fieser, S. D. Schimler, L. A. Mitchell, E. G. Wilborn, A. John, L. T. Hogan, B. Benson, A. M. LaPointe, W. B. Tolman, *Chem. Comm.* **2018**, 54, 7669-7672.
- [147] H. Siegel, M. Eggersdorfer, **2000**.
- [148] V. V. A. Baeyer, *Ber. Dtsch. Chem. Ges.* **1899**, 32, 3625.
- [149] J. Le Paih, J.-F. Frison, C. Bolm, *Oxidation of Carbonyl Compounds in Modern Oxidation Methods*, Weinheim, **2005**.
- [150] C. Bolm, C. Palazzi, O. Beckmann, *Metal-catalyzed Baeyer-Villiger Reactions in Transition Metals for Organic Synthesis, Vol. 2*, Weinheim, **2004**.
- [151] I. Polyak, M. T. Reetz, W. Thiel, *J. Am. Chem. Soc.* **2012**, 134, 2732-2741.
- [152] G. J. ten Brink, I. W. Arends, R. A. Sheldon, *Chem. Rev.* **2004**, 104, 4105-4124.
- [153] Z. Q. Lei, L. L. Wei, R. R. Wang, G. F. Ma, *Catal. Comm.* **2008**, 9, 2467-2469.
- [154] J. G. Cannon, J. E. Garst, *J. Pharm. Sci.* **1975**, 64, 1059.
- [155] L. Wu, S. Dutta, M. Mascal, *ChemSusChem* **2015**, 8, 1167.
- [156] S. Dutta, L. Wu, M. Mascal, *Green Chem.* **2015**, 17, 2335.
- [157] M. J. Fink, M. D. Mihovilovic, *Chem. Comm.* **2015**, 51, 2874-2877.
- [158] T. Fukuyama, S. Maetani, I. Ryu, in *Comprehensive Organic Synthesis, Vol. 3*, 2nd Edition ed., Elsevier Amsterdam NL, **2014**, pp. 1073-1100.
- [159] W. Fang, H. Zhu, Q. Deng, S. Liu, X. Liu, Y. Shen, T. Tu, *Synthesis* **2014**, 46, 1689-1708.
- [160] R. Grigg, S.P. Mutton, *Tetrahedron* **2010**, 66, 5515-5548.
- [161] W. Fang, H. Zhu, Q. Deng, S. Liu, X. Liu, Y. Shen, T. Tu, *Synthesis* **2014**, 46, 1689-1708.
- [162] K. Dong, X. Fang, S. Gülak, R. Franke, A. Spannenberg, H. Neumann, R. Jackstell, M. Beller, *Nat. Commun.* **2017**, 8, 14117.
- [163] M. Beller, B. Cornils, C. D. Frohning, C. W. Kohlpaintner, *J Mol. Catal. a-Chem.* **1995**, 104, 17-85.
- [164] M. A. Ortuno, B. Dereli, C. J. Cramer, *Inorg Chem* **2016**, 55, 4124-4131.
- [165] A. John, M. A. Hillmyer, W. B. Tolman, *Organometallics* **2017**, 36, 506-509.
- [166] N. Chatani, H. Tatamidani, Y. Ie, F. Kakiuchi, S. Murai, *J. Am. Chem. Soc* **2001**, 123, 4849-4850.
- [167] S. Ko, Y. Na, S. Chang, *J. Am. Chem. Soc.* **2002**, 124, 750-751.
- [168] M. S. Stephan, A. J. J. M. Teunissen, G. K. M. Verzijl, J. G. de Vries, *Angew. Chem. Int. Ed.* **1998**, 37, 662-664.
- [169] J. G. de Vries, *Dalton trans.* **2006**, 421-429.
- [170] S. Nobuyoshi, I. Daisuke, Y. Nichikei, F. Takahide, Japan, 2014.
- [171] G. Macchione, S. Maza, M. Mar Kayser, J. L. de Paz, P. M. Nieto, *Eur. J. Org. Chem.* **2014**, 2014, 3868-3884.
- [172] A. John, M. O. Miranda, K. Ding, B. Dereli, M. A. Ortuño, A. M. LaPointe, G. W. Coates, C. J. Cramer, W. B. Tolman, *Organometallics* **2016**, 35, 2391-2400.
- [173] S. M. Sen, J. Han, J. S. Luterbacher, A. D. Martin, J. A. Dumesic, C. Maravelias, *Comput. Aided Chem. Eng* **2014**, 34, 615-620.
- [174] A. Mamoru, *J. Catal.* **1987**, 106, 273 - 279.

- [175] Y. Muranaka, T. Suzuki, H. Sawanishi, I. Hasegawa, K. Mae, *Ind. Eng. Chem. Res.* **2014**, 53, 11611-11621.
- [176] Y. Gong, L. Lin, B. Zhang, *Chin. J Chem.* **2012**, 30, 327-332.
- [177] J. G.M. Bremner, D.G. Jones, I. C. I. Ltd.), GB, **1945**.
- [178] J. A. Dumesic, R. M. West, US7960592B1, **2011**.
- [179] K. Min, S. Kim, T. Yum, Y. Kim, B. I. Sang, Y. Um, *Appl. Microbiol. Biotechnol.* **2013**, 97, 5627-5634.
- [180] X. Wang, J. Zeng, X. Lu, J. Xin, S. Zhang, *Ind. Eng. Chem. Res.* **2019**, 58, 11841-11848.
- [181] A. G. Gayubo, A. T. Aguayo, A. E. Sánchez del Campo, P. L. Benito, J. Bilbao, *Stud. Surf. Sci. Catal.* **1999**, 126, 129-136.
- [182] M.-F. S. G. Reyniers, G. F. Froment, *Ind. Eng. Chem. Res.* **1995**, 34, 773-785.
- [183] A. G. Gayubo, A. T. Aguayo, A. E. Sánchez del Campo, P. L. Benito, J. Bilbao, in *Stud. Surf. Sci. Catal., Vol. 126* (Eds.: B. Delmon, G. F. Froment), Elsevier, **1999**, pp. 129-136.
- [184] I. Böttger, B. Pettinger, T. Schedel-Niedrig, A. Knop-Gericke, R. Schlögl, in *Stud. Surf. Sci. Catal., Vol. 133* (Eds.: G. F. Froment, K. C. Waugh), Elsevier, **2001**, pp. 57-70.
- [185] A. V. Miller, V. V. Kaichev, I. P. Prosvirin, V. I. Bukhtiyarov, *J. Phys. Chem. C* **2013**, 117, 8189-8197.
- [186] N. Onishi, G. Laurenczy, M. Beller, Y. Himeda, *Coord. Chem. Rev.* **2018**, 373, 317-332.
- [187] M. Andérez-Fernández, L. K. Vogt, S. Fischer, W. Zhou, H. Jiao, M. Garbe, S. Elangovan, K. Junge, H. Junge, R. Ludwig, M. Beller, *Angew. Chem. Int. Ed.* **2017**, 56, 559-562.
- [188] C. G. S. Lima, J. L. Monteiro, T. de Melo Lima, M. Weber Paixão, A. G. Corrêa, *ChemSusChem* **2018**, 11, 25-47.
- [189] A. L. Maximov, A. V. Zolotukhina, A. A. Mamedli, L. A. Kulikov, E. A. Karakhanov, *ChemCatChem* **2018**, 10, 222-233.
- [190] Y. Wu, R. P. Singh, L. Deng, *J. Am. Chem. Soc.* **2011**, 133, 12458-12461.
- [191] W. Skorianetz, G. Ohloff, *Helv. Chim. Acta* **1975**, 58, 1272-1275.
- [192] Z. P. Xu, C. Y. Mok, W. S. Chin, H. H. Huang, S. Li, W. Huang, *J. Chem. Soc., Perkin Trans. 2* **1999**, 725-730.
- [193] J. Würmel, J. M. Simmie, M. M. Losty, C. D. McKenna, *J. Phys. Chem. A* **2015**, 119, 6919-6927.
- [194] R. De Bruycker, H.-H. Carstensen, J. M. Simmie, K. M. Van Geem, G. B. Marin, *Proc. Combust. Inst.* **2015**, 35, 515-523.
- [195] S. Y. Tee, K. Y. Win, W. S. Teo, L.-D. Koh, S. Liu, C. P. Teng, M.-Y. Han, *Adv Sci (Weinh)* **2017**, 4, 1600337-1600337.
- [196] C. Chen, US006632765B1, **2003**.
- [197] Q. Bao, T. Bu, J. Yan, C. Zhang, C. Ning, Y. Zhang, M. Hao, W. Zhang, Z. Wang, *Catal. Lett.* **2017**, 147, 1540-1550.
- [198] E. V. Makshina, J. Canadell, J. v. Krieken, E. Peeters, M. Dusselier, B. F. Sels, *ChemCatChem* **2019**, 11, 180-201.
- [199] L. Craciun, G. Benn, J. Dewing, G. Schriver, W. Peer, B. Siebenhaar, U. Siegrist, US20050222458A1, **2005**.
- [200] B. Sarkar, C. Pendem, L. N. S. Konathala, R. Tiwari, T. Sasaki, R. Bal, *Chem. Comm.* **2014**, 50, 9707-9710.
- [201] L. Craciun, G. Benn, J. Dewing, G. Schriver, W. Peer, B. Siebenhaar, U. Siegrist, US20110112330A1, **2011**.
- [202] X. C. Jiang, C. H. Zhou, R. Tesser, M. D. Serio, D. S. Tong, J. R. Zhang, *Ind. Eng. Chem. Res.* **2018**, 57, 10736-10753.
- [203] S. Dey, S. K. G. and, A. Sudalai, *Org. Biomol. Chem.* **2015**, 13, 10631-10640.
- [204] M. Lilga, J. White, J. Holladay, A. Zacher, D. Muzatko, R. Orth, US20070219391A1, **2007**.
- [205] L. E. Bogan, M. A. Silvano, D. L. Zolotorofe, US20090076297A1, **2009**.

- [206] W. P. Ratchford and C. H. Fisher, *Ind. Eng. Chem.* **1945**, 37.
- [207] J. E. Godlewski, J. E. Velásquez, D. I. Collias, US20130296602A1, **2013**.
- [208] E. V. Makshina, J. Canadell, J. van Krieken, E. Peeters, M. Dusselier, B. F. Sels, *ChemCatChem* **2018**, 11, 180-201.
- [209] A. S. Amarasekara, L. H. Nguyen, N. C. Okorie, S. M. Jamal, *Green Chem.* **2017**, 19, 1570-1575.
- [210] A.-N. Parvulescu, A. L. de Oliveira, M. Lejkowski, N. T. Woerz, M. Hartmann, K. Amakawa, M. Goebel, U. Mueller, M. Feyen, Y. Liu, US20150343431A1, **2015**.
- [211] J. G. Cannon, J. E. Garst, *J. Pharm. Sci.* **1975**, 64, 1059-1061.
- [212] W. P. Ratchford, C. H. Fisher, *Ind. Eng. Chem.* **1945**, 37, 382-387.
- [213] R. C. Larock, *Comprehensive Organic Transformations*, 2nd ed., NY, USA, **1999**.